Notes on colours:

- Referee's comments are given in black.
- Authors' comments are given in red.
- Texts from the revised manuscript are given in blue.

Referee 1

Interactive comment on "CSIB v1: a sea-ice biogeochemical model for the NEMO community ocean modelling framework" by Hakase Hayashida et al.

A. Randelhoff (Referee)
achim.randelhoff@takuvik.ulaval.ca

Received and published: 19 September 2018

Hayashida et al. report here on their implementation of a sea ice biogeochemical model into the NEMO framework. The strength of NEMO is the ability to compare different submodules, and thus to isolate the overall impact of very specific parameterizations and submodels. This is an important step in refining existing models and towards singling out future research directions in this ambitious field of mechanistic modelling of (Arctic) ocean biogeochemistry.
I found the paper generally well-written and laid out clearly; find some suggested improvements below.

We thank the referee for his positive comments and thorough feedback on our manuscript. Below, we provided our responses to the referee's comments and revised our manuscript based on these comments as much as possible.

Major issues:
Section 3.1: I am not entirely convinced by your analysis. The "break points" you see in the time series appear to be quite arbitrary; they probably make sense to you based on your familiarity with models and previous studies, but a reader might want to see a statistical analysis that supports your claims. That being said, I am not entirely sure to what extent you need these spinup times for your later analysis; you are probably able to carry through the rest of your paper without most of the claims put forward in this section. If they are important in their own right, I would recommend considering a more rigorous presentation.

We agree that the break points discussed in the time series during spin up are quite arbitrary and that it would be more desirable to make these claims using statistical analysis. Our analysis here is qualitative, and so chose the break points based on the findings from previous model studies. As the referee also pointed out, this spin-up section does not affect the conclusions of the rest of the paper. However, presenting the results during model spin-up can be helpful for future studies. Therefore, we decided to move this section into an appendix section (Appendix B), and revised the text accordingly.

The paper should probably also explain more generally why it focuses on the period

1969-79 for spin-up and 1979 for all experiments, especially since e.g. snowfall climatology (and likely all other data) are much scarcer for that period than later ones. The Arctic also looked very different in 1979 from what it is today, so you should give a good reason if you expect that your comparisons from the 1970s are relevant today as well.

We agree that the model can be better evaluated for more recent period than the period considered in the present study. We extended our simulation up to 2015 and evaluated with more recent observational data (Hayashida 2018, PhD thesis), but these results are planned to be published as separate papers considering the contents of the present study, which is intended as a model description paper. We revised the manuscript to clarify these points (P2 L31):

"We note that this study is intended as a model description paper, and the analysis focuses on results for the year 1979, corresponding to the end of a decadal model spin up. The analysis of the simulation beyond 1979, in which more observational data are available for evaluation (Hayashida 2018b), is planned to be published as a journal article separately."

Hayashida, H. (2018): Modelling sea-ice and oceanic dimethylsulfide production and emissions in the Arctic, PhD thesis, University of Victoria, Victoria, BC, Canada, http://dspace.library.uvic.ca/handle/1828/10486

Minor comments and suggestions:
General:
Some of your figures have colorbars that are of very little use (examples: Fig. 8, Fig. 14b+c, Fig. 16c, ...) because they are scaled linearly and some extreme regions mask the variability over most of the map. Assuming you produce your figures using matplotlib, you could look into https://matplotlib.org/users/colormapnorms.html.

Re: Fig.8, 14b: Using a linear scale for the colorbar allows us to easily distinguish between high and low productive regions, where the contribution of the latter region to the total production (area integrated) is negligible. Hence, we would prefer not to change these figures.

Re: Fig.14c: We revised the figure by reducing the range of the colorbar scale so that the contrast is stronger.

Re: Fig.16c: We revised the figure by adopting the log scale and changing the colormap to "YlBuGn".

You mix present and past tense occasionally (e.g. Section 3.3.1; p20 line 9ff; ...).

Revised to use present tense consistently in Results and Discussion section.

Specific:
p1
15 spell out LIM2/3, PISCES

Revised as suggested.

p2
23 "horizontal transport of ...": Technically correct (here as elsewhere), but it might be more intuitive to explain that you mean transport with sea ice drift.

Revised as suggested by adding “associated with sea ice drift” at the end of the sentence.

27 You may want to quickly mention in this section why you develop another sea ice BGC model after several others already exist. I assume it is because the NEMO framework allows model intercomparison, your overarching goal, and it did not have any yet?

Yes. NEMO does not have any sea-ice biogeochemical model component (except the offline version of Tedesco et al. 2017, as noted on P2 L19 in the original manuscript) and also having one for NEMO allows intercomparison. We revised the manuscript to mention about intercomparison in this paragraph (P2 L27):

“These implementations allow more realistic simulation of sea-ice biogeochemistry and intercomparison of process-based ice algae models.”

p3
Tab. 1: Specify that i0 is for the uppermost layer, be it snow or ice or both (which I think it is based on p25, l.14, as Maykut & Untersteiner had apparently measured it for snow-free surfaces, but correct me if I am wrong). Mention briefly (here or in the text) what you mean by "ice algal skeletal layer".

The referee is correct that i0 defined in the paper refers to either snow or ice surface. However, in this Table, we compare i0 for snow surface among studies. We revised the table caption and first row by replacing “i0” with “i0 (snow surface)” to clarify that we are comparing i0 for snow surface. And throughout the manuscript, we replaced “i0” with “i0 for snow surface” for clarification where applicable.

Replaced “the thickness of ice algal skeletal layer” with “the vertical extent of the biologically-active layer at ice base”.

9ff. " a thin layer...": Is this synonymous with the "scattering layer" of sea ice optics? What happens when there is less than 10 cm of snow+ice? Does this fraction penetrate only below 10 cm, after which different attenuation coefficients are applied, or is transmissivity below this "thin layer" set to 1?

Yes, the surface thin layer defined in the present study is synonymous with the scattering layer of sea ice optics. When the snow+ice thickness is less than 10 cm, the penetrating fraction (i0) enters the underlying seawater. The Beer-Lambert law is applied for the penetrating fraction. We revised the schematic to clarify these points (Figure 1). We also revised the manuscript to use the term surface scattering layer (SSL) for consistency with the sea ice optics literature.

11 Two times "this" is repetitive

Removed as suggested.

p4
Fig. 1: Again, is this "surface thin layer" the same as the scattering layer? In this schematic, you could also indicate if there is additional attenuation below this "surface thin layer".

Yes, the surface thin layer is identical to the surface scattering layer. In the revised figure caption for Fig.1, we indicate that the radiation penetrating below the SSL attenuates following the Beer-Lambert law.

9 I think I understand what you are saying, but in my mind the point of mechanistic modelling is exactly to include more and more parameterizations. Is PISCES' performance not good enough to justify the extra computational costs it would imply as compared to CanOE?

As the reviewer points out, extra computational costs can be justified if the model performs better. CanOE has been developed as an advanced/more sophisticated biogeochemical model for the Canadian Earth System Model version 5 (CanESM5), compared to the simpler NPZD version CMOC (Canadian Model of Ocean Carbon) used in CanESM2 with the idea to limit the complexities as much as possible, while allowing to address insufficiencies in CMOC (e.g. single NPZD model are either tuned towards low nutrient or high nutrient oceans). PISCES includes complexities that do not necessarily warrant the additional computational resources, as well as some which have limited foundations. Preliminary results of a model intercomparison study (Steiner et al., in prep.) for primary production in the Arctic do not necessarily suggest superior performance for PISCES. We would also argue that the point of mechanistic modelling is to improve the parameterizations in a way so they better represent the real world and improve the correspondence between model and observations. That does not necessarily mean including more and more parameterizations. Some parameterisations might be more accurate but do very little to the overall model improvement.

15-16 I can live with the sentence but found it a tad vague, probably because I did not understand what you mean by "state of the ecosystem". In terms of nutrient budget modelling, part of the ecosystem *is* the sulfur cycle so the inverse statement is a tautology.

Replaced "state of the ecosystem" by "conditions of primary and secondary producers".

p5
11-12 43% in units of W/m^2? I also assume you mean "43% of the downwelling shortwave radiation reaching the sea surface"

Revised as suggested.

p6
Fig. 2: "stoichiometry": stoichiometries

Revised as suggested.

p7
4 Plase explain what "[e]ddy diffusion tendencies" are. How are they computed (explicitly)?

Eddy diffusion tendencies are the rate of change in a sea-ice biogeochemical state variable due to horizontal transport by unresolved motions (the second term in Equation 2). They are computed by evaluating the second order diffusive operator using the Crank-Nicholson method. We revised the manuscript to add this information (P7 L23):

"Diffusion is computed within the ice pack by evaluating the second-order diffusive operator using the Crank-Nicholson scheme (Crank and Nicolson, 1996), while it is set to zero at the ice edge."

10 By "concentrations", I assume you mean sea ice bulk, not brine concentrations. Since salinity gets a special treatment, are there problems of mass conservation during ice freezing because of changes in ratios of nutrients to salinity?

Yes, the term "concentrations" refers to sea ice bulk concentrations. As noted in the original manuscript (P7 L16), Equation 3 does violate mass conservation. However, it has negligible impacts on ocean biogeochemistry given the relatively-thin sea ice biologically-active layer (3 cm). Salinity and nutrients in sea ice are modelled separately. While salinity is non-zero throughout the ice column, nutrients (and other sea-ice BGC variables) are represented as having zero concentration above the biologically-active bottom-ice layer. We revised the manuscript to clarify that it is the bottom 3 cm of newly-formed ice that has the same concentration as the underlying seawater (P7 L28) and that the concentration above is zero (P8 L9):

"The bottom 3 cm of newly-formed ice is assumed to contain the same concentrations of biogeochemical state variables as those in the underlying water column." (P7 L28)

"Above the bottom sea-ice biogeochemical layer, the concentrations are set to zero for all biogeochemical tracers." (P8 L9)

11 Add "the concentration (X) of any ..."

Revised as suggested.

18-19 "minimum biomass threshold": I assume this threshold is also arbitrary, not based on field measurements?

The threshold is taken from our earlier model study (Mortenson et al. 2017) which is based on observed range (Garrison et al. 1983). Thus, it is not entirely arbitrary. We revised the manuscript to clarify this point (P8 L7):

"This threshold is derived based on the observed range of ice algal biomass in young sea ice (Garrison et al., 1983) and by assuming a fixed carbon-to-chlorophyll ice algal cell quota (Mortenson et al., 2017)."

Garrison et al. (1983): A physical mechanism for establishing algal populations in frazil ice. Nature, *306*(5941), 363.

29 You say you use the molecular diffusive exchange of nutrients, but my impression is your model would not resolve the molecular sublayer (a few mm from the ice-ocean interface). Without having checked I assume you use combined turbulent-molecular diffusion coefficients, but you may want to include the right references here, especially since such coefficients have never been measured (as far as I know) for tracers other than momentum, heat, and salinity.

As the referee pointed out, it is the combined turbulent-molecular diffusion; the effects of turbulence are accounted as the molecular sublayer is parameterized as a function of friction velocity (Equation 27

of Mortenson et al. 2017), and the molecular diffusion coefficient is derived from measurements for dissolved silica in seawater at 2 degree-C (Rebreanu et al. 2008). We added this discussion in the revised manuscript (P8 L23):

"For 1), the effects of turbulence are approximated by parameterizing the molecular sublayer as a function of friction velocity, and molecular diffusion is calculated using the observed diffusion coefficient of dissolved silica measured in seawater at 2 ◦C (Rebreanu et al., 2008)."

Rebreanu et al. (2008), The diffusion coefficient of dissolved silica revisited. *Marine chemistry*, *112*(3-4), 230-233.

30 Flooding due to negative sea ice freeboard does not count towards flushing?

Flooding due to negative sea ice freeboard is accounted and considered as part of surface ablation in the text. We added this information in the revised manuscript (P8 L22):

"flushing of these variables by flow of water through the ice from rainfall and surface melting (including flooding due to negative freeboard)."

p8
2-3 "designed to be the most realistic ...": "realistic" is as such a bit vague and you might want to rephrase as something like "thought to be most realistic among all choices considered in this paper".

Revised as suggested.

p10
1 "initialized to arbitrarily low values": I do not understand what "arbitrarily low" means.

Replaced "arbitrarily low values" with "very low values (e.g. 0.01 mmol C m-3 for the carbon contents of phytoplankton, zooplankton, and detritus)".

5 "while the other two boundaries (along North America and Eurasia) were assumed to be closed": So how was riverine (freshwater) input distributed into the ocean?

We distribute riverine freshwater flux into specified grid cells based on Dai and Trenberth (2002) as described in the original manuscript (P10 L13). It is independent of lateral boundaries. We realize that this can be better explained visually, and thus, included a figure displaying the locations of "river mouths" where riverine input is deposited in the revised manuscript (Figure 5 and P11 L23 of the revised manuscript):

"Figure 5 shows the seasonal and interannual variability (a and b) and spatial distribution (c) of the total discharge over the pan-Arctic."

13-14 "... was neglected, and therefore ... not addressed": This is a tautology. Is there a reason why? Lack of data? Too small? Too hard?

Lack of adequate data to prescribe riverine concentrations of biogeochemical variables in the model domain. We revised the sentence accordingly (P11 L25):

"The river discharge of biogeochemical state variables was neglected due to the lack of adequate data."

p11
Tab. 3: Typo in units of rn_ahtrc_0, should probably be m2s-1.

Revised as suggested.

6 "modified": How? Were only the data quality flags adjusted?

We contacted Clark Pennelly who provided the data and confirmed that there was actually no modification to the atmospheric data values; the only changes were indexing and ordering of latitudinal coordinates and renaming variables. We revised the text slightly to indicate that there was no modification to the data values including the missing data flags (P11 L34):

"As a substitute, we used a version provided by Clark Pennelly at the University of Alberta (personal communication) which addressed the missing data flag errors without any modifications to the atmospheric data (the only changes were indexing and ordering of latitudinal coordinates and remaining variables)."

10 So just to be sure; You used the 1979 snowfall for all years 69-78, but for all the other variables you use the 69-78 time series data?

The 1979 snowfall and total precipitation are used for 1969-1978, while for all the other variables we use the 1969-1978 time series data. We revised the manuscript to clarify this point (P12 L5):

"However, in EXP0, we prescribed the total precipitation and snowfall for 1979 repeatedly for the simulation over the period 1969-1978, while keeping the remaining atmospheric variables the same as the original DFS dataset."

15-16 You may want to consider additionally archiving the current version (e.g. using a doi) upon publication.

As suggested, we archived the current version and produced a DOI. We added this reference to the revised manuscript (P12 L12):

"For a complete list of the parameters, readers are referred to the source-code archive (Hayashida, 2018)."

18-19 "were adjusted to improve": How adjusted, and by what measure did you check that they "improved" sea ice volume etc.? Maybe insert reference to later if this is part of the discussion of the model runs.

We adjusted these parameters by running a number of simulations, every time with a different combination of the parameters. By "improve", we meant their comparison with PIOMAS. We revised this sentence accordingly (P13 L1):

"The other two parameters (hiccrit and pstar) were adjusted to improve the fit with the PIOMAS data product (Section 2.6) in terms of sea-ice volume and extent for 1979 (Section 3.1.1)."

19-20 "were adjusted to simulate reasonable": Same as in the previous sentence.

By reasonable, we mean compared to previous studies. As suggested, we inserted a reference to the later section where we show comparison in the revised manuscript (P13 L3):

"Lastly, two parameters of CanOE (Tref and chldeg) were adjusted to simulate reasonable annual primary production in the Arctic Ocean (Section 3.2)."

p12
18 Repetition: "the the Pan-Arctic"

Revised as suggested.

p13
7 "diagnose potential drifts": Unclear to me. In addition, how do you separate this (effects such as potential mass non-conservation in some tracers) from the inherent "spin-up dynamics" (meaning the adjustment from some relatively arbitrary initial condition to a state that is permitted by model dynamics)?

As discussed in response to the major comment 1 above, our simulation is too short to separate the drifts from the inherent spin-up dynamics quantitatively. Thus, we removed this sentence and revised this section (Appendix B).

p15
4ff. What is the reason for not simply masking the respective regions from the PIOMAS dataset in order to compare your model outputs across the same regions?

As suggested, we interpolated the PIOMAS product onto our model grid to perform grid-to-grid comparison over the same domain (Figure 7), and accordingly updated the time series comparing the sea ice volume and extent between our model and PIOMAS (Figure 6). Because the spatial coverage of SIIV3 differs from our model domain, we excluded its ice extent time series from the figure in the revised manuscript.

28 Is the occurence of such thick ice off Siberia in PIOMAS discussed in any of the literature about PIOMAS? I am mostly asking out of curiosity, I agree with your conclusion that it is likely an artifact.

This thick ice off Siberia is also present (although smaller magnitude) in PIOMAS for August 1993 (Figure 10b of Zhang and Rothrock (2003)). However, it was not discussed in that literature. We also did not find any other literature discussing this feature.

Zhang and Rothrock (2003), Modeling global sea ice with a thickness and enthalpy distribution model in generalized curvilinear coordinates. *Monthly Weather Review*, *131*(5), 845-861.

p18
13 "confined to shelf regions" (excluding the Barents Sea)

Revised as suggested.

29 space between ’Figure’ and ’8d’

Revised as suggested.

29 "in both qualitative and quantitative ...": I feel "in quantitative ..." is enough already as it entails the other.

Removed “qualitative”.

p20
Section 3.4: "subsurface chlorophyll a maximum": Maxima at around 5–10 m are hardly comparable to the severals tens of meters usually found in the Arctic; splitting by Atlantic/Pacific sectors might be worthwhile here due to their very different hydrographies, just as extending the profiles in the plots deeper (to e.g. 40 m).

We agree that averaging over smaller regions would make the results closer to what we find in observations. We looked at the vertical time series at various locations and confirmed that the subsurface chlorophyll maxima (SCM) can be found at deeper depths, comparable to observations (see the figure below, which shows the vertical time series at the grid cell corresponding to 170 degree W and 70 degree N in the Chukchi Sea. The SCM depth (>20 m) is comparable to observations, e.g., Brown et al. 2015). A detailed discussion on SCM simulated by CanOE is included in Steiner et al. (in prep.).

Brown et al. (2015), Characterizing the subsurface chlorophyll a maximum in the Chukchi Sea and Canada Basin. *Deep Sea Research Part II: Topical Studies in Oceanography*, *118*, 88-104.

However, the focus of the analysis in this section is to quantify the impacts on air-sea gas (DMS) flux at a larger scale (pan-Arctic), and so the pan-Arctic averaging was used. We revised the manuscript to discuss this point (P19 L22):

“Note that the meltwater lens and the subsurface maxima are respectively thicker and shallower than those observed by field measurements (e.g., Brown et al., 2015) because of averaging over the pan-Arctic domain. The purpose of this spatial averaging is to quantify the impacts at a larger scale rather than assessing localized effects.”

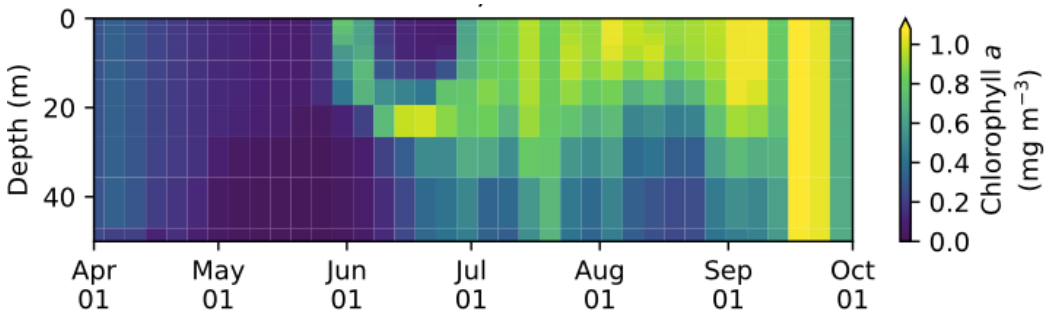

Fig. 9 gives the impression that the surface mixed layer is not deep enough (compared to what I think observations would show), hence surface mixing might be too weak in the model. Could this also be the reason for strong DMS gradients in the upper 10-15 meters?

As in the previous comment, Fig.9 shows pan-Arctic averages which tend to average/smear out mixing depths which could be much higher at specific locations and points in time.

Do you think including under-water PAR irradiance in Fig. 9 could help with the interpretation of the results?

We do not think that the addition of PAR to Fig.9 would aid in the interpretation of the results. It is already clear from the existing figure that the SCM is associated with the depletion of surface nitrate (chlorophyll maxima following the nitracline).

24ff. I am not sure what these gradients in DMS tell me. You state "DMS flux would be underestimated", but can you spell out what exactly is being underestimated? The real flux, the modelled flux? Is the DMS flux calculation currently based on the 1-m concentration or the 12-m concentration, and why does the formula not use the one that would be appropriate for your model? How many percent would the underestimation be? 15% under- (over-?) estimation in the surface ocean DMS concentration as such does not sound so bad, but the effect on the flux probably depends on the air concentration.

Here, we meant that the modelled flux would be underestimated if the model had coarse vertical resolution (i.e. 12 m), as the averaging over 12 m dilutes the DMS concentration. The difference in DMS concentration linearly translates into the modelled flux by definition of the flux paramterization. The parameterization would be independent of model vertical resolution. We agree that the flux depends on the atmospheric concentration as well, which can be important if atmospheric boundary layers are low and the atmospheric concentration is high (Steiner & Denman, 2008). However, in general, the atmospheric concentration of DMS is orders of magnitudes smaller than the surface-water concentration, therefore should have negligible effect on the flux difference between the cases. Neglecting these atmospheric conditions is a common approach for ocean models that are not coupled to atmospheric models. We revised this paragraph accordingly (P20 L4):

“Here, the averaging over a thicker layer results in dilution of the DMS concentration in the uppermost layer represented in the model. Considering that this difference is present primarily during the ice melt period, and therefore that the sea-surface DMS is released into the atmosphere, the modelled sea-to-air DMS flux would be underestimated by a similar amount in the absence of fine vertical resolution in the upper water column.”

Steiner and Denman (2008): Parameter sensitivities in a 1-D model for DMS and sulphur cycling in the upper ocean. Deep Sea Research Part I: Oceanographic Research Papers.

p22
8 "mm dˆ(-1)": Does this mean amount of meltwater equivalent, snow...?

Yes. We added this information in the revised manuscript (P20 L18):

"The monthly CORE-II dataset varies from approximately 1 to 2.4 mm d−1 (meltwater equivalent), while …"

p23
5 "extremely-low": extremely low

Revised as suggested.

14ff. So if these model-internal parameters can have such a big and non-intuitive effect on accumulated snow depth, why do you tune/adjust/modify the input snowfall dataset instead of the model parameters? (I also kept wondering, what happens to the thickness of the snow cover during ice dynamics (i.e. convergence)? Is total snow mass being conserved?)

The model sensitivity to the parameter nn_fsbc is somewhat unexpected because snow accumulation should not be sensitive to this parameter as long as the frequency of computation of surface boundary conditions (defined by nn_fsbc) is higher than that of the input snowfall dataset. While tuning this parameter did improve the simulated snow depth (as demonstrated by EXP1 and EXP2), this tuning is quite arbitrary without known constraints and therefore is not preferable. Furthermore, the tuning might have other implications which we did not assess in the present study. On the other hand, the usage of high-frequency atmospheric forcing is desirable simply because it is more realistic. We revised the manuscript to add this discussion (P22 L13):

"This high sensitivity to the choice of nn_fsbc is somewhat unexpected given that the tested range (1-10 time steps, equivalent to 20-200 minutes) is far less than the temporal resolution of the CORE-II dataset. A more detailed analysis of the model sensitivity to nn_fsbc is outside the scope of this study. Nevertheless, this analysis suggests that the issue with the usage of monthly or climatological-daily snowfall dataset can be resolved by tuning this parameter (as demonstrated in EXP1 and EXP2). However, the tuning of this parameter without known constraints is quite arbitrary and might have other implications for modelled dynamics. The usage of high-frequency atmospheric forcing dataset is recommended whenever possible to prevent the issue discussed here."

Total snow/ice mass is conserved in LIM2 and the convergence is simulated for sea-ice physical variables.

Section 4.2: Briefly remind the reader what i0 is.

Revised as suggested.

p25
14 "This value" referring to Castellani et al.'s 0.3?

Yes. We replaced "This value" with "This value (0.3)" in the revised manuscript.

p26
Section 4.3: I am a bit confused as to what you mean by "neglecting" advection/eddy diffusion. What happens instead when ice concentration changes from or to zero in a grid cell? Are sea ice BGC parameters somehow reset, do they pick up from where they were last time, whenever ice re-appears? I am especially thinking of nutrient and

biomass budgets. Are these still being conserved?
Again, note my earlier reservation about calling this "advection", you may want to specify that you are talking about moving sea ice, and hence moving BGC variables around with the ice (I think).

Neglecting advection/eddy diffusion means tendencies of BGC variables associated with horizontal motions of are artificially suppressed. Comparing this sensitivity run with the standard run allows us to quantify the contribution of horizontal transport to the overall budget. When ice concentration changes from zero to a non-zero value, sea-ice BGC concentrations are set to those in the underlying water column as described in Sec.2.3.2 of the original manuscript. As described in that section, this formulation does violate the mass conservation but the effect is small given the thin-layer (3 cm) of sea-ice BGC. When ice concentration changes to zero, sea-ice BGC concentrations are set to zero as they are all lost in the grid cell.

As suggested, we revised the manuscript to specify that we are talking about moving sea ice (P26 L5):

"These results indicate that the overall effect of horizontal transport associated with moving sea ice over the pan-Arctic is an increase in these quantities."

Section 4.4: Which parameter(s) is/are being modified concretely to "neglect" "the shading"?

We neglected the shading effect by setting the light extinction coefficient for ice algae to zero. We added this information in the revised manuscript (P26 L20):

"In EXP5, the shading effect of ice algae on light transfer through the ice is artificially suppressed in order to assess its impact on under-ice NPP. Effectively, this is done by setting the light extinction coefficient for ice algae to zero (Equation 15 of Mortenson et al. (2017))."

p28
31ff I think you can be more explicit here: What I understand is that ice algae shading can affect pelagic bloom *timing*, but will not affect annual pan-Arctic NPP. Regarding "patchiness of ice algal distribution": If you mean patchiness at the subgrid scale then I do not think your model accounts for this anyway; so perhaps it should not be part of the argument.

Revised as suggested to be more explicit by adding the word "timing".

By "patchiness of ice algal distribution", we do not mean sub-grid scale, but the pan-Arctic distribution is patchy (i.e. confined to shelf regions) as described earlier in this section. We clarified this point in the revised manuscript (P28 L24):

"However, given the patchiness of ice algal distribution (mostly confined to shelf regions) and the control of the light through the open-water fraction, the impact of the shading on the pan-Arctic under-ice annual NPP is negligible."

p29
Fig.15: I think including ice+snow transmissivity, or snow depth, or lead fraction, or something else of the sort should be included here to separate the rise in under-ice

PAR into the two factors "increasing sun angle" and "more transparent ice cover" as the season progresses.

While separating the increase in under-ice PAR into the two factors can be useful, we do not think that including any of those suggested variables would allow us to distinguish the two because those suggested variables are dependent on both of the two factors. For example, increasing sun angle would lead to more melting which leads to more transparent ice cover. Thus, we kept the figure as is.

p30
4 "were necessary to properly simulate": I am unsure what "properly" means here.

Replaced “properly” with “adequately”.

Referee 2

Interactive comment on “CSIB v1: a sea-ice biogeochemical model for the NEMO community ocean modelling framework” by Hakase Hayashida et al. Anonymous Referee #2
Received and published: 2 October 2018

This paper describes one more Pan-Arctic coupled model. I think it is a well-written paper and it seems to fit the scope of the journal. I have a few general comments/questions (below) and several minor comments/corrections made directly on the paper pdf (attached). I think this paper may be accepted after minor to moderate modifications. I suggest that authors address my general comments below to help the reader understanding better some of the modeling options taken here. This can be done with some small addition of text to the original manuscript. I also suggest that authors have a look at my minor comments/questions and choose the best way to address them. In general these should be quite easy to handle.

We thank the referee for his/her positive comments and constructive feedback on our manuscript. We revised the manuscript based on the comments/corrections made directly on the submitted manuscript as much as possible. Please see https://www.geosci-model-dev-discuss.net/gmd-2018-191/gmd-2018-191-AC2-supplement.pdf where we added our responses to the referee's comments/corrections.

Below we provide responses to the general comments/questions.

General comments/questions
1) I think that the effort made here to test the model and compare it with observations is quite important. This is frequently lacking in modeling studies that emphasize obtained results without a proper assessment of model performance. The modes implemented here is compared with observations temporarily and spatially (both horizontally and vertically). I think this is a good example. I guess authors could improve a bit the comparison by including some statistical measures of model performance such, as for example, the Nash Sutcliffe model efficiency and the Percentage model bias synthesized in Allen et al. (2017). In this case they could perhaps make comparisons across time and space simultaneously and come up with some objective qualitative assessment of model performance.

We appreciate the suggestion to perform more objective analysis of our model results that can be helpful for readers. As suggested, we quantified the model performance using the percentage model difference as a measure. This measure was used to compare: 1) the annual-mean ice volume and extent (Section 3.1.1; P14 L17); and 2) the March- and September-mean ice thickness distributions (Section 3.1.2; P16 L2 and L12) between our model and PIOMAS in the revised manuscript. In short, the comparison 1 was better than the comparison 2, indicating that our model agrees well with PIOMAS in terms of simulating the overall structure, but not so (although still reasonable; 30-40% difference) in spatial patterns.

2) Why a "new" Pan-Arctic model? I think it would help if authors justified the reasons for selecting a specific sea-ice biogeochemistry model, especially considering that the selected model simulates only bottom-ice biogeochemistry while, since the 90s, several authors adopted vertically resolved sea-ice biogeochemistry models, suggesting the importance of the stocks of algae, nutrients, etc., in upper ice layers through their contribution to vertically integrated production (e.g. Arrigo et al., 1993; Vancoppenolle et al., 2010; Pogson et al., 2011; Duarte et al., 2015). I have the impression that the emphasis on bottom sea-ice biogeochemistry comes from the larger availability of studies on land-fast ice, with a typical large accumulation of ice algae at the bottom few centimeters. However, studies in the pack ice over the open ocean show quite a different picture, where maximum may occur at various depths (e.g. Melnikov et al., 2002; Olsen et al., 2017).

The purpose of our model development work here is its in-line coupling implementation specifically into NEMO, which has not been done previously.

While vertically resolved sea-ice biogeochemistry models are more desirable, we argue that its implementation into a 3-D modelling framework is impractical due to computational costs. Note that all of the previous model studies that adopted the vertically resolved sea-ice models are based on 1-D column frameworks. To the best of our knowledge, the CICE model is the only model system that has the capability to vertically resolve sea-ice BGC (Jeffery et al. 2016). However, other 3-D sea-ice physical models, such as the LIM model used in the present study, do not resolve multi vertical layers (only 2 sea-ice layers), hence vertically resolving sea-ice BGC seems impractical. We revised Section 2.3 to explain this point and acknowledge the fact that biomass above the bottom ice layer can be substantial (P7 L5):

"Sea-ice biogeochemical processes are assumed to take place in a layer of fixed thickness at the ice base. Hence, this bottom- ice biogeochemical layer is not explicitly modelled and does not correspond to one of the two ice layers in LIM. Although algal biomass in ice core samples above this layer can be substantial (e.g., Melnikov et al., 2002; Olsen et al., 2017), resolving vertical distributions of sea-ice biogeochemistry in 3-D models is computationally impractical at present."

Jeffery et al. (2016): Biogeochemistry of Cice: The Los Alamos Sea Ice Model Documentation and Software User's Manual Zbgc_colpkg Modifications to Version 5

3) Why testing the model for a period when available data is much less than in recent years and, therefore, it becomes much more difficult to properly evaluate model performance? In fact and with regard to the biogeochemical data, author's comparisons with other data sources may be biased by the differences in the temporal frames of various studies.

We agree that the model can be better evaluated for more recent period than the period considered in

the present study. We extended our simulation up to 2015 and evaluated with more recent observational data (Hayashida 2018, PhD thesis), but these results are planned to be published as separate papers considering the contents of the present study, which is intended as a model description paper. We revised the manuscript to clarify these points (P2 L31):

"We note that this study is intended as a model description paper, and the analysis focuses on results for the year 1979, corresponding to the end of a decadal model spin up. The analysis of the simulation beyond 1979, in which more observational data are available for evaluation (Hayashida 2018b), is planned to be published as a journal article separately."

Hayashida, H. (2018): Modelling sea-ice and oceanic dimethylsulfide production and emissions in the Arctic, PhD thesis, University of Victoria, Victoria, BC, Canada, http://dspace.library.uvic.ca/handle/1828/10486

References Allen, J. I., Holt, J. T., Blackford, J., & Proctor, R. (2007). Error quantification of a high-resolution coupled hydrodynamic-ecosystem coastal-ocean model: Part 2. Chlorophyll-a, nutrients and SPM. Journal of Marine Systems, 68(3-4), 381-404. doi: C2 10.1016/j.jmarsys.2007.01.005 Arrigo, K. R., Kremer, J. N., & Sullivan, C. W. (1993). A Simulated Antarctic Fast Ice Ecosystem. JOURNAL OF GEOPHYSICAL RESEARCH, 98, 17. Duarte, P., Assmy, P., Hop, H., Spreen, G., Gerland, S., & Hudson, S. R. (2015). The importance of vertical resolution in sea ice algae production models. Journal of Marine Systems, 145, 69-90. doi: 10.1016/j.jmarsys.2014.12.004 Melnikov, I. A., Kolosova, E. G., Welch, H. E., & Zhitina, L. S. (2002). Sea ice biological communities and nutrient dynamics in the Canada Basin of the Arctic Ocean. Deep-Sea Research Part I-Oceanographic Research Papers, 49(9), 1623-1649. doi: Pii S0967-0637(02)00042-0 Doi 10.1016/S0967-0637(02)00042-0 Olsen, L. M., Laney, S. R., Duarte, P., Kauko, H. M., Fernandez-Mendez, M., Mundy, C. J., . . . Assmy, P. (2017). The seeding of ice algal blooms in Arctic pack ice: The multiyear ice seed repository hypothesis. Journal of Geophysical Research-Biogeosciences, 122(7), 1529-1548. doi: 10.1002/2016JG003668 Pogson, L., Tremblay, B., Lavoie, D., Michel, C., & Vancoppenolle, M. (2011). Develop- ment and validation of a one-dimensional snow-ice algae model against observations in Resolute Passage, Canadian Arctic Archipelago. Journal of Geophysical Research- Oceans, 116. doi: Artn C04010 10.1029/2010jc006119 Vancoppenolle, M., Goosse, H., de Montety, A., Fichefet, T., Tremblay, B., & Tison, J. L. (2010). Modeling brine and nutrient dynamics in Antarctic sea ice: The case of dissolved silica. Journal of Geophysical Research-Oceans, 115. doi: Artn C02005 10.1029/2009jc005369

Please also note the supplement to this comment: https://www.geosci-model-dev-discuss.net/gmd-2018-191/gmd-2018-191-RC2- supplement.pdf

Please see https://www.geosci-model-dev-discuss.net/gmd-2018-191/gmd-2018-191-AC2-supplement.pdf where we added our responses to the referee's comments/corrections.

Interactive comment on Geosci. Model Dev. Discuss., https://doi.org/10.5194/gmd-2018-191, 2018.

Referee 3

Interactive comment on "CSIB v1: a sea-ice biogeochemical model for the NEMO community ocean modelling framework" by Hakase Hayashida et al.
Anonymous Referee #3
Received and published: 4 October 2018
Geoscientific Model Development Discussions (Ms. No. gmd-2018-191) Title: CSIB v1: a sea-ice biogeochemical model for the NEMO community ocean modelling framework Authors: Hakase Hayashida, James R. Christian, Amber M. Holdsworth, Xianmin Hu, Adam H. Monahan, Eric Mortenson, Paul G. Myers, Olivier G. J. Riche, Tessa Sou, and Nadja S. Steiner

#Summary
The authors described a newly developed 3-D sea ice biogeochemical model embedded on the pan-Arctic NEMO and CanOE framework and then evaluated its basic performance with available validation datasets. Several sensitivity experiments were also performed to verify unknown parameter values such as shortwave absorption in the snow surface layer and light shading effect of ice algae. The paper was well written, and most parts of the presented analyses are quite reasonable. On the other hand, the target period of 1970s seems to be too old and short for model evaluation with reliable observational data. Computational cost should not be a primary reason because a simulation for more recent years can also be performed in the same manner. If there are another circumstances, please explain specifically.

We thank the referee for his/her positive and helpful comments on our manuscript. We revised the manuscript to reflect the referee's suggestions as much as possible. Below, we provide our responses to the referee's comments, including the responses to the questions posed in the #Summary section.

#Major Comments
One of my major concerns is that the model target period for 1969-1979 is so old. Such an experiment is regarded as a spin-up one but is not usually chosen for main analyses due to lower accuracy of atmospheric forcing datasets and lack of field measurements. In addition, most results in the sensitivity experiments are seen only in 1979. Hence potential readers cannot judge whether the presented anomalies are typical or unique features. The authors may have insufficient computational resource. Even in that case, they can run the model for more recent years (e.g., from 2000 or 2010) and/or use decadal mean forcing (e.g., 1990s or 2000s). Then discussion with decadal changes would provide more interesting scientific findings. Is it impossible?

We agree that the model can be better evaluated for the more recent period than the period considered in the present study. We did in fact conduct the simulation up to 2015 and performed a detailed evaluation with more recent observational data (Hayashida 2018b PhD thesis). We initially had planned one publication combining the technical information and the full evaluation of model variables, but the amount of information was simply too much to put it into one paper. Hence, we revised it to have one initial paper including the model description as well as several technical aspects (sensitivity experiments) focusing on the spinup period and one paper with detailed evaluation and science content covering the time period 1979-2015. We revised the manuscript to clarify these points (P2 L31):

"We note that this study is intended as a model description paper, and the analysis focuses on results for the year 1979, corresponding to the end of a decadal model spin up. The analysis of the simulation

beyond 1979, in which more observational data are available for evaluation (Hayashida 2018b), is planned to be published as a journal article separately."

Hayashida, H. (2018): Modelling sea-ice and oceanic dimethylsulfide production and emissions in the Arctic, PhD thesis, University of Victoria, Victoria, BC, Canada, http://dspace.library.uvic.ca/handle/1828/10486

Second concern is that the authors show GPP for ice algae and NPP for phytoplankton. It is a little confusing. I know that some reasons are described in the manuscript and that their difference is minor. However, I expect that the authors rerun their model to produce NPP for ice algae or GPP for phytoplankton. It is important to reduce extra cares for potential readers throughout the manuscript.

We appreciate the concern raised by the referee regarding GPP vs NPP. We re-visited the literature and also had discussions with colleagues, and we are now convinced that the first (source) term in the model equation for ice algae is representative of NPP for ice algae. In other words, we now consider what we considered GPP in the original manuscript as NPP. The logic for this decision is as follows:

The specific growth rate of ice algae (d^-1) prescribed in our model is based on Eppley (1972), who derived this parameter based on measurements of particulate matter production. From Sakshaug et al. (1997) and Hashimoto et al. (2005) (quoted below), it is understood that particulate matter production is a measure closer to NPP than GPP. Therefore, we consider that the first term in the model equation for ice algae, the product of growth rate and biomass, as NPP.

"*Net primary productivity is related to the 'growth rate', which can be defined as the net turnover rate for particulate carbon (not including production of DOC), provided that the cells are in steady-state (balanced) growth (Eppley, 1981)*". --Sakshaug et al. (1997)

"*Generally, the primary production is estimated from the rate of uptake of inorganic carbon into particulate carbon and/or the rate of evolution of oxygen into the water. In incubations of 24 h, the former method is considered to provide the values closest to net primary production (NPP), while the latter comes closest to gross primary production (GPP) (e.g., Falkowski and Raven 1997).*" -- Hashimoto et al. (2005)

Eppley (1972): Temperature and phytoplankton growth in the sea.
Sakshaug et al. (1997): Parameters of photosynthesis: definitions, theory and interpretation of results.
Hashimoto et al. (2005): Relationship between net and gross primary production in the Sagami Bay, Japan.

As a result of this decision, we revised the manuscript to replace GPP with NPP for ice algae and also revised Section 2.5.3 (Output) where we describe NPP (P13 L10):

"Ice algal NPP is assumed to equal the growth term in the model equation (Mortenson et al., 2017), as the specific growth rate associated with that term is derived from Eppley (1972). This rate is a measure of particulate production, which is considered to provide values closer to NPP than gross primary productivity (GPP) (e.g., Sakshaug et al., 1997; Hashimoto et al., 2005). Thus, the loss due to respiration is implicitly included in the growth term in the model equation for ice algae."

#Detailed Comments
[Introduction] >Line 6 in Page 2 Terminology of "mechanistic model" is unfamiliar, at least for me.

“Numerical model” is more standard, right?

We replaced ‘mechanistic’ with ‘process-based’. ‘process-based’ distinguishes the model from other numerical models such as statistical models.

[Section 2] >Section 2.3 What are “unresolved (eddy diffusion) motions of sea ice” described here. I know that eddy diffusion in ocean models represents sub-grid seawater exchange driven by mesoscale eddies. However, lateral exchange of (solid) sea ice packs due to eddy activity hardly occurs except a part of marginal ice zones. Some sea ice models adopt eddy diffusion only to damp numerical instability depending on advection schemes. Do the authors assume other physical processes in the central Arctic for this term? I find a sentence “Readers are referred to Vancoppenolle et al. (2012)”. But I appreciate that the authors explain more details, because a sensitivity experiment related with “eddy diffusion” term is presented in this manuscript.

As described by the reviewer, the diffusion term in the LIM model is designed to dampen numerical instabilities but can also be considered as turbulent-like component of sea ice motion. We revised this section accordingly (P7 L21):

“Diffusion, on the other hand, is represents transport by unresolved motions (random component of sea-ice motion analogous to turbulence in fluids; Thorndike, 1986; Rampal et al., 2009, 2016), and is often tuned to improve numerical stability.”

>Section 2.3.3 Let me confirm whether ambient temperature controlling algal growth rate is kept at a freezing point of underlying seawater or not.

It is set to the temperature of underlying seawater. We revised the manuscript to clarify this (P8 L14):

“The growth rate of ice algae is dependent on ambient temperature (of underlying seawater),“

[Section 3]
>Line 21 in Page 18 Please correct a unit of Dupont’s PP.

Revised as suggested.

>Line 1 in Page 20 What kinds of formulation or parameters are necessary to represent mat and stand contributions? Why did not the authors consider them in the present model?

By mat and strand communities, we are referring to macroscopic ice-algal aggregates (e.g. *Melosira arctica*) that are different from ice-algal blooms not just in terms of size but also in terms of physiology (Assmy et al. 2013). Therefore, we would need to add another state variable in order to represent mat and strand communities. We did not consider them in the present model because their contribution to the pan-Arctic NPP is negligible compared to ice-algal blooms because of their limited area coverage (Assmy et al. 2013). Given this finding, the old estimates by Legendre et al. (1992) quoted in the manuscript are quite speculative also knowing the underlying assumption in their estimates (discussed in detail in Deal et al. 2011). We included this discussion in the revised manuscript for clarification (P19 L8):

“Although the upper end accounts for contribution from mat and strand communities that are not represented in our model, their contribution to the pan-Arctic production should be small as their

spatial distribution is generally localized (e.g., Assmy et al., 2013)."

Assmy et al. (2013): Floating ice-algal aggregates below melting Arctic sea ice. PLOS ONE.

[Section 4]
>Section 4.1 (EXP1 and 2) It took a time for me to understand the purpose of these sensitivity experiments. Is it right that CORE-II provides only monthly mean data for snowfall and that DFS snow- fall has daily mean time series only from 1979? Has daily climatology for 1979-2012 been used in the case of simulation before 1978? If yes, a simulation for more recent years does not cause this problem. Anyway, I recommend that the authors explain backgrounds for this analysis more clearly. In addition, this subsection describes only snow depth comparison. How about impacts of forcing choice on ice algal PP?

Yes, CORE-II provides only monthly mean data, while DFS provides daily mean data for individual years from 1979 and daily-climatological mean data prior to 1979. We revised the manuscript to clarify the purpose of these sensitivity experiments (P20 L12):

"Note that the temporal resolution of the snowfall and total precipitation fields in the CORE-II dataset is monthly. In EXP2, the snowfall and total precipitation fields over the period 1969-1978 are replaced by their respective 1979-2012 daily climatological values as in the original DFS dataset (Dussin et al., 2016). Comparing between EXP0 and EXP1 allows us to assess the impacts of atmospheric forcing (DFS vs CORE-II), while comparing between EXP1 and EXP2 allows us to assess the impacts of snowfall dataset (daily vs daily climatology) on modelled snow depth."

The impacts of forcing choice on ice algal PP were not assessed because we think that models should simulate reasonable snow depth before incorporating sea-ice biogeochemistry, as snow is a driver for light-limited ice algal growth. While we expect that EXP1 and EXP2 would have resulted in higher ice algal PP, quantifying these would not be so valuable because snow depth was not simulated realistically.

>Section 4.2 (EXP3) It may cause misleading that "Using these higher i0 reduces light limitation, and hence enhances ice algal primary production", even though light penetration through snow column is overestimated. Since formulation and parameter values of light limitation term largely differ between models as described in the previous paragraph, light intensity at the skeletal layer is not always directly linked to ice algal PP. I recommend that the authors describe this part more carefully.

As suggested by the referee, we revised the manuscript to describe this part more carefully (P23 L30):

"The overall impact of i0 on ice algal production depends on the choice of formulation and parameter(s) for the light limitation function as discussed previously."

>Section 4.3 (EXP4) Why is "space opening" necessary for new ice algal growth? It can also be considered that higher algal biomass causes higher PP as long as nutrient is available. Please explain a limitation factor. As mentioned above, the authors should specify more detailed processes of "eddy diffusion" of sea-ice biogeochemical state variables. In addition, can individual impact of this eddy diffusion term be estimated? Sea ice drift patterns also have large interannual variability depending on wind stress fields. Therefore, I am afraid that the presented anomalies in a single year are not representative in the pan-Arctic region.

Space opening helps ice algal growth because the ice algal loss term has quadratic dependency on biomass. Hence, the growth is more efficient at lower biomass. We agree with the referee that the nutrient advection can further promote higher PP in the productive regions, which may partly explain the no change in the nitrate concentration in these region (Fig. 14c in the revised manuscript). We revised the manuscript to clarify these two possible explanations (P26 L13):

"One possible explanation for these spatial differences is that the horizontal transport of sea ice takes ice algae out of regions of high productivity into regions of low productivity. This allows more efficient growth by maintaining the loss due to viral infection and aggregation (represented by the quadratic mortality term in the model) at relatively low values in the productive regions. Another factor is the horizontal transport of nutrients into these regions which are taken up by ice algae and results in the further increase in ice algal production."

As mentioned in the response above, we described sea-ice diffusion more carefully. Here, the focus is on the horizontal transport of sea ice (advection + diffusion) rather than advection vs diffusion, therefore, we did not save and evaluate model output for individual contributions. We agree that the interannual variability can be large due to wind stress fields, and therefore our results are not representative of long-term average. However, the quantities we presented are representative of the pan-Arctic average (for a particular year and using particular forcing and model). We revised the manuscript to note on the interannual variability (P26 L6 as well as P30 L9):

"However, we note that these values could be quite different in other years given the large interannual variability in wind stress fields driving sea ice drift patterns." (P26 L6)

"While we believe that these findings would be qualitatively similar in other years, it would be worthwhile to quantify their interannual variability." (P30 L9)

>Section 4.4 (EXP5) I do not understand that "the reduction in nutrient drawdown under regions of large ice algal biomass enhances nutrient advection into regions of low ice algal biomass". Why is nutrient advection enhanced by biogeochemical processes? Definition of bloom onset using bottom-ice PAR looks unnatural for me, because under-ice NPP is also calculated in the present model. The authors may try to compare with Castellani et al. (2017) more directly. But the target year is quite different between two studies so that this information is not so valuable.

We did more analysis on this and found that nutrient limitation is already so high in these regions of increased NPP that additional supply via advection should not have an impact. We then found that the NPP increase is dominated by small phytoplankton, but the reasons for this response of the modelled ecosystem to a perturbation to light are unclear. In the revised manuscript, we removed the possible explanation about nutrient, added a figure showing the increase in NPP dominated by small phytoplankton, and revised the text accordingly (P26 L29):

"However, in some regions, shading results in a slight increase in under-ice NPP which is dominated by small phytoplankton (Figure 16c). The underlying mechanisms for this response of the modelled ecosystem to a perturbation to light are unclear."

Definition of bloom onset using bottom-ice PAR was used in this analysis in order to directly compare with Castellani et al. (2017). We revised the manuscript to note the difference in the target year between the two studies (P28 L8):

"Furthermore, direct comparison is difficult due to the difference in the target year of simulation; Castellani et al. (2017) simulated 2012, while we consider 1979."

[Section 5]
>Line 5 in Page 30 Again, validation in a single old year is insufficient to appeal the model performance, especially in terms of sea ice volume and extent.

We agree with the referee that a single year comparison is not sufficient to appeal the model performance; this is left for future studies as noted in our response to the referee's major comment 1. We revised the manuscript accordingly (P28 L32):

"Results of the reference simulation (EXP0) were discussed and compared with previous studies, with a focus on the year 1979; more thorough evaluation of the model performance over the recent decades is planned for future studies."

[Figure]
>Spatial maps I recommend that names of major countries or cities are overlaid.

We revised Figure 5 to add names of major countries/regions.

>Time Series Values of vertical axis should be smart (e.g., every 1 or 10).

We modified the vertical axis of the time series to be spaced uniformly throughout the manuscript.

>Figure 3 Magenta contours are hardly distinguishable from red contours.

We replaced the magenta with cyan and removed the 3000 m isobath, as such detail is not needed for the paper.

>Figure 4 Is total number of vertical layer same between NAA1 and NAA6 versions (i.e., 46 layers)? This figure is confusing. How about replacing vertical axis to water depths?

Yes, the total number of vertical layer is the same (46 layers) between the two configurations. The figure below shows the case where the vertical axis is replaced by water depths. We don't think that this figure is particularly better than the original figure. Comparing each layer between the two configurations in the original figure clearly demonstrates the point that NAA1 has finer resolution than NAA6, so we keep the figure unchanged.

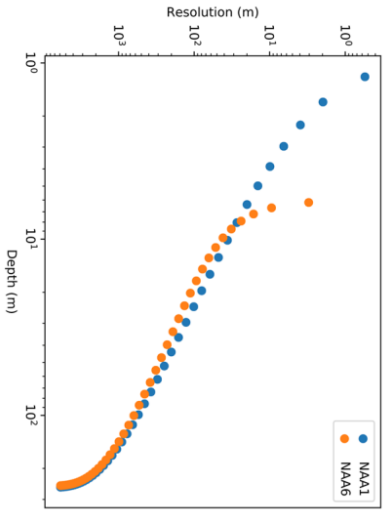

>Figure 6 Although area total amounts are shown in Figure 5, why are only GPP and NPP values in this figure plotted using "per unit area"? I think that the pan-Arctic average value is meaningless because of large spatial variability.

We agree that there is inconsistency in the representation of GPP and NPP between Fig5 and Fig6. However, we argue that either of these (areal integral or areal average) provides the same information about temporal variability by definition (areal integral = areal average * area of Arctic Circle, in this context), and therefore we do not think that they need to be changed especially since there is no observation data to compare the areal integral of GPP or NPP on a seasonal scale (e.g. m-2 d-1). As for the interannual time series (Fig5 in the submitted manuscript), we used annual areal integrals to compare with previous studies (as discussed in the manuscript).

>Figure 10 Please insert a zero line in (b). And I am wondering why the 1-m average minus the 12-m average shows negative for most periods.

We inserted a horizontal line at y = 0 in Fig10b. Regarding the second point, the caption was incorrect; it should have been 12-m average minus 1-m average. We appreciate the referee for catching this error. Both the figure and the caption were revised accordingly.

>Figure 16 Contrast of a color bar in (c) seems to be weak.

We changed the colormap to show more contrast in the revised manuscript.

[Table]
>Table 3 Unit of eddy diffusivity should be mˆ2/s.

Revised as suggested.

Interactive comment on Geosci. Model Dev. Discuss., https://doi.org/10.5194/gmd-2018-191, 2018.

CSIB v1: a sea-ice biogeochemical model for the NEMO community ocean modelling framework

Hakase Hayashida[1,2], James R. Christian[3,1], Amber M. Holdsworth[3], Xianmin Hu[4], Adam H. Monahan[1], Eric Mortenson[1], Paul G. Myers[5], Olivier G. J. Riche[3], Tessa Sou[3], and Nadja S. Steiner[3,1]

[1]School of Earth and Ocean Sciences, University of Victoria, Victoria, British Columbia, Canada
[2]*Now at Institute for Marine and Antarctic Studies, University of Tasmania, Hobart, Tasmania, Australia
[3]Fisheries and Oceans Canada, Institute of Ocean Sciences, Sidney, British Columbia, Canada
[4]Fisheries and Oceans Canada, Bedford Institute of Oceanography, Dartmouth, Nova Scotia, Canada
[5]Department of Earth and Atmospheric Sciences, University of Alberta, Edmonton, Alberta, Canada

Correspondence to: Nadja Steiner (nadja.steiner@canada.ca)

Abstract. ~~Numerical~~ Process-based models are a useful tool for studying marine ecosystems and associated biogeochemical processes in ice-covered regions where observations are scarce. To this end, CSIB v1 (Canadian Sea-ice Biogeochemistry version 1), a new sea-ice biogeochemical model has been developed and embedded into the Nucleus for European Modelling of the Ocean (NEMO) modelling system. This model consists of a three-compartment (ice algae, nitrate, and ammonium) sea-ice ecosystem and a two-compartment (dimethylsulfoniopropionate and dimethylsulfide) sea-ice sulfur cycle which are coupled to pelagic ecosystem and sulfur-cycle models at the sea ice-ocean interface. In addition to biological and chemical sources and sinks, the model simulates the horizontal transport of biogeochemical state variables within sea ice through a one-way coupling to a dynamic-thermodynamic sea-ice model (LIM2~~). This paper describes technical aspects of implementing sea-ice biogeochemistry into NEMO and provides~~ ; the Louvain-la-Neuve sea Ice Model version 2). The model results for 1979 (after a decadal spin-up) are presented and compared to observations and previous model studies for a brief discussion on the ~~results of several model experiments. Results of~~ model performance. Furthermore, this paper provides discussion on technical aspects of implementing the sea-ice biogeochemistry and assesses the ~~reference simulation were evaluated by comparing the model outputs to observations and previous modelling studies. Additional simulations were conducted to assess the~~ model sensitivity to 1) the temporal resolution of the snowfall forcing data, 2) the representation of light penetration through snow, 3) ~~advective and eddy-diffusive~~ the horizontal transport of sea-ice biogeochemical state variables, and 4) light attenuation by ice algae. The sea-ice biogeochemical model has been developed within the generic framework of NEMO to facilitate its use within different configurations and domains, and can be adapted for use with other NEMO-based submodels such as LIM3 ~~and PISCES~~(the Louvain-la-Neuve sea Ice Model version 3) and PISCES (Pelagic Interactions Scheme for Carbon and Ecosystem Studies).

1 Introduction

Biogeochemical processes at the sea ice-ocean interface play an active role in polar marine ecosystems and global cycling of important chemical elements and compounds. For example, microalgae that ~~heavily~~ colonize the base of sea ice in spring can have a strong influence on ~~the~~ primary production of ~~underlying~~ phytoplankton through light attenuation, nutrient drawdown, and seeding as well as on ~~the~~ secondary production by ~~being the~~ providing a food source for ~~pelagic and benthic grazers~~ grazers (Arrigo, 2014). Furthermore, these ecological processes regulate the production and removal of greenhouse gases (e.g., carbon dioxide and nitrous oxide) and other climatically-important gases (e.g., dimethylsulfide) in ice-covered regions, and the exchange of these gases with the overlying atmosphere ~~(~~(Vancoppenolle et al., 2013).

However, our current understanding of many of these processes remains limited due to both logistical and technical challenges for field observations ~~(Miller et al., 2015). Mechanistic~~ (Miller et al., 2015). Process-based models representing sea-ice biogeochemistry can both fill gaps between sparse measurements and aid in the interpretation of these measurements. Furthermore, these models can be used in systematic intercomparisons that can build confidence in our understanding of polar marine science such as has been done for pelagic ecosystem models ~~(e.g. Popova et al., 2012; Jin et al., 2015)~~(e.g., Popova et al., 2012; Jin et al., 2

.

Although considerable effort has been invested in developing ~~mechanistic~~ process-based models for sea-ice ~~bigeochemistry~~ biogeochemistry over the last three decades following the pioneering work of Arrigo et al. (1991), most of these models were applied in one-dimensional (1D) ~~framework~~ frameworks, and the results are therefore ~~applicable only to a particular location of interest~~ limited to particular locations (see Vancoppenolle and Tedesco, 2016). Only a few of these models have been applied in three-dimensional (3D) framework coupled to either a regional or global sea ice-ocean general circulation model (see Table ~~1~~1 for a list of 3D model configurations developed for pan-Arctic studies). More efforts toward developing such 3D sea-ice biogeochemical models are needed to better understand the large-scale variability in biogeochemical processes within sea ice and their role in underlying pelagic and benthic ecosystems.

In this study, we present CSIB v1 (Canadian Sea-Ice Biogeochemistry version 1), a new sea-ice biogeochemical model implemented into the Nucleus for European Modelling of the Ocean (NEMO), a state-of-the-art modelling framework for oceanographic research (www.nemo-ocean.eu). To the best of our knowledge, Tedesco et al. (2017) is the only previous study in which a sea-ice biogeochemical model has been coupled to NEMO. However, the coupling ~~was~~ is done in an offline configuration in that study. An important advance of the present study is that the model is written within the NEMO code to allow in-line coupling (i.e., physical dynamics are computed simultaneously with biogeochemistry) and the computation of ~~the~~ horizontal transport of sea-ice biogeochemical state variables associated with sea ice drift. These implementations allow more realistic simulation of sea-ice biogeochemistry and intercomparison of process-based ice algae models. The main objectives of the present study are to: describe the development of the coupled model in a pan-Arctic configuration (Section ~~2~~2); ~~evaluate the results of a multi-year reference~~ present the basic feature of the simulation (Section ~~3~~3); and assess the model sensitivity to modifications of parameters and parameterizations (Section ~~4~~4). Key findings of the present study are summarized in Section ~~5.~~5. We note that this study is intended as a model description paper, and the analysis focuses on results for the year 1979,

Table 1. Comparison of pan-Arctic 3D sea-ice biogeochemical model configurations developed in various framework. dx: the horizontal resolution; dzo: the vertical resolution of the uppermost water column; dzi: the ~~thickness~~ vertical extent of ~~ice algal skeletal~~ the biologically-active layer at ice base; i_0 (snow surface): the fraction of incoming shortwave radiation ~~which~~ that penetrates through the snow surface; Shading: ~~the~~ attenuation of light by ice algae; ~~and~~ Runoff: ~~the~~ river discharge of nitrate.

Reference	Framework	dx	dzo	dzi	~~$i_{0,snow}$~~ i_0 (snow surface)	Shading	Runoff
Dupont (2012)	MOM	~ 50 km	3.45 m	5 cm	0	no	yes
Jin et al. (2012)	POP	~ 40-50 km	10 m	3 cm	0	no*	no*
Watanabe et al. (2015)	COCO	~ 5 km	2 m	2 cm	1*	no	no*
Castellani et al. (2017)	MITgcm	~ 28 km	10 m	5 cm	0.3	yes	no
This study ~~(EXP0)~~	NEMO	10-14.5 km	1 m	3 cm	0.15	yes	no

*Confirmed through personal communication with the lead author.

corresponding to the end of a decadal model spin up. The analysis of the simulation beyond 1979, in which more observational data are available for evaluation (Hayashida, 2018b), is planned to be published as a journal article separately.

2 Model description and setup

The fundamental constituents of NEMO are the following three submodels: ocean physics, sea-ice physics, and ocean biogeochemistry. In the present study, we adopted version 3.4 of NEMO (NEMO v3.4; Madec, 2008) and developed within it an additional submodel, sea-ice biogeochemistry. Technical details on the code structure of the model developed in this study are provided in Appendix A for those who are interested in using the newly-added sea-ice biogeochemical model.

2.1 Ocean and sea ice physics (OPA-LIM2)

The physical ocean submodel is the Océan PArallélisé (OPA), which is a free-surface, hydrostatic, primitive-equation model developed for regional and global ~~ocean circulation studies~~ ocean circulation studies (Madec, 2008). OPA is coupled to the submodel for sea-ice physics, namely the Louvain-la-Neuve sea Ice Model (LIM). The present study uses version 2 of LIM (LIM2; Fichefet and Maqueda, 1997; Bouillon et al., 2009) , consisting of a three-layer (one for snow and two for ice) dynamic-thermodynamic model.

To model ambient light available for ice algae and under-ice phytoplankton properly, we modified the module ~~which~~ that computes the shortwave radiative transfer through snow and sea ice as shown schematically in Figure 1. In this module, the unreflected fraction (1-a) of the incoming shortwave radiation (F_{sw}) is parameterized as either being absorbed within a thin layer of surface snow and/or ice ~~(defined as having thickness of~~ or penetrating below this layer. This thin layer at the surface is known as the surface scattering layer (SSL; Grenfell and Maykut, 1977), and is defined in the model as the uppermost 10 cm of snow and/or ice column in NEMO v3.4~~) or penetrating through the snow and/or ice interior underneath this layer. This~~ . When the sum of snow depth and ice thickness is less than 10 cm, the SSL equals this total thickness. The penetrating fraction

is determined by ~~a coefficient , i_0,~~ the coefficient i_0, which is set to zero ~~for snow surface~~ in the presence of snow in the default configuration of LIM2 following Maykut and Untersteiner (1971). While this assumption of complete blockage of light may be a reasonable approximation for thermodynamic processes of snow and sea ice, ~~this approximation~~ it is problematic for modelling sea-ice biogeochemistry. Specifically, the assumption implies that primary producers can not photosynthesize until snow disappears completely, which is inconsistent with the findings of many field observations that measure high algal biomass at the base of snow-covered sea ice ~~(e.g. Leu et al., 2015)~~(e.g., Leu et al., 2015). Furthermore, i_0 for snow surface has been set to non-zero values in other sea-ice models in the case of thin or melting snow (Flato and Brown, 1996; Abraham et al., 2015). For these reasons, we use a non-zero value of ~~i_0~~ i_0 for snow surface and parameterize the light transmission through the snow column below the specified surface layer following the Beer-Lambert law. The value of i_0 for snow surface was set to 0.15 following the 1D sea-ice biogeochemical modelling work of Vancoppenolle et al. (2010). The attenuation coefficient of snow was set to 10 m^{-1}, which falls within the observed range for melting and freezing snow ~~(Grenfell and Maykut, 1977) . The model~~ (Grenfell and Maykut, 1977). Model sensitivity to i_0 for snow surface is discussed in Section 4.2.

2.2 Ocean biogeochemistry (CanOE)

The submodel for ocean biogeochemistry adopted in the present study is the Canadian Ocean Ecosystem Model (CanOE), developed by the ocean modelling group at the Canadian Centre for Climate Modelling and Analysis ~~(Christian et al, in prep.).~~ (Christian et al, in prep.; see Appendix A3 of Hayashida, 2018b). This model has been developed for the latest version of the Canadian Earth System Model (Arora et al., 2011), which will be used in the next phase of the Coupled Model Intercomparison Project (CMIP6). CanOE simulates the lower trophic levels of marine ecosystems (nutrients, phytoplankton, zooplankton, and detritus) and biogeochemical cycling of key elements (carbon, oxygen, nitrogen, and iron). This model is built around the basic code structure of the Pelagic Interactions Scheme for Carbon and Ecosystem Studies (PISCES) version 2, the default submodel for ocean biogeochemistry of NEMO (Aumont et al., 2015). One advantage of CanOE over PISCES is that it is computationally ~~more efficient~~ less expensive as a result of having fewer state variables (19 vs 24) and fewer computationally expensive parameterizations ~~(Christian et al, in prep.).~~ (Christian et al, in prep.; see Appendix A3 of Hayashida, 2018b). In the present study, we made two modifications to CanOE. The first modification is the addition of an ocean sulfur-cycle model and the second modification is the parameterization of the photosynthetically active radiation (PAR).

2.2.1 Addition of an ocean sulfur cycle

Figure 2 shows a schematic of CanOE including the ocean sulfur cycle and the sea-ice biogeochemistry. ~~The sulfur cycle model consists~~ Here, the sulfur cycle is restricted to sources and sinks of two state variables: dissolved dimethylsulfoniopropionate (DMSPd) and ~~dimethylsulfide (DMS)~~DMS. The ocean sulfur cycle is one-way coupled to CanOE as ~~sulfur cycle processes~~ the sources and sinks of DMSPd and DMS depend on the ~~state of the ecosystem~~conditions of primary and secondary producers, but not vice versa. The ocean sulfur-cycle model is based on Hayashida et al. (2017) with the following two modifications. First, the cellular DMSP content of modelled phytoplankton is derived from their carbon content as opposed to the chlorophyll content as in Hayashida et al. (2017). This change was made because there are more observation-based estimates of the intracellular

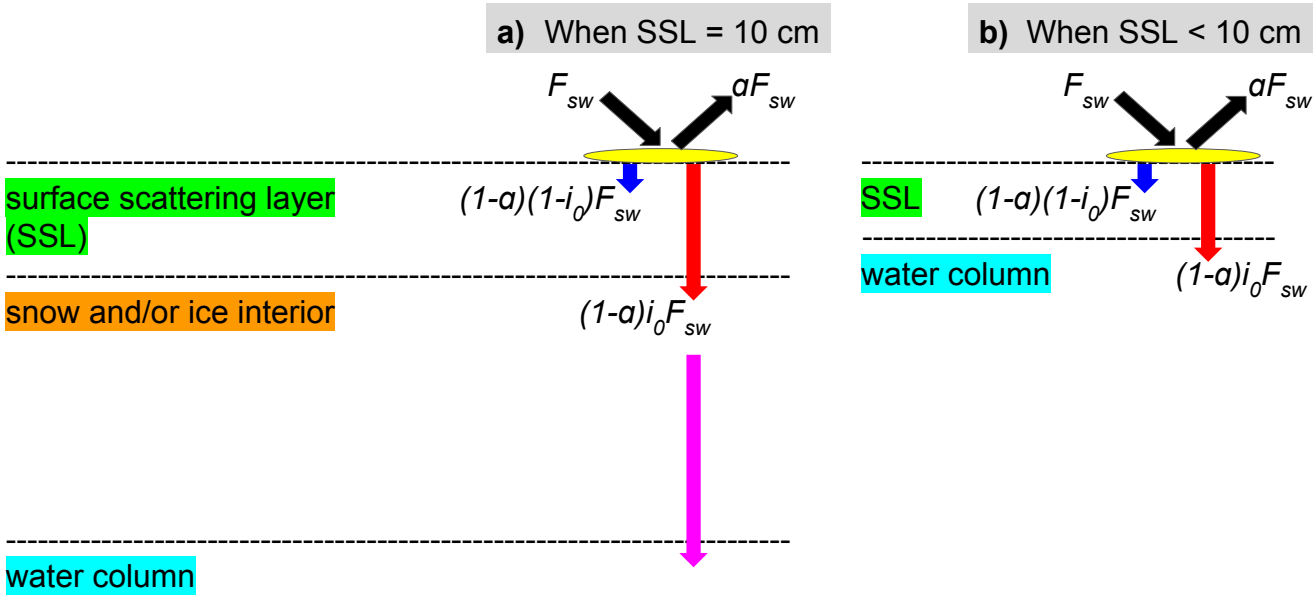

Figure 1. Shortwave radiative transfer through snow and sea ice ~~modified from Figure 3.4 of Vancoppenolle et al. (2012)~~in the LIM2/LIM3 model. ~~F_{sw}~~ F_{sw} represents the incoming shortwave radiation, a fraction of which is reflected due to the surface albedo of snow or ice (a). The remaining ~~fraction~~ radiation is either absorbed within the ~~surface thin layer~~ SSL (~~$(1-a)(1-i_0)F_{sw}$~~ $(1-a)(1-i_0)F_{sw}$; blue arrows) or penetrates below the SSL ($(1-a)i_0F_{sw}$; red arrows). a) When the SSL is 10 cm, the radiation penetrating into the snow and/or ice interior which attenuates following the Beer-Lambert law and reaches the water column ~~below this layer~~ (~~$(1-a)i_0F_{sw}$~~ magenta arrow). b) When the SSL is less than 10 cm, the penetrating radiation directly reaches the water column. Modified from Figure 3.4 of Vancoppenolle et al. (2012)

DMSP-to-carbon (DMSP:C) ratio ~~has been considered more thoroughly in observations~~ than the DMSP-to-chlorophyll a ratio ~~(e.g. Stefels et al., 2007)~~(e.g., Stefels et al., 2007). The DMSP:C ratios for small and large phytoplankton (respectively high and low DMSP producers) are set to 12 and 4 mmol:mol.

Also, the parameterization of sea-to-air flux of DMS was modified to account for the non-linear dependence of the flux on the open-water fraction (Loose et al., 2009):

$$F = f_{ow}^{0.4} k_{dms} DMS \quad (1)$$

where F is the DMS flux (μmol m^{-2} s^{-1}), f_{ow} is the open-water fraction (-), k_{dms} is the gas transfer velocity (m s^{-1}), and DMS (nM) is the DMS concentration in the uppermost layer of the water column.

2.2.2 Correction to the fractionation of under-ice PAR

The second modification to CanOE was made to the PAR fraction of incident solar radiation. PAR is the shortwave radiation in the 400-700 nm wavelength range, which is available for photosynthesis. In CanOE, PAR ~~reaching the sea surface~~ is 43% of the downwelling shortwave radiation reaching the sea surface, a well established estimate for PAR in open water ~~(e.g. Morel, 1988)~~ (e.g., Morel, 1988). However, this assumption underestimates PAR reaching the sea surface under sea ice. The shortwave radiation penetrating through snow and ice is almost entirely PAR, as radiation outside of the 400-700 nm range is absorbed by the snow and ice ~~(e.g. Zeebe et al., 1996)~~(e.g., Zeebe et al., 1996). Thus, we have set the fraction of the downwelling shortwave radiation to unity (instead of 43%) when computing the sea-surface PAR under sea ice.

2.3 Sea-ice biogeochemistry

The submodel for sea-ice biogeochemistry is a modified version of a three-compartment (ice algae, nitrate, and ammonium) ecosystem based on Mortenson et al. (2017) and a two-compartment (DMS and DMSPd) sulfur cycle based on Hayashida et al. (2017).

Sea-ice biogeochemical processes are assumed to take place in a layer of fixed thickness at the ice base. Hence, this bottom-ice biogeochemical layer is not explicitly modelled and does not correspond to one of the two ice layers in LIM. Although algal biomass in ice core samples above this layer can be substantial (e.g., Melnikov et al., 2002; Olsen et al., 2017), resolving vertical distributions of sea-ice biogeochemistry in 3-D models is computationally impractical at present. The governing equation for any sea-ice biogeochemical state variable is:

$$\frac{\partial X}{\partial t} = -\nabla \cdot \left(\overrightarrow{U} X\right) + D\nabla^2 X + \mathrm{SMS}\left(X\right) \tag{2}$$

where X denotes the concentration of the state variable, $\overrightarrow{U}$ denotes the horizontal velocity field of sea ice, and D denotes the horizontal eddy diffusion coefficient. The first ~~and second~~ two terms on the right hand side of Equation ~~2 represent horizontal transport by resolved (advection)and unresolved (eddy diffusion) motions, respectively~~2 represent tendencies associated with horizontal motion of sea ice (Section 2.3.1). The third term represents biological and chemical sources and sinks~~of the state variable X~~. Note that while LIM2 computes the impact of mechanical redistribution (i.e., deformation due to ridging/rafting) on sea ice physical properties, these processes are neglected in computations of the ~~sea ice biogeochemical state variable tendencies~~ sea-ice biogeochemical state variables in the present study as the model uses a simple representation of the sea-ice biogeochemical layer as a layer of fixed thickness (3 cm) at the ice base.

2.3.1 ~~Advection and diffusion~~Horizontal transport

Horizontal ~~advection and eddy diffusion~~ transport of sea-ice biogeochemical state variables ~~are~~ is computed simultaneously and in the same way as the sea ice physical properties of LIM2 (i.e., snow and sea ice volume, heat content, and areal coverage). ~~For advection, the~~ Specifically, it is done by solving the advection-diffusion equation for sea ice. Advection (by which we refer to the transport associated with the resolved motion of sea ice) is computed using the scheme of Prather (1986)~~is applied.~~

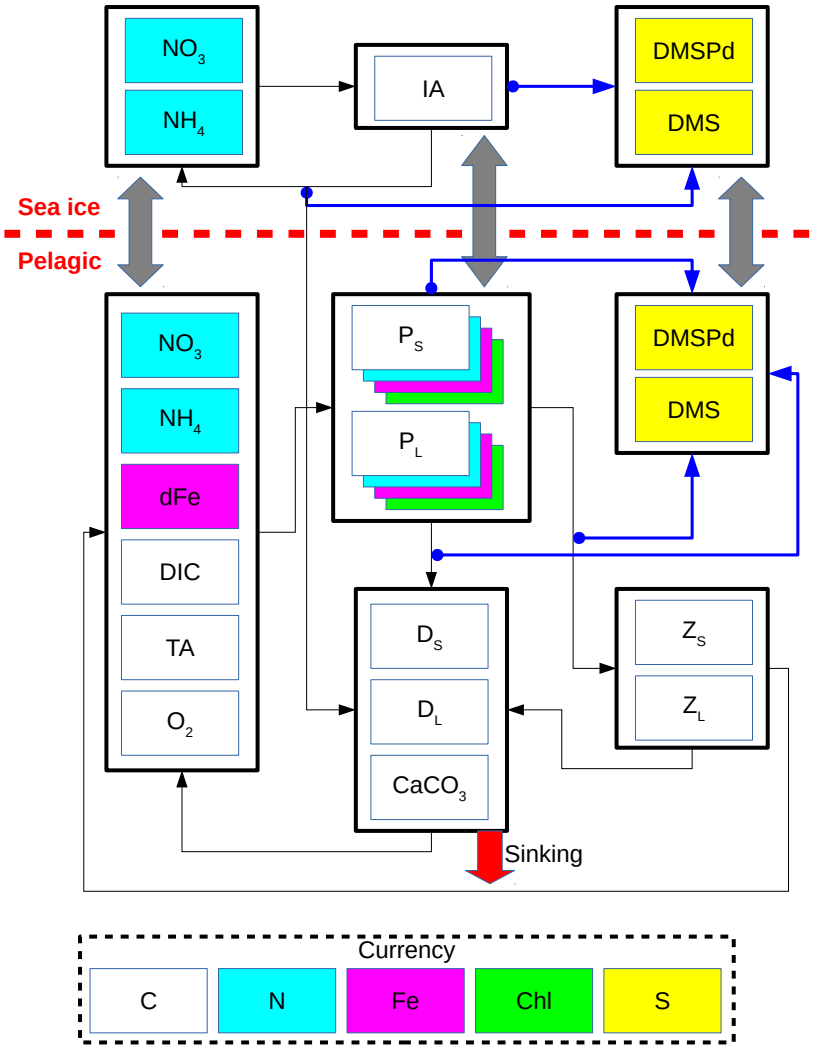

Figure 2. Schematic of the CanOE pelagic ecosystem model and associated sea-ice biogeochemistry and pelagic sulfur-cycle models. Black arrows indicate fluxes of carbon (C)/nitrogen (N)/iron (Fe) between compartments; blue arrows indicate sources of dissolved dimethylsulfoniopropionate (DMSPd); gray arrows indicate ice-ocean fluxes of nitrate (NO_3), ammonium (NH_4), ice algae (IA)/large phytoplankton (P_L), DMSPd, and dimethylsulfide (DMS). Flows of dissolved oxygen (O_2) are opposite to those of dissolved inorganic carbon (DIC) and are not explicitly illustrated. Detritus (D_S and D_L) and zooplankton (Z_S and Z_L) are denominated in C units but have implicit N and Fe pools according to fixed elemental ratios; phytoplankton (P_S and P_L) have separate state variables for each currency. O_2 and total alkalinity (TA) ~~are~~ have their own currencies, but are shown as white here for simplicity; their sources and sinks follow well established ~~stoichiometry~~ stoichiometries relative to those of DIC. Sources and sinks of TA associated with the nitrogen cycle ~~-~~(Wolf-Gladrow et al., 2007) are included but not shown in the figure. The state variables dFe and $CaCO_3$ represent dissolved iron and calcium carbonate, respectively. The currencies Chl and S represent the chlorophyll a and sulfur, respectively.

~~Eddy diffusion tendencies are computed explicitly and are~~ . Diffusion, on the other hand, represents transport by unresolved motions (random component of sea-ice motion analogous to turbulence in fluids; Thorndike, 1986; Rampal et al., 2009, 2016) , and is often tuned to improve numerical stability. Diffusion is computed within the ice pack by evaluating the second-order diffusive operator using the Crank-Nicholson scheme (Crank and Nicolson, 1996), while it is set to zero at the ice edge. The horizontal diffusion coefficient (D) is set to 5 m^2 s^{-1}, as suggested by Vancoppenolle et al. (2012). ~~Readers are referred to Vancoppenolle et al. (2012) for further description of these processes.~~ The impacts of ~~advection and diffusion on modelled sea-ice~~ horizontal transport of sea ice on modelled biogeochemical state variables are discussed in Section ~~4~~.3.

2.3.2 New ice formation

~~In case of simulated horizontal accretion (i.e. an increase in sea ice concentration due to thermodynamic growth), the~~ The bottom 3 cm of newly-formed ice is assumed to contain the same concentrations of ~~sea-ice~~ biogeochemical state variables as those in the underlying water column. Thus, the concentration (X) of any sea-ice biogeochemical state variable is updated as follows:

$$X = \frac{SIC_{t-1}}{SIC_t} X^* + \frac{SIC_t - SIC_{t-1}}{SIC_t} X_{ui} \tag{3}$$

where SIC_{t-1} and SIC_t respectively denote the sea-ice concentrations in the previous and current time step. X^* denotes the concentration of the sea-ice biogeochemical state variables (meltwater equivalent) after the computation of advection and diffusion but prior to the computation of biological and chemical sources and sinks. X_{ui} denotes the concentration of the biogeochemical state variable in the uppermost layer of the water column under the ice. Equation ~~3~~ neglects the density difference between sea ice and seawater, and therefore violates mass conservation. However, this simplification has negligible effect on ocean biogeochemistry given the relatively-thin sea-ice biogeochemical layer ~~as demonstrated in Hayashida et al. (2017)~~ (Hayashida et al., 2017). For ice algae only, a minimum biomass ~~threshold~~ is set at 10 mmol C m^{-3} in order to mimic reasonable overwintering biomass ~~(Mortenson et al., 2017).~~ . This threshold is derived based on the observed range of ice algal biomass in young sea ice (Garrison et al., 1983) and by assuming a fixed carbon-to-chlorophyll ice algal cell quota (Mortenson et al., 2017). Above the bottom sea-ice biogeochemical layer, the concentrations are set to zero for all biogeochemical tracers.

2.3.3 Biological and chemical sources and sinks

The biological and chemical processes represented as sources and sinks of the sea-ice biogeochemical state variables are described in detail in Mortenson et al. (2017) and Hayashida et al. (2017). For the ecosystem component, these processes include photosynthesis, mortality, and remineralization of dead organic matter. The growth rate of ice algae is dependent on ambient temperature (of underlying seawater), PAR, and nutrient concentrations (nitrate and ammonium). Note that the growth rate dependence on ice melt considered in Mortenson et al. (2017) has been neglected in the present study because: 1) our preliminary results indicated that ice algal blooms were generally insensitive to it; 2) the parameterization for ice melt

limitation was applied for a specific location and might not be appropriate for other locations; and 3) the parameterization lacks observational evidence.

In addition to the computation of biological and chemical sources and sinks, processes relevant to the ice-ocean fluxes are computed, including~~molecular~~ : 1) turbulent-molecular diffusive exchange of nutrients~~,~~ ; 2) release of all state variables into the water column due to basal ablation~~, and~~ ; and 3) flushing of these variables ~~through flows~~ by flow of water through the ice from rainfall and surface ~~ablation.~~

2.4 ~~Experiments~~

~~In this study, we consider six model experiments (Table 2). The first experiment is a reference simulation (EXP0), designed to be the most realistic model solution which best agrees with observations. The 11-year duration of EXP0 is considered sufficient for the spin up of sea-ice and near-surface pelagic variables based on previous Arctic biogeochemical model studies (e.g. Dupont, 2012; Jin . The setup of EXP0 is described below. The rest of the experiments (EXP1-5) are designed to assess the sensitivity of the model simulations to changes in uncertain forcing data and parameter values.~~

~~List of model experiments Name Description DurationEXP0 Reference simulation. 1969-1979EXP1 Same as EXP0 except that the atmospheric forcing was replaced by~~ melting (including flooding due to negative freeboard). For 1), the ~~CORE-II dataset. 1969-1979EXP2 Same as EXP0 except that the snowfall and total precipitation for 1969-1978 were replaced by the original DFS dataset (i.e. daily-mean climatology). 1969-1979EXP3 Same as year 1979 of EXP0 except that the light penetration through snow was impeded (i.e. i_0 was set to zero as in the original LIM2). 1979EXP4 Same as year 1979 of EXP0 except that the advection and diffusion of sea-ice biogeochemical state variables were neglected (i.e. set to zero). 1979EXP5 Same as year 1979 of EXP0 except that the shading effect of ice algae was neglected (i. e. set to zero). 1979~~effects of turbulence are approximated by parameterizing the molecular sublayer as a function of friction velocity, and molecular diffusion is calculated using the observed diffusion coefficient of dissolved silica measured in seawater at 2 °C (Rebreanu et al., 2008).

2.3.1 ~~Domain~~

2.4 Spatial domain

The model domain is based on the North Atlantic and Arctic (NAA) configuration developed by the ocean modelling group at the University of Alberta (http://knossos.eas.ualberta.ca/anha/model_configuration.php#naa). This configuration was built on the curvilinear orthogonal coordinate system of NEMO that has been successfully applied to study the freshwater budget of the Arctic Ocean in present ~~-~~(Hu and Myers, 2013) and future climates ~~-~~(Hu and Myers, 2014), as well as to investigate pelagic ecosystem processes in the Canada Basin ~~-~~(Steiner et al., 2015). The NAA domain includes the Arctic Ocean, the Canadian Arctic Archipelago, the northern Bering Sea, the ~~northern~~ North Atlantic Ocean, and the Nordic Seas (Figure ~~-~~3). The horizontal resolution of the 568 $\times$ 400 grid varies from 10 km along the North American boundary to 14.5 km along the Eurasian boundary. Vertically, the ocean is divided into 46 layers with variable resolution, from approximately 1 m in the

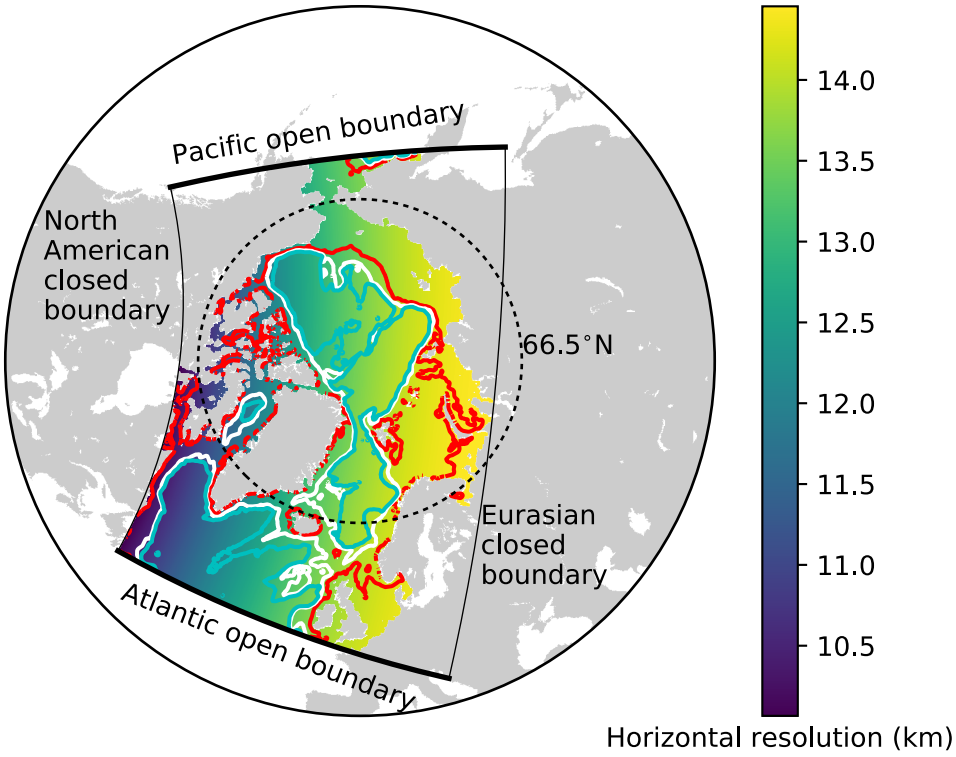

Figure 3. The domain of the North Atlantic and Arctic (NAA) configuration. The colour map represents the horizontal resolution and the contour lines denote the isobaths at 100 m (red), 1000 m (white), and 2000 m (~~magenta), and 3000 m (~~cyan). The thick (thin) solid black lines indicate the locations of Atlantic and Pacific open (North American and Eurasian closed) boundaries.

uppermost layer to 255 m in the bottommost layer. This vertical resolution is finer than that of the original NAA configuration in the upper layers (Figure ~~4~~). The bathymetry is based on the 1 arc-min global relief data ~~(~~ETOPO1; Amante and Eakins, 2009) as described by Hu and Myers (2013). For numerical stability, each ocean grid cell is set to have at least 7 vertical levels, corresponding to a depth of approximately 20 m.

2.5 Experiments

We consider six model experiments (Table 2). The first experiment is a reference simulation (EXP0), which is intended as the most realistic among all simulations considered in this study. The 11-year duration of EXP0 is considered sufficient for the spin up of sea-ice and near-surface pelagic variables based on previous Arctic biogeochemical model studies (e.g., Dupont, 2012; Jin et al., 2012

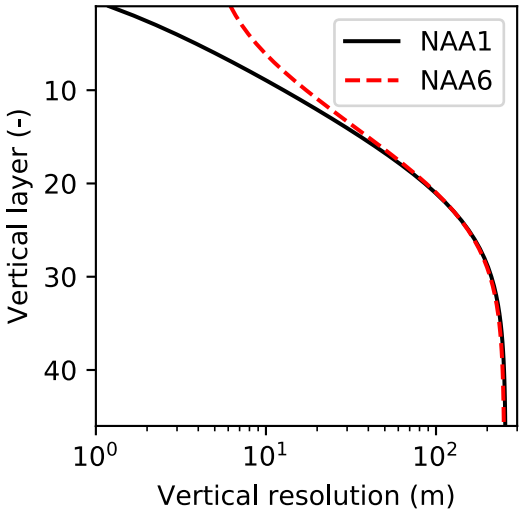

Figure 4. Comparison of the vertical resolution of the ocean model between the original NAA configuration (NAA6, i.e. approximately 6 m in the uppermost layer) and the configuration adopted in the present study (NAA1, i.e. approximately 1 m in the uppermost layer). Note the log scale on the x axis.

. The results during this spin-up period are presented in Appendix B. The setup of EXP0 is described below. The remaining experiments (EXP1-5) are designed to assess the sensitivity of the model simulations to changes in uncertain forcing data and parameter values.

2.5.1 Initial and lateral boundary conditions, runoff, and atmospheric forcing

The ocean was initialized from rest with temperature and salinity fields for January 1969 derived from the Ocean Reanalysis System 4 (ORAS4; Balmaseda et al., 2013). The initial snow depth, ice thickness, and ice concentration were respectively set to 0.1 m, 2.5 m, and 0.95 for grid cells with temperatures within 2 °C of the seawater freezing point. Elsewhere, these values were set to zero. The initial concentrations of nitrate, dissolved inorganic carbon, and total alkalinity were taken from the annual-mean fields of the GLobal Ocean Data Analysis Project version 2 (GLODAP2; Lauvset et al., 2016). The initial concentrations of dissolved oxygen were set to the annual-mean fields from the World Ocean Atlas 2013 Version 2 (WOA13; Garcia et al., 2014). The initial concentration of dissolved iron was set to 0.6 nM in the entire domain (Aumont et al., 2015). Because the model simulation starts at a time of low biological production (i.e., January 1), the remaining biogeochemical state variables in the ocean were initialized uniformly in space to ~~arbitrarily low values .~~ very low values (e.g., 0.01 mmol C m^{-3} for the carbon contents of phytoplankton, zooplankton, and detritus). The initial concentrations of sea-ice biogeochemical state variables were set to the same values as their respective variables in the uppermost layer of the ocean.

Table 2. List of model experiments

Name	Description	Duration
EXP0	Reference simulation.	1969-1979
EXP1	Same as EXP0 except that the atmospheric forcing was replaced by the CORE-II dataset.	1969-1979
EXP2	Same as EXP0 except that the snowfall and total precipitation for 1969-1978 were replaced by the original DFS dataset (i.e., daily-mean climatology).	1969-1979
EXP3	Same as year 1979 of EXP0 except that the light penetration through snow was impeded (i.e., i_0 for snow surface) was set to zero as in the original LIM2).	1979
EXP4	Same as year 1979 of EXP0 except that the advection and diffusion of sea-ice biogeochemical state variables were artificially suppressed (not computed).	1979
EXP5	Same as year 1979 of EXP0 except that the shading effect of ice algae was artificially suppressed.	1979

Open boundary conditions were applied by a radiation-relaxation algorithm (Madec, 2008) along the Atlantic and Pacific boundaries of the model domain, while the other two boundaries (along North America and Eurasia) were assumed to be closed (Figure 3). The boundary temperature, salinity, and zonal and meridional current fields were interpolated from the interannual monthly-mean fields of ORAS4. The open boundary conditions for ocean biogeochemical state variables were the same as their initial conditions. The relaxation timescales were set to 1 day for inflow and 15 days for outflow. These values are identical to those used in Dupont et al. (2015), but differ from the original NAA configuration (Hu and Myers, 2013). Our preliminary experiments suggested that these changes were needed to prevent salinity drift. Because the feature to prescribe the open boundary conditions for the sea-ice prognostic variables was not available in NEMO version 3.4, these were set to zero for the sea-ice prognostic variables of LIM2 as well as the sea-ice biogeochemical state variables; this feature is available in the ~~succeeding~~ subsequent version of NEMO (version 3.6).

River discharge of freshwater was derived from the interannual monthly-mean product of ~~Dai and Trenberth (2002).~~ Dai and Trenberth (2002). Figure 5 shows the seasonal and interannual variability (a and b) and spatial distribution (c) of the total discharge over the pan-Arctic. The river discharge of biogeochemical state variables was neglected ~~, and therefore, was not addressed in this study~~due to the lack of adequate data. Additional external supplies of nutrients (~~i.e.~~ dust deposition and sediment mobilization) ~~, which can be represented in CanOE,~~ were neglected due to the lack of reliable data. Partial pressure of carbon dioxide in the atmosphere was derived from the monthly-mean Mauna Loa CO_2 data (www.esrl.noaa.gov/gmd/ccgg/trends/data.html).

The surface atmospheric conditions used to drive the sea-ice and ocean model simulations were derived from the Drakkar Forcing Set 5.2 ~~(DFS; ?)~~(DFS; Dussin et al., 2016). The DFS dataset is high resolution in space (0.7°) and time (3-hourly for

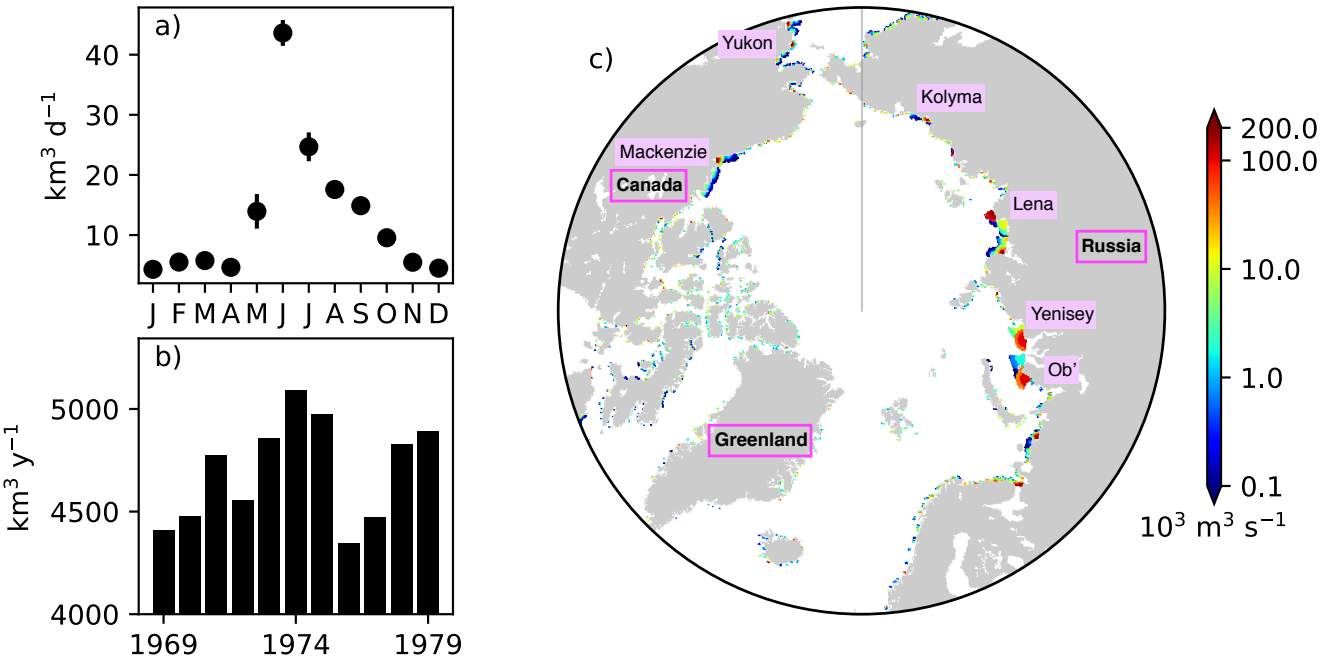

Figure 5. River runoff of freshwater prescribed in the model. a) Annual cycle of daily discharge and b) interannual variability in annual discharge integrated over the region north of 60°N. c) Spatial distribution of annual discharge rate averaged over the period 1969-1979. In a), the errorbars indicate the standard deviations over the period 1969-1979. In c), note the log scale on the colorbar, and names of major rivers and countries/regions are labelled.

zonal and meridional wind speed at 10 m height and air temperature and specific humidity at 2 m height; and daily for incoming shortwave and longwave radiation, total precipitation, and snowfall). It is based on a combination of ERA-40 and ERA-interim reanalysis products –(Uppala et al., 2005; Dee et al., 2011). The original DFS dataset (www.servdap.legi.grenoble-inp.fr/meom/DFS5.2/ALL) has missing data flags which cause a simulation crash in some years. As a substitute, we used a ~~modified~~ version provided by Clark Pennelly at the University of Alberta (personal communication) ~~. Furthermore~~which addressed the missing data flag errors without any modifications to the atmospheric data (the only changes were indexing and ordering of latitudinal coordinates and remaining variables). The total precipitation and snowfall prior to 1979 in the original DFS dataset were set to the 1979-2012 daily climatology due to the lack of adequate observations to construct the dataset for those years individually (Dussin et al., 2016). However, in EXP0, ~~the DFS snowfall and the total precipitation for year~~ we prescribed the total precipitation and snowfall for 1979 ~~were used~~ repeatedly for the simulation over the period 1969-1978, ~~as opposed to the 1979-2012 daily climatology (due to the lack of adequate observations to construct the dataset for those years individually; ?)~~ while keeping the remaining atmospheric variables the same as the original DFS dataset. This modification was necessary to simulate adequate snow depths (discussed further in Section ~~4~~.1).

Table 3. List of selected model parameters in the NEMO namelists

Name	Description	Unit	Value
	namelist		
rn_aht_0	Horizontal eddy diffusivity for oceanic active tracers	m^{-2} s^{-1}	5
	namelist_ice_lim2		
ahi0	Horizontal eddy diffusivity for sea-ice properties	m^{-2} s^{-1}	5
hiccrit	Thickness of newly-formed ice	m	0.6
pstar	Ice strength parameter	N m^{-2}	23,000
	namelist_top		
rn_ahtrc_0	Horizontal eddy diffusivity for passive tracers	m^{-2} s^{-2} $^{-1}$	5
	namelist_pisces		
Tref	Reference temperature for photosynthesis, grazing, and remineralization	°C	10
chldeg	~~Chrolophyll~~ Chlorophyll oxidation rate	d^{-1}	0

2.5.2 Additional settings

The time step of the model integration was 20 minutes. Unlike Hu and Myers (2013), no additional treatments for modelled temperature, salinity and wind-stress fields near the open boundaries were necessary since no obvious drift was apparent in the simulated fields. Table ~~-~~3 displays some of the model parameters that were modified from their default values in NEMOv3.4. For a complete list of the parameters, readers are referred to the source-code ~~repository ()~~archive (Hayashida, 2018a). The coefficients for horizontal eddy diffusion for oceanic and sea-ice tracers (rn_aht_0, ahi0, and rn_ahtrc_0) were reduced to keep diffusion relatively small compared to resolved dynamical processes, as recommended by Vancoppenolle et al. (2012). The other two parameters (hiccrit and pstar) were adjusted to improve the ~~modelled sea ice~~ fit with the PIOMAS data product (Section 2.6) in terms of sea-ice volume and extent for 1979 (Section 3.1.1). Lastly, two parameters of CanOE (Tref and chldeg) were adjusted to simulate reasonable annual primary production in the Arctic Ocean (Section 3.2).

2.5.3 Output

The output of the model experiments was saved as annual means for the first ten years (1969-1978) and five-day means for the final year (1979). Ice (snow) volume was defined as the sum of the product of grid-cell-mean ice thickness (snow depth) and the grid-cell area. Ice extent was defined as the areal sum of all grid cells with an ice concentration of at least 0.15. Primary productivity ~~within sea ice~~ of ice algae and phytoplankton was quantified in terms of depth-integrated (bottom 3 cm ~~) gross primary productivity (GPP), whereas primary productivity within water column was expressed in terms of depth-integrated (~~of sea ice and upper 90 m of water column, respectively) net primary productivity (NPP). ~~GPP was used for ice algae because the linear loss term for ice algae in our model accounts for processes other than just respiration, and therefore NPP cannot be derived simply by subtracting the linear loss term from the photosynthetic growth (i. e. GPP) . In~~

~~any case, the difference between NPP and GPP may be small~~ Ice algal NPP is assumed to equal the growth term in the model equation (Mortenson et al., 2017), as the specific growth rate associated with that term is derived from Eppley (1972) . This rate is a measure of particulate production, which is considered to provide values closer to NPP than gross primary productivity (GPP) (e.g., Sakshaug et al., 1997; Hashimoto et al., 2005). Thus, the loss due to respiration is implicitly included in the growth term in the model equation for ice algae~~, as a previous incubation experiment suggests that NPP accounts for 60 to 100 % of GPP in the bottom layer of Arctic sea ice (Table 4 of Gosselin et al., 1997)~~. On the other hand, CanOE has an explicit representation of respirational loss, and so phytoplankton NPP is defined as the growth minus the respiratory cost of biosynthesis (Christian et al, in prep.; see Appendix A3 of Hayashida, 2018b). Any grid cell whose ice concentration is 0.15 or greater was considered "under-ice" following Zhang et al. (2010). To investigate the interannual variability in pan-Arctic primary productivity, the ice algal ~~GPP~~NPP, phytoplankton NPP, and under-ice NPP were integrated annually and horizontally to derive respective pan-Arctic annual quantities. The term pan-Arctic is defined here as the region north of the Arctic Circle (66.5 °N). The pan-Arctic mean refers to an area-weighted average over the region north of the Arctic Circle. This areal restriction allows consistent comparison to some previous studies ~~(e.g. Legendre et al., 1992; Jin et al., 2012).~~ (e.g., Legendre et al., 1992; Jin et al., 2012).

2.5.4 ~~PIOMAS and SIIV3 data products~~

2.6 PIOMAS data product

The modelled sea-ice properties were evaluated against the ~~following observationally-based data products: the the~~ output of the Pan-Arctic Ice Ocean Modeling and Assimilation System (PIOMAS)~~and Sea Ice Index Version 3 (SIIV3) data products. Although these products are considered here as the best data products presently available, note that these products have their own biases that could result in mismatches with our model results.~~

~~PIOMAS~~ , which is a regional coupled sea ice-ocean circulation model that ~~also~~ assimilates some observational data ~~(~~Zhang and Rothrock, 2003; Schweiger et al., 2011). The ~~daily-mean time series of PIOMAS ice volume were obtained from . The~~ monthly-mean ice thickness and ice concentration gridded data products of PIOMAS were ~~also used for spatial comparison (Dirkson et al., 2016).~~

~~SIIV3 provides an estimate for ice extent based on sea-ice concentration fields derived from passive microwave radiometers (Windnagel e . The daily-mean SIIV3 ice extent time series were obtained from the National Snow and Ice Data Center website (). For the year 1979, this~~ interpolated onto the NAA grid in order to perform a grid-to-grid comparison across the same domain. Although the PIOMAS data product is ~~available for 182 days (i.e. every other day on average), which is sufficient to compare with the 5-day-mean model output.~~

3 ~~Reference simulation (EXP0)~~

2.1 ~~Interannual variability during spin up~~

The annual-mean time series of modelled snow and ice volumes, ice extent, seawater nitrate, and ice algal and phytoplankton biomass over the 11 years of EXP0 are shown in Figure B1. This time period can be considered as sufficiently long to spin up some of these quantities, while others may require additional years to spin up. However, none of these quantities reach a steady state in the current setup as the model was driven by interannual surface and lateral boundary conditions. The aim of the present analysis is to diagnose potential drifts by examining the character of temporal variability starting from the initial year. In summary, no substantial drifts are simulated in any of the quantities considered.

The annual-mean modelled snow volume stabilized around 0.8×10^3 km^3 after an initial drop of about 0.1×10^3 km^3 from year 1969 to 1970 (Figure B1a), indicating a spin-up period of a year or so. In contrast, the annual-mean modelled ice volume variations showed an initial reduction during 1969-1971 followed by an overall increase during 1973-1979. The relatively short duration of this simulation does not allow us to distinguish between trends and slow interannual variability, so we cannot determine if the ice volume has spun up based solely on this analysis; this is addressed in a follow up study. A previous pan-Arctic regional model study of Watanabe (2013) showed a spin-up period of 10 years for modelled ice volume based on a simulation using a fixed annual cycle atmospheric forcing and restoring of temperature and salinity.

Modelled ice extent showed a decrease in the first 6 years followed by a stabilization in the last 5 years, suggesting that this quantity spun up at year 1975 (FigureB1b). This spin-up time is similar to that found in considered here as the pan-Arctic model study of Jin et al. (2012), in which their modelled ice area and extent became comparable to the observations after the first 6 years of simulationbest presently available, note that it has its own biases that could result in mismatches with our model results.

The annual-mean modelled seawater nitrate concentration integrated over the upper 90 m of the water column in the entire model domain showed both increases and decreases during the 11 years (FigureB1b), although the size of the fluctuation ($\sim$20 mmol N m^{-2}) is small relative to its mean state ($\sim$490 mmol N m^{-2}). Similarly to ice volume, a longer simulation would be needed to distinguish between trends and interannual variability in the modelled nitrate concentration. A previous pan-Arctic model study of Dupont (2012) indicated a spin-up period of at least a decade for nitrate in the upper 100 m water column for the model domain he considered. The modelled primary producers (ice algae and phytoplankton) appear to have spun up within a year of the model simulation, as their annual primary production fluctuates around a steady mean following the first year (Figure B1c).

Time series of annual-mean modelled a) snow and ice volumes, b) ice extent and depth-integrated (90 m) seawater nitrate concentration, and c) depth-integrated (3 cm) ice algal GPP and depth-integrated (90 m) phytoplankton NPP in EXP0. The depth-integrated quantities represent averages over the entire model domain.

3 Reference simulation (EXP0)

3.1 Comparison of sea-ice physical properties with PIOMAS ~~and SIV3 during the year~~ in 1979

3.1.1 Seasonal variability

To assess the ~~performance of the model simulation of~~ model performance in simulating sea ice, the seasonal variability of modelled ice volume and extent in EXP0 ~~were~~ are compared to PIOMAS ~~and SIV3~~ (Figure 6a and b) for ~~the year 1979. This year corresponds to the first full year available for these data products. The ice volume in~~ 1979 (after a decadal spin up). In both EXP0 and PIOMAS~~was at its~~ , the annual maximum in ~~late April (April 25 vs 28) and at its annual minimum in September (September 10 vs 21). The ice extent in EXP0~~ ice volume (extent) takes place in April (March), while both the ice volume and ~~SIVV3 was at its annual maximum in March(March 24 vs 1)and at its annual minimum in September (September 25 vs 21). Given the difference in the frequency of the model output and these data products (5-day vs daily), the timings of the ice volume maximum and the ice extent minimum are comparable. The most prominent disagreement is in the timing of the ice extent maximum in which EXP0 lags by a few weeks. The seasonal recession of Arctic sea ice started later in EXP0 partly because our domain excludes lower-latitude regions that were ice-covered in 1979 (e.g. the Sea of Okhotsk and the Gulf of Saint Lawrence), and the seasonal retreat of sea ice in these areas occurred earlier (confirmed using the Sea Ice Spatial Comparison Tool:).~~

~~The ice volume is slightly~~ extent are at their annual minima in September. The ice volume is consistently higher in EXP0 than PIOMAS~~throughout the year, with the largest difference of about 3000 km^3 taking place in May-June. The~~ . The difference in the annual-mean ice volume over the NAA domain is 3.9 km^3 (17%). In contrast, the ice ~~extent, on the other hand, is generally lower in EXP0 than SIV3, and their difference is greater than 1~~extent comparison is much better with the difference of 0.1 $\times 10^6$ ~~km^2 during the season of greatest extent (December-May). Much of this difference can be attributed to the fact that the model domain excludes regions that are usually ice covered during that period, such as Hudson Bay (covering a surface area of 1.23$\times 10^6$ km^2) and the Sea of Okhotsk (1.58$\times 10^6$ km^2). During the remainder of the year, the modelled ice extent is in closer agreement with SIV3 (especially in August-September) .~~ (1%) in the annual means.

3.1.2 Spatial variability

Figure ~~-~~7 shows the spatial variability in modelled March- and September-mean ice thickness fields in EXP0 and PIOMAS. The extent of modelled Arctic sea ice can be inferred from the ~~locations of~~ location of the ice edge, defined here as the 0.15 contour of ice concentration ~~of 0.15 (Figure~~ (Figure 7a,b,d,e). Overall, the locations of the ice edge within our model domain are similar between EXP0 and PIOMAS for both March and September. Beyond the model domain, the ice coverage in March extends to Hudson Bay and the Sea of Okhotsk in PIOMAS (Figure 7b). The March-mean ice thickness distribution in EXP0 ~~consists of: a zonal~~ includes a band of >5-m-thick ice along the coast ~~between north of Greenland and north of the western edge of the Canadian Arcite Archipelago ;~~ of the Canadian Arctic Archipelago extending east to Greenland, and a region of relatively thick ice (∼4 m) in the Arctic Basin north of the East Siberian Sea (Figure 7a). The ~~zonal~~ band is also present

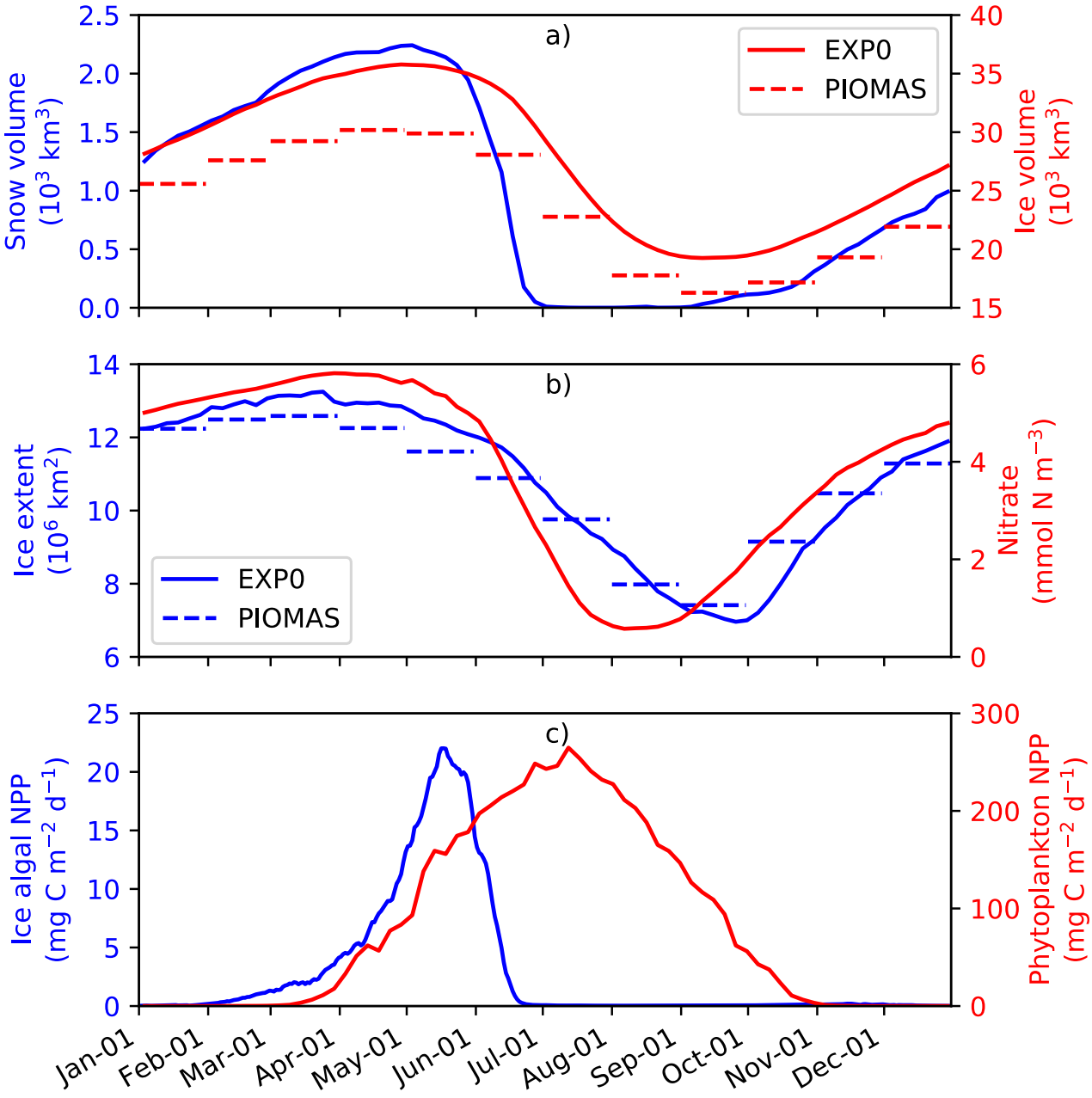

Figure 6. Time series of 5-day-mean modelled a) snow and ice volumes, b) ice extent and pan-Arctic-mean surface seawater nitrate concentration, and c) pan-Arctic ice algal and ~~phytoplaknton daily~~ phytoplankton NPP during 1979 in EXP0. The dashed lines in a) and b) represent the ~~daily-mean~~ monthly-mean PIOMAS ice volume and extent~~of PIOMAS and SIIV3~~, respectively.

in PIOMAS, although it is restricted to the north of Greenland (Figure 7b). The thick ice region in the Arctic Basin north of the East Siberian Sea, on the other hand, is absent in PIOMAS. Besides these ~~regions entailing the zonal band and the blob~~particular regions, EXP0 generally ~~simulated~~ simulates thicker ice than PIOMAS in the Greenland Sea and various shelf regions (Figure 7c). On the other hand, EXP0 ~~simulated~~ simulates thinner ice than PIOMAS ~~in~~ on the Canadian Polar Shelf ~~,~~ and in the Chukchi Sea, the Barents Sea, the Kara Sea, and an area near the North Pole (Figure 7c). Overall, the mean absolute difference in the ice thickness distribution over the NAA domain is 0.43 m (30%). Note that the difference is still calculated even if the ice is absent by considering thickness of 0 m. Also, note that even though PIOMAS assimilates data, it is still a model product, and therefore the difference is not a definite measure of accuracy.

In September, the most notable features in the ice thickness distribution are the presence of ~~: thin~~ thinner (<2 m) ice ~~(relative to the surroundings)~~ in an area near the North Pole in EXP0 (Figure 7d) ~~; and thick~~ and thicker (>5 m) ice along the coast of Siberia in PIOMAS (Figure 7e). The latter feature seems unrealistic considering that: it is thicker in September than in March; and it is thicker than the multi-year ice present along the band north of the Canadian Arctic Archipelago and Greenland. Both of these features ~~result in negative values in the ice thickness difference between the model and~~ constitute negative ice thickness anomalies in the model relative to PIOMAS (Figure 7f). ~~Besides these regions, the~~ The difference is also negative and ~~high~~ large (∼3 m) ~~in~~ on the Canadian Polar Shelf; this could be due to the fact that the horizontal resolution of PIOMAS (∼22 km; Zhang et al. (2010)) ~~may be~~ is too coarse to resolve the circulation through these relatively narrow channels, resulting in the simulation of too thick first-year ice in this region at this particular time of the year. The ice thickness ~~difference is positive in~~ is greater in EXP0 than in PIOMAS in the Arctic Basin, part of the East Siberian Sea, and the Laptev Sea as well as along the eastern coast of Greenland. The mean absolute difference is 0.31 m (38%), similar to the March comparison.

3.2 Primary productivity of ice algae and phytoplankton

3.2.1 Seasonal variability

Figure 6 shows the seasonal variability in modelled pan-Arctic-mean ice algal ~~GPP~~ NPP and phytoplankton NPP during 1979 (panel c) along with relevant environmental factors (panels a and b). ~~The ice algal GPP started~~ Ice algal NPP starts increasing in early February, ~~peaked~~ peaks in mid May, sharply ~~declined~~ declines in late May-early June, and ~~was~~ is near zero by late June. The start of the decline of the ice algal ~~GPP coincided~~ NPP coincides with the decline of the ice volume (Figure 6a) demonstrating that the decline ~~was~~ is driven by the release of ice algae as a result of ice melt. The seasonal progression of the ice algal production is similar to Jin et al. (2012). The phytoplankton NPP ~~started~~ starts increasing in early March, ~~peaked~~ peaks in early July, and ~~decreased~~ decreases to near zero by the end of October (Figure 6d). At the peak in phytoplankton NPP, the pan-Arctic-mean surface seawater nitrate concentration ~~was~~ is below 1 mmol N m^{-3} and ~~remained~~ remains so until the end of August (Figure 6b).

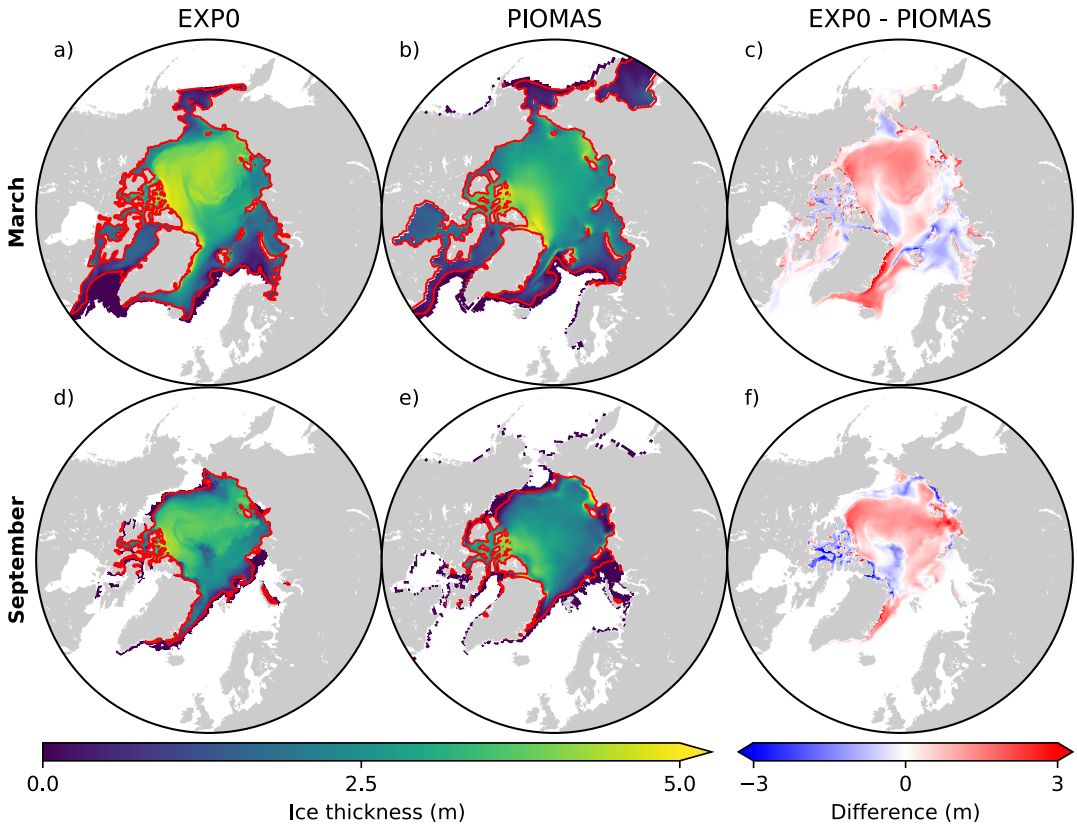

Figure 7. Spatial distributions of monthly-mean ice thickness in EXP0 (a,d) and the PIOMAS product interpolated onto the NAA grid (b,e) and their difference (c,f) for March and September in 1979. ~~In a), b), d), and e), the~~ The red lines represent the ice edge, defined here as the 0.15 contour of ice concentration~~of 0.15. In c) and f), the comparison is restricted to the NAA domain because the ice thickness fields of PIOMAS were interpolated onto the NAA grid in order to perform a grid-to-grid comparison.~~

3.2.2 Spatial variability

Figure 8 shows the spatial distribution of annual-mean snow depth and , surface seawater nitrate , and ice algal annual GPP and phytoplankton annual concentration, ice algal NPP, and phytoplankton NPP for 1979. The largest values of ice algal annual GPP NPP (>10 g C m^{-2} y^{-1}) are present on the Canadian Polar Shelf and in the coastal regions of Baffin Bay, the Canadian Polar Shelf, the Chukchi Sea, the East Siberian Sea, and the Kara Sea (Figure 8c). All of these regions have relatively thin snow (less than 0.1 m; Figure 8a), demonstrating the control of light on ice algal growth. In contrast, the nutrient control on ice algal production is less pronounced; although high ice algal GPP NPP usually concides with high surface seawater nitrate, it is also present in a few areas where the nitrate levels are relatively low (Baffin Bay and Chukchi Sea; Figure 8b). Overall, ice algal production is mostly confined to shelf regions (water depth <100 m; Figure 3excluding the Barents Sea), consistent with previous model studies (Deal et al., 2011; Dupont, 2012; Jin et al., 2012, 2018). However, the values reported in Deal et al. (2011), Jin et al. (2012), and Jin et al. (2018) are representative of NPP, while those of Dupont (2012) and the present study represent GPP; comparisons should be made with this difference in mind. (Deal et al., 2011; Dupont, 2012; Jin et al., 2012, 2018).

There are a few noteworthy similarities and differences in the spatial variability in modelled ice algal annual production between the present study and previous model studies. All studies show a moderate-to-high level of ice algal production in Baffin Bay. In contrast, disagreement in the ice algal production is found along the eastern coast of Greenland and in the Bering Sea; the values along the eastern coast of Greenland are moderate (5-10 g C m^{-2} y^{-1}) in Deal et al. (2011) and Jin et al. (2012), while they are low (less than 5 g C m^{-2} y^{-1}) in Dupont (2012), Jin et al. (2018), and the present study. Similarly, although Bering Sea is identified as a region of high ice algal production by Deal et al. (2011), Jin et al. (2012), and Jin et al. (2018), Dupont (2012) and the present study simulate low ice algal production in this region. A possible explanation for the lower ice algal production in this region in the latter studies is due to an insufficient nutrient supply from the Pacific boundary as discussed in Dupont (2012). Lastly, the recent study by Jin et al. (2018) finds the Sea of Okhotsk to be a region of elevated ice algal annual production, which we are unable to assess in the present study due to the limited model domain. We also note the difference in the temporal coverage of simulations among these studies, which can explain some of the differences in these results.

The modelled phytoplankton annual NPP is high (>100 g C m^{-2} y^{-1}) in the Atlantic and the Pacific sectors with little to no ice cover, moderate (50-100 g C m^{-2} y^{-1}) in the shelf seas along the North American and the Eurasian continents, and low (<50 g C m^{-2} y^{-1}) in the interior of the Arctic Ocean (Figure 8d). These findings are in both qualitative and quantitative agreement with the results of five different models and satellite-based estimates (Figure 1 of Popova et al., 2012).

3.2.3 Interannual variability

The modelled pan-Arctic ice algal annual GPP NPP in EXP0 ranged ranges from 10.5 to 18.2 Tg C y^{-1} for the period 1970-1979, excluding the initial spin-up year. While this value is on the lower end of the range of observation-based NPP estimates (9-73 Tg C y^{-1}; Legendre et al., 1992), the upper bound (73 it is close to the decadal mean of the annual NPP (10.1 Tg C y^{-1}) for 1998-2007) simulated by Jin et al. (2012). The pan-Arctic estimates by Legendre et al. (1992) are quite

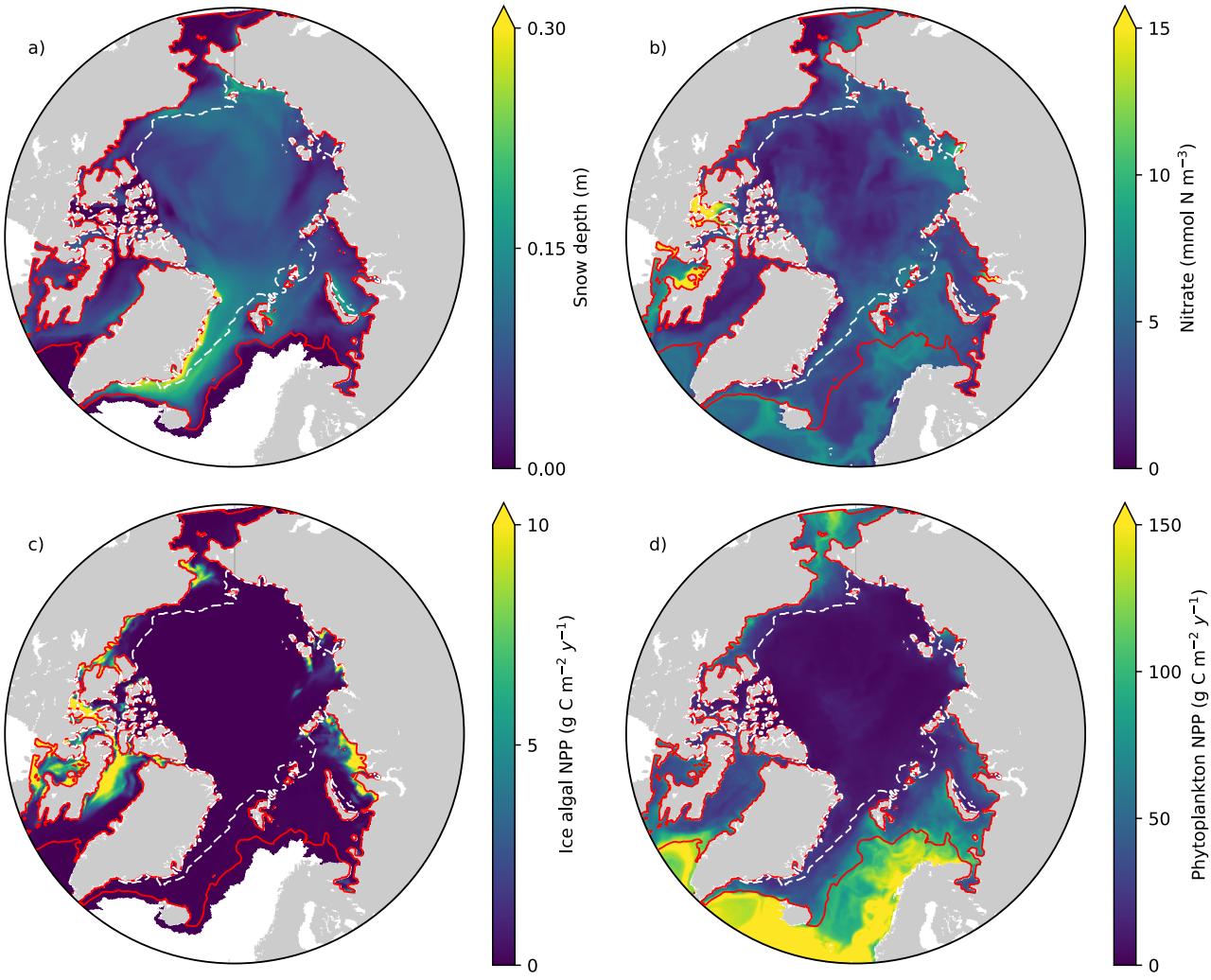

Figure 8. Spatial distribution of annual-mean a) snow depth and b) surface seawater nitrate concentration, and c) depth-integrated (bottom 3 cm) ice algal annual ~~GPP~~ NPP and d) depth-integrated (upper 90 m) phytoplankton annual NPP in 1979 in EXP0. The ~~solid and dashed~~ red and white lines represent the 0.15 contour of monthly-mean ice concentration ~~of 0.15~~ in March and September, respectively.

speculative as they are based on the integration of a single ice algal production value over a specified ice area (discussed in detail in Deal et al. (2011)). The close agreement between the two model-based estimates suggests that the lower end of the observation-based estimates is more plausible than their upper end. Although the upper end accounts for contribution from mat and strand communities that are not represented in our model~~. Furthermore, this value is close to the decadal mean of the annual NPP (10.1 Tg C y^{-1} for 1998-2007) simulated by Jin et al. (2012)~~, their contribution to the pan-Arctic production should be small as their spatial distribution is generally localized (e.g., Assmy et al., 2013). Direct comparisons with the results of Deal et al. (2011) and Dupont (2012) are not possible because the reported values in those studies include contributions from below the Arctic Circle. The modelled pan-Arctic phytoplankton annual NPP in EXP0 ~~ranged~~ ranges from 378 to 465 Tg C y^{-1}, which is in line with the observation-based estimate (>329 Tg C y^{-1}; Total High Arctic) of Sakshaug (2004), the satellite-based estimate (419 Tg C y^{-1} for 1998-2006) of Pabi et al. (2008), and the model-based estimate (627 Tg C y^{-1} for 1998-2006) of Jin et al. (2012).

3.3 Vertical distribution of salinity, nitrate, chlorophyll a, and DMS in the upper water column

The seasonal variability of pan-Arctic-mean seawater salinity, nitrate, chlorophyll a, and DMS in the upper 15 m of the water column is shown in Figure ~~-~~9. During the summer, a prominent freshening of the uppermost layer occurs as a result of ice melt (Figure ~~-~~9a). This freshening results in formation of a thin layer of low-salinity water known as a meltwater lens, which ~~strengthened the stratification and reduced the~~ strengthens stratification and reduces mixing with the underlying water column. The formation of the lens ~~coincided~~ coincides with the bloom of modelled phytoplankton, resulting in the depletion of nitrate first in the uppermost model layer and then in the underlying layers (Figure ~~-~~9b). Nutrient depletion in the near surface waters then results in formation of subsurface chlorophyll a and DMS maxima during the latter half of July (Figure ~~-~~9c and d). Note that the meltwater lens and the subsurface maxima are respectively thicker and shallower than those observed by field measurements (e.g., Brown et al., 2015) because of averaging over the pan-Arctic domain. The purpose of this spatial averaging is to quantify the impacts at a larger scale rather than assessing localized effects.

These ice-associated physical and biogeochemical processes ~~took~~ take place within a relatively shallow upper water column (~10 m), and would have been impossible to simulate with a model of coarse vertical resolution. It is for this reason that the near-surface vertical resolution of the NAA configuration considered in the present study is finer than that of the original configuration ~~-~~(6 m in the uppermost layer; Hu and Myers, 2013). Although modelling these small-scale processes probably has negligible effect on bulk quantities such as depth-integrated NPP, it can have an impact on processes ~~happening right~~ at the air-sea or ice-sea interface (e.g., gas fluxes). To illustrate this point, the time series of modelled pan-Arctic-mean seawater DMS concentration in the uppermost layer of the water column (about 1 m) ~~was~~ is compared with the concentration averaged over the top four layers (about 12 m) as a proxy for values simulated by a coarse-vertical-resolution model (Figure ~~-~~10).

Modelled DMS concentration is higher in the uppermost layer than ~~in~~ the 12-m ~~layer~~ average throughout most of April-September, ~~but slightly smaller~~ while it is slightly lower in August (Figure ~~-10b~~10a). The concentration difference is ~~largest~~ highest (up to about 20 %) in June-July ~~. The largest DMS concentrations are found in the upper 1 m until the formation of the subsurface maximum (Figure 9c~~(Figure 10b). Overall, the annual-mean DMS concentration averaged over the upper 12 m of

the water column is 9 % lower than in the upper 1 m. Here, the averaging over a thicker layer results in dilution of the DMS concentration in the uppermost layer represented in the model. Considering that this difference is present primarily during the ice melt period, and therefore that the sea-surface DMS is ~~capable of being~~ released into the atmosphere, the modelled sea-to-air DMS flux would be underestimated by a similar amount ~~using the 12-m resolution time series~~in the absence of fine vertical resolution in the upper water column.

4 Sensitivity experiments (EXP1-5)

4.1 Snowfall forcing frequency (EXP1 and 2)

Two sensitivity experiments (EXP1 and EXP2) ~~were~~ are performed with the identical setup as EXP0 except for a change to the atmospheric forcing. In EXP1, all the forcing fields ~~were~~ are replaced by the CORE-II dataset ~~used~~ as in the original NAA configuration ~~(Hu and Myers, 2013).~~ (Hu and Myers, 2013). Note that the temporal resolution of the snowfall and total precipitation fields in the CORE-II dataset is monthly. In EXP2, the snowfall and total precipitation fields over the period 1969-1978 ~~were~~ are replaced by their respective 1979-2012 daily climatological values as in the original DFS dataset ~~(?)~~ (Dussin et al., 2016). Comparing between EXP0 and EXP1 allows us to assess the impacts of atmospheric forcing (DFS vs CORE-II), while comparing between EXP1 and EXP2 allows us to assess the impacts of snowfall dataset (daily vs daily climatology) on modelled snow depth.

A comparison of the pan-Arctic-mean snowfall rates between the CORE-II and DFS datasets illustrates the differences between ~~these datasets (Figure~~ them (Figure 11a). The monthly CORE-II dataset varies from approximately 1 to 2.4 mm d^{-1} (meltwater equivalent), while the range of the DFS dataset is three times as large (from ~~nearly~~ near 0 to about 4.4 mm d^{-1} for the year 1979) most likely due to the difference in the temporal resolution of the datasets. The lack of high frequency variability in the DFS daily climatology is evident from the comparison of the DFS dataset between 1969-1978 and 1979. The daily climatology ranges approximately from 0.2 to 2.2 mm d^{-1}, less than ~~a~~ half of the range for the individual daily averages for 1979. The annual-mean CORE-II snowfall rate is higher than that of the DFS dataset in all of these years. ~~Between the~~ The annual mean of the DFS daily climatology ~~and~~ is slightly greater than that of the individual daily averages for ~~1979, the former is slightly higher.~~ 1979.

Figure ~~-~~11b shows a comparison of the modelled pan-Arctic annual-mean snow depth among EXP0, EXP1, and EXP2. The snow depth ~~was~~ is substantially lower in EXP1 and EXP2 than in EXP0 throughout the period 1969-1979, except for 1969 (in which year the snow depth is affected by its initial value). In EXP2, the ~~extremely-low~~ extremely low snow depth somewhat ~~recovered~~ recovers in 1979.

Figure ~~-~~11c-e shows a spatial comparison of the modelled annual-mean snow depth over the period 1970-1978 (excluding the first and ~~the~~ last year of ~~simulations~~simulation). There is a clear difference in the distribution between EXP0 and the other two experiments; the ice pack ~~was~~ is generally covered by moderate amount of snow (~0.1 m) in EXP0, while in EXP1 and EXP2, most regions ~~were~~ are nearly snow-free. These results of the latter two experiments are inconsistent with the available snow depth climatology indicating the presence of considerably thicker (>0.2 m) annual-mean snow cover over the Arctic

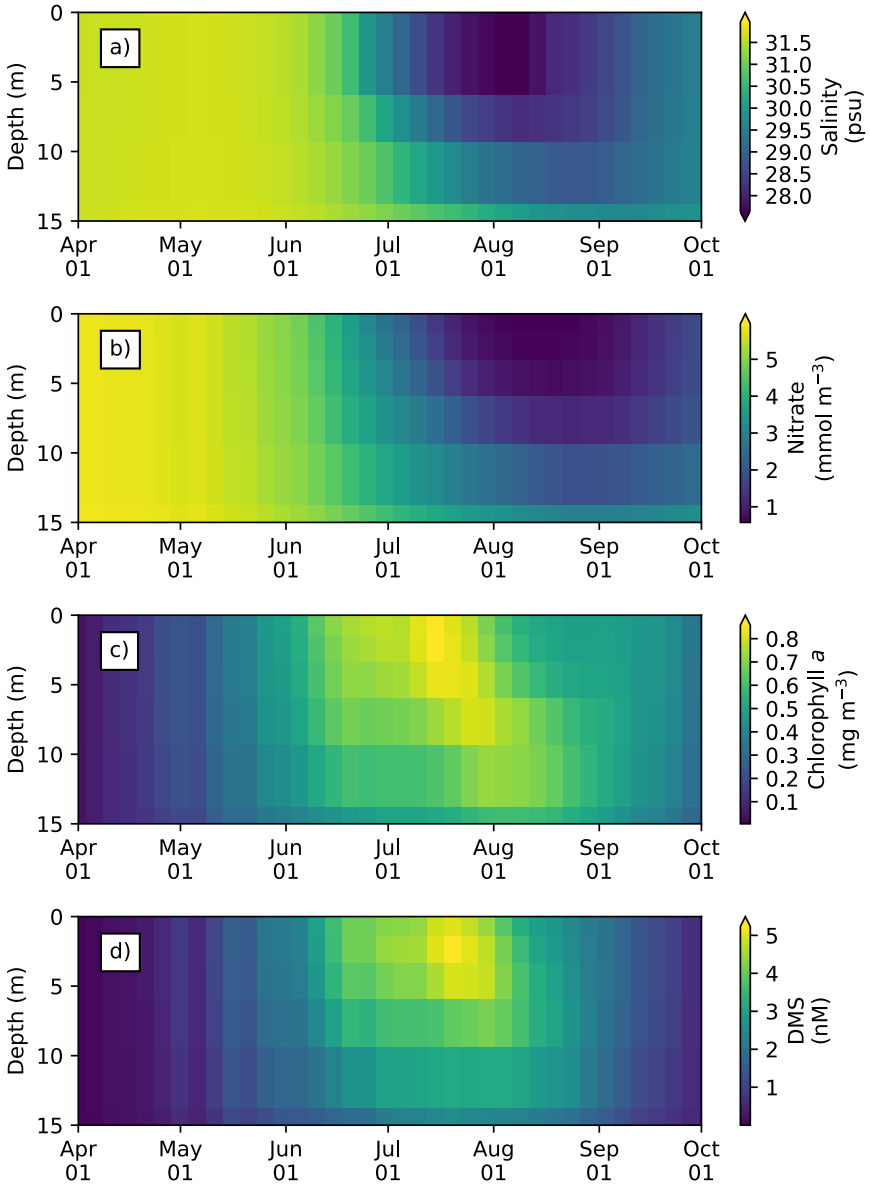

Figure 9. Time series of 5-day- and pan-Arctic-mean seawater a) salinity, and concentrations of b) nitrate, c) chlorophyll *a*, and d) DMS in the upper 15 m of the water column during April-September in 1979 of EXP0.

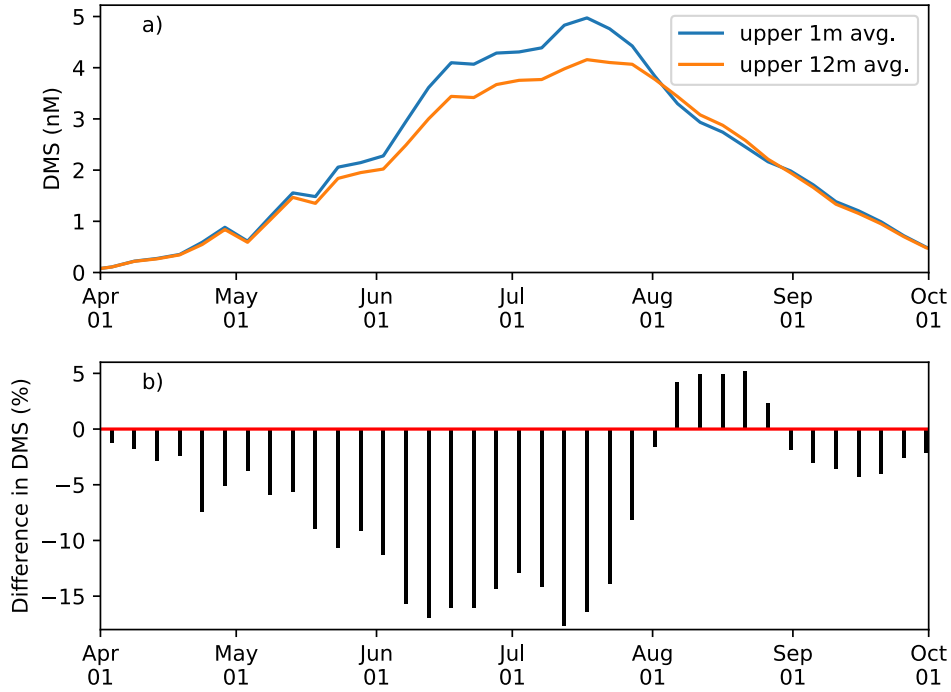

Figure 10. a) Time series of 5-day- and pan-Arctic-mean seawater DMS concentration a) in the uppermost layer (∼1 m; blue) and averaged over the upper four layers (∼12 m; orange) during April-September in 1979 of EXP0. b) The percentage difference between the two time series (the ~~1-m~~ 12-m average minus the ~~12-m~~ 1-m average, divided by the 1-m average).

Basin ~~-~~(Warren et al., 1999). As a result of these biases, the modified DFS dataset ~~was~~ is used as the reference simulation, rather than the CORE-II dataset or the original DFS dataset.

It is interesting that the modelled pan-Arctic annual-mean snow depth ~~was~~ is higher in EXP0 than EXP1 even though the prescribed annual-mean snowfall rate ~~was~~ is consistently higher in the latter experiment (Figure ~~-~~11a). Furthermore, the recovery of the modelled snow depth in 1979 of EXP2 is also interesting given that there is essentially no change in the total snowfall amounts between 1978 and 1979. These results indicate a high sensitivity of the modelled snow depth to the ~~frequency range contained in~~ temporal resolution of the snowfall dataset. This interpretation is reinforced by the fact that the modelled snow depth is also sensitive to the parameter nn_fsbc, which defines the frequency of the computation of surface boundary conditions and sea-ice physics relative to that of ocean dynamics. Figure ~~-~~12 compares the annual-mean modelled snow depths for year 1970 of EXP2 with those of the simulations that varied nn_fsbc from the default value of 1 (i.e., the time step for surface boundary condition and sea-ice physics is identical to the ocean time step) to 5 and 10 (i.e., surface boundary condition and sea-ice physics are computed at every 5 and 10 ocean time steps, respectively). We ~~found~~ find that setting nn_fsbc to 5 ~~and~~ or 10 ~~both increased the pan-Arctic-mean~~ increased the modelled snow depth ~~although regional differences exist (Figure~~

quite remarkably (Figure 12). This high sensitivity to the ~~frequency content of~~ choice of nn_fsbc is somewhat unexpected given that the tested range (1-10 time steps, equivalent to 20-200 minutes) is far less than the temporal resolution of the ~~input snowfall dataset and the frequency of coupling to the ocean is a model artifact~~CORE-II dataset. A more detailed analysis of ~~this artifact (and its elimination) is outside of~~ the model sensitivity to nn_fsbc is outside the scope of this study. Nevertheless, this analysis suggests that the issue with the usage of monthly or climatological-daily snowfall dataset can be resolved by tuning this parameter (as demonstrated in EXP1 and EXP2). However, the tuning of this parameter without known constraints is quite arbitrary and might have other implications for modelled dynamics. The usage of high-frequency atmospheric forcing dataset is therefore recommended whenever possible to prevent the issue discussed here.

4.2 Light penetration through snow column (EXP3)

Figure ~~-~~13 compares the modelled sea-ice physical and biogeochemical properties in 1979 in EXP0 with those of EXP3, in which i_0 for snow ~~was~~ surface is set to the default LIM2 value of zero. The results for modelled snow and ice volume ~~were~~ are almost identical between the two experiments (Figure ~~-~~13a), indicating a low sensitivity of these physical quantities to the change in i_0 for the snow surface. On the other hand, an appreciable difference in the modelled bottom-ice PAR prior to the melt season in June results in a large difference in the modelled ice algal ~~GPP (Figure~~ NPP (Figure 13b). ~~By construction, the ice algal GPP~~ Ice algal NPP in EXP3 is restricted to snow-free regions, so an increase in the ice algal ~~GPP~~ NPP due to the change in i_0 for snow surface reflects production in snow-covered regions (Figure ~~-~~13c). The pan-Arctic ice algal annual ~~GPP~~ NPP of EXP3 is 3.5 Tg C y^{-1}, only about a quarter of the value obtained in EXP0. ~~The~~ This value is much lower than those ~~of the~~ obtained in previous studies (see Section ~~-~~3.2.3). This result emphasizes the importance of correct representation of the light penetration through ~~the snowcolumn~~snow, and shows that the original LIM2 provides inadequate light for ice algal growth, resulting in insufficient ~~pan-Arctic ice algal annual GPP~~ice algal NPP. Note that the default value of i_0 for the snow surface is also set to zero in LIM3 ~~-~~(Vancoppenolle et al., 2012).

Previous 3D sea-ice biogeochemical models ~~differed~~ differ in their choices of values for i_0 ~~(Table~~ for the snow surface (Table 1). The studies of Dupont (2012) and Jin et al. (2012) set this value to zero, yet their values for simulated ice algal productivity ~~were~~ are relatively high. However, these models ~~used~~ use special parametarizations for irradiance and light limitation, respectively, which likely ~~resulted~~ result in realistic ice algal primary production values despite the ~~impedence~~ lack of light penetration through snow~~column. Dupont (2012) imposed~~ . Dupont (2012) imposes a minimum lead fraction of 0.01 in any grid cell, supplying enough ambient light for ice algal growth. In Jin et al. (2012), the light limitation parameter ~~-~~(the ratio of light-limited slope and maximal photosynthetic rate; see Table 2 of Jin et al., 2006) ~~was~~ is set to a very high value, nearly double the upper limit of the observed range reported in Table 2 of Lavoie et al. (2005). This reduction in light limitation allows the modelled ice algae to grow faster even under low light conditions upon snow disappearance.

Two other regional modelling studies ~~prescribed~~ prescribe non-zero values of i_0 for snow surface. Castellani et al. (2017) set i_0 for snow surface to 0.3 based on the measurements over snow-free ice surface ~~-~~(Grenfell and Maykut, 1977). As such, this value (0.3) should be viewed as an overestimate. Similarly, the light penetration through snow ~~column was~~ is also overestimated in Watanabe et al. (2015), as i_0 ~~was~~ for snow surface is effectively unity in their study. Using these higher i_0 for snow surface

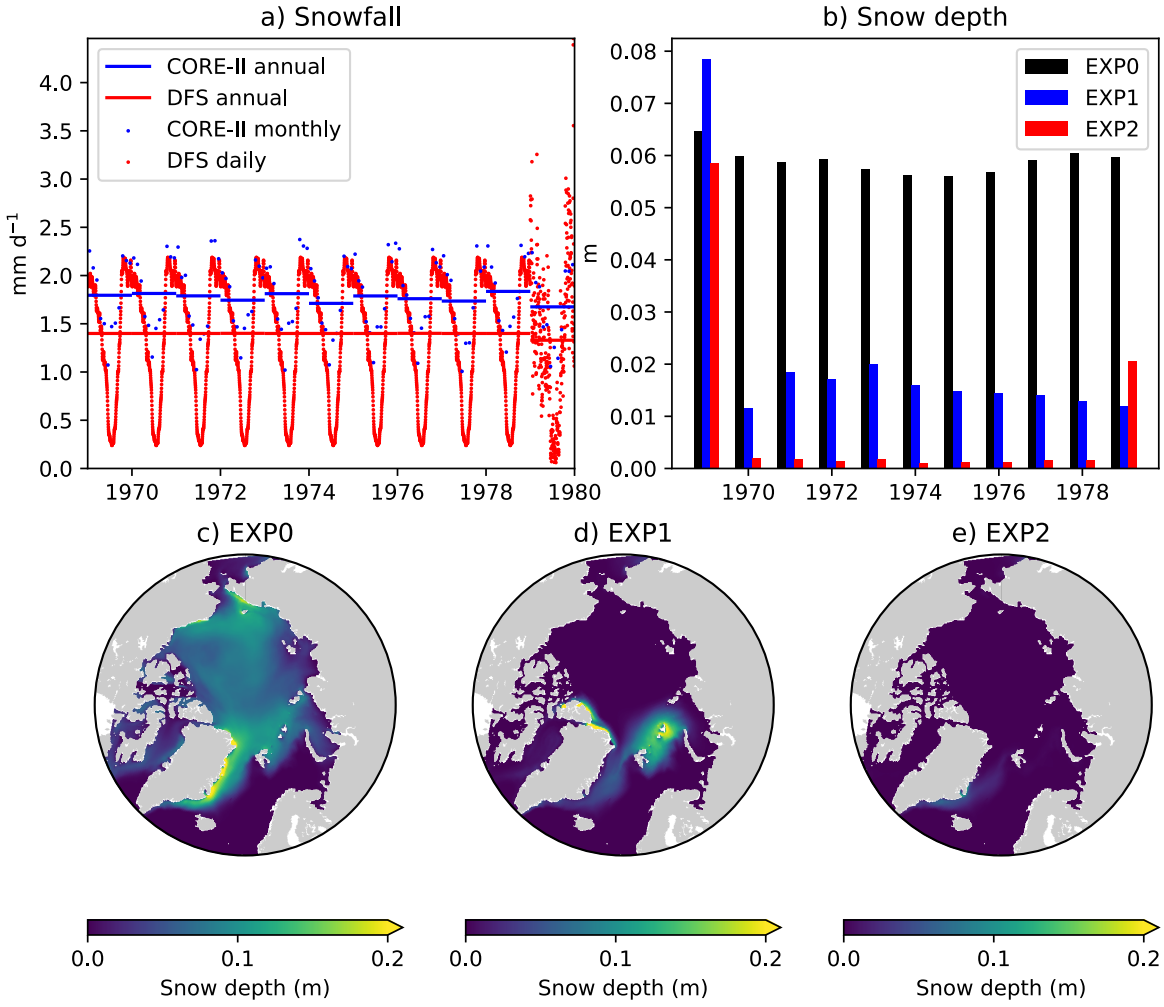

Figure 11. Model sensitivity to snowfall forcing frequency. Time series of pan-Arctic-mean a) prescribed snowfall rate of the CORE-II (blue) and DFS (red) datasets and b) modelled annual-mean snow depth in EXP0 (black), EXP1 (blue), and EXP2 (red). Spatial maps of modelled annual-mean snow depth for the period 1970-1978 in c) EXP0, d) EXP1, and e) EXP2. The units for the snowfall rate ~~was~~ are converted from kg m^{-2} s^{-1} to mm d^{-1} using a constant snow density of 330 kg m^{-3}, which is the value assumed in LIM2.

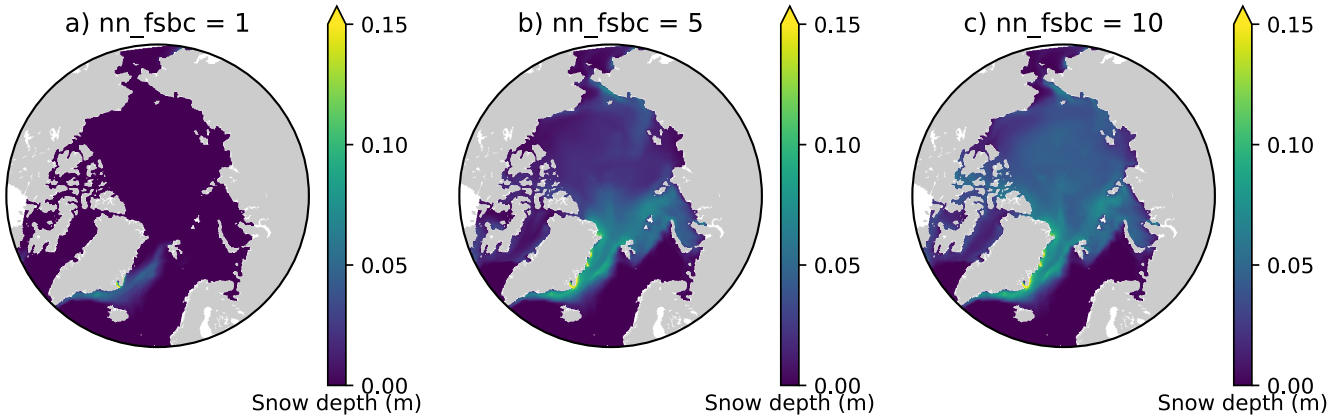

Figure 12. Sensitivity of modelled snow depth to the parameter nn_fsbc, which defines the frequency of the computation of surface boundary conditions and sea-ice physics relative to that of ocean dynamics. Spatial distribution of annual-mean modelled snow depth for ~~year~~ 1970 when nn_fsbc is set to a) 1, b) 5, and c) 10.

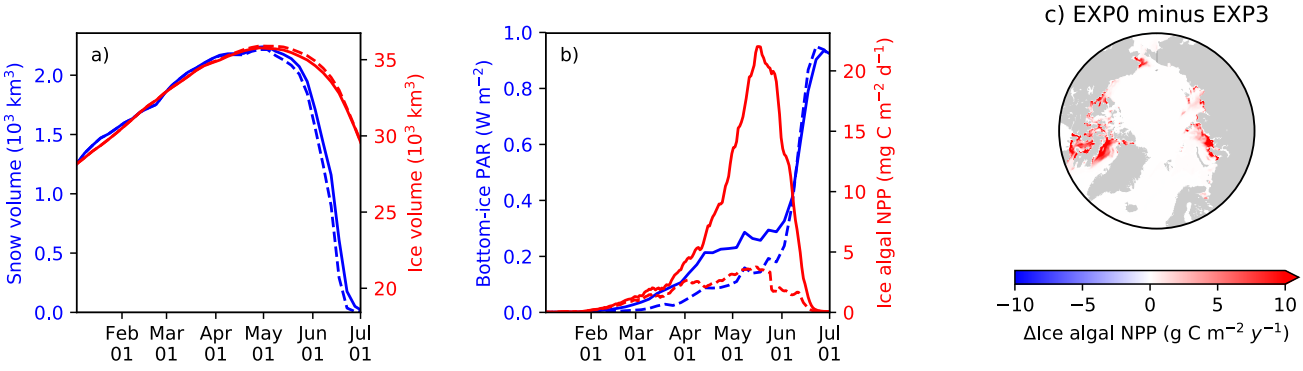

Figure 13. Model sensitivity to light penetration through snow. Time series comparison of modelled 5-day-mean a) snow volume (blue) and ice volume (red) and b) bottom-ice PAR (blue) and ice algal ~~GPP~~ NPP (red) in 1979 between EXP0 (solid) and EXP3 (dashed). c) Spatial distribution of the difference in the ice algal annual ~~GPP~~ NPP between EXP0 and EXP3.

reduces light limitation ~~, and hence enhances ice algal primary production~~ for ice algal growth. The overall impact of i_0 on ice algal production depends on the choice of formulation and parameter(s) for the light limitation function as discussed previously.

To the best of the authors' knowledge, no studies have ever reported an observed value for i_0 for snow surface. For a snow-free ice surface, Grenfell and Maykut (1977) ~~reported the~~ report values ranging between 0.18 and 0.63 depending on both the ice type and whether the incoming shortwave radiation is direct or diffuse. Observation-based estimates of i_0 for snow surface would be useful in order to reduce the uncertainty of ice algal and under-ice phytoplankton growth in models.

4.3 ~~Advection and eddy diffusion of sea-ice biogeochemical state variables~~ Horizontal transport associated with moving sea ice (EXP4)

EXP4 ~~was~~ is conducted with the identical model formulation as EXP0 except that the advection and ~~eddy~~ diffusion of sea-ice biogeochemical state variables ~~were neglected.~~ (the effect of horizontal transport associated with moving sea ice) are artificially suppressed (i.e., the first two terms on the right hand side of Equation 2 are removed). Note that the advection and diffusion of sea-ice physical state variables ~~were~~ are retained in EXP4, ~~and therefore,~~ so there is no ~~change in the~~ difference in these variables between EXP0 and EXP4.

A time series comparison of the modelled pan-Arctic-mean bottom-ice nitrate and ice algal ~~GPP for the year~~ NPP for 1979 shows that these quantities are always higher in EXP0 than EXP4 (Figure 14a). The pan-Arctic annual-mean bottom-ice nitrate and the ice algal annual ~~GPP~~ NPP are higher in EXP0 than EXP4 by 2 and 16 %, respectively. These results indicate that the overall effect of ~~advection and eddy diffusion~~ horizontal transport associated with moving sea ice over the pan-Arctic is an increase in these ~~quantites.~~ quantities. However, we note that these values could be quite different in other years given the large interannual variability in wind stress fields driving sea ice drift patterns.

Although the overall effect is an enhancement, the spatial distribution shows regions of local ~~increases and decreases (Figure~~ increase and decrease (Figure 14c-d). The difference in nitrate concentration between the two experiments is relatively high off the west coast of Baffin Island, ~~in which~~ where the bottom-ice nitrate concentration is relatively high in EXP0 (Figure 14b), whereas the difference is relatively small ~~in~~ on the Canadian Polar Shelf (Figure 14c). The difference in ~~the spatial distribution of the ice algal GPP~~ ice algal NPP is relatively high in regions of high ice algal ~~GPP~~ NPP except for the Canadian Polar Shelf (Figure 14d), which is a region of relatively slow ice motion (Figure 14e). ~~A~~ One possible explanation for these spatial differences is that the horizontal transport ~~within~~ of sea ice takes ice algae out of regions of high productivity into regions of low productivity~~, opening up space for new growth in the~~. This allows more efficient growth by maintaining the loss due to viral infection and aggregation (represented by the quadratic mortality term in the model) at relatively low values in the productive regions. Another factor is the horizontal transport of nutrients into these regions which are taken up by ice algae and results in the further increase in ice algal production.

4.4 Shading of ice algae (EXP5)

In EXP5, the shading effect of ice algae on light transfer through the ice ~~was neglected~~ is artificially suppressed in order to assess its impact on under-ice NPP. Effectively, this is done by setting the light extinction coefficient for ice algae to zero (Equation 15 of Mortenson et al. (2017)). On the pan-Arctic scale, there is almost no ~~impact~~effect, as shown in Figure 15a. The differences in the pan-Arctic- and annual-mean under-ice PAR and the pan-Arctic under-ice annual NPP between EXP0 and EXP5 are ~~only~~ 2 % and 1 %, respectively.

Consistent with the patchiness of the ice algal distribution (Figure 8c), the shading effect is rather localized as shown in Figure 15b-e. The influence on under-ice PAR is assessed for the month of the ice algal bloom peak (May; Figure 6c). ~~By construction, the~~ The spatial distribution of the difference in the under-ice PAR between EXP0 and EXP5 is simply a reflection

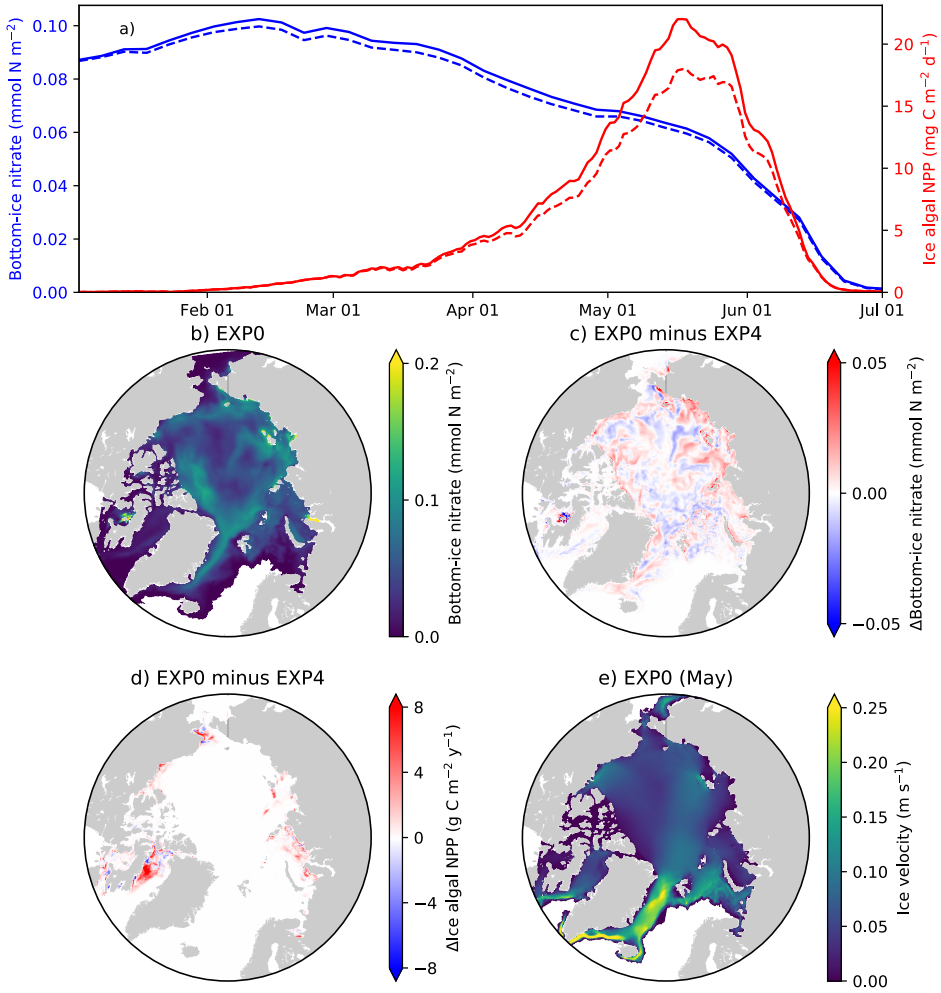

Figure 14. Model sensitivity to the ~~advection and diffusion~~ horizontal transport of sea-ice biogeochemical state variables. a) Time series comparison of 5-day- and pan-Arctic-mean modelled bottom-ice nitrate (blue) and ice algal daily ~~GPP~~ NPP (red) during January-June of 1979 between EXP0 (solid) and EXP4 (dashed). Spatial maps of the annual-mean bottom-ice nitrate in b) EXP0 and c) its difference between EXP0 and EXP4, d) the difference in the ice algal annual ~~GPP~~ NPP between EXP0 and EXP4, and e) the magnitude of the ice velocity during May.

of ice algal abundance (Figure 15c). Similarly, a general decrease in the under-ice NPP is found due to shading in the regions of high ~~modelled ice algae~~ice algal production. However, in some regions, ~~the~~ shading results in a slight increase in ~~the~~ under-ice NPP which is dominated by small phytoplankton (Figure 16c). The underlying mechanisms for this response of the modelled ecosystem to a perturbation to light are unclear. ~~A possible explanation for this phenomenon is that the reduction in nutrient drawdown under regions of large ice algal biomass enchances nutrient advection into regions of low ice algal biomass.~~

The shading effect of ice algae was recently examined in the model study ~~by~~ of Castellani et al. (2017). Their results showed that the effect has ~~stronger~~ greater influence at higher latitudes due to low ambient light. Furthermore, they hypothesized that the onset of the under-ice phytoplankton bloom north of 80°N can be delayed by up to 40 days depending on how their modelled under-ice PAR is affected by shading.

It is difficult to directly compare the results of the present study with those of Castellani et al. (2017), primarily due to the difference in the definition of the term under-ice. As described in Section 2.5.3, in the present study, a grid cell is considered "under-ice" as long as the ice concentration is 0.15 or above. Because of the high surface albedo and strong light attenuation by snow and ice, the under-ice PAR defined in the present study is therefore dominated by the light through the open-water fraction. Consequently, the under-ice NPP is controlled by the light through the open-water fraction and does not show a strong influence by the shading of ice algae. Furthermore, direct comparison is difficult due to the difference in the target year of simulation; Castellani et al. (2017) simulated 2012, while we consider 1979.

~~To~~ Nevertheless, to carry out an analysis comparable to that of Castellani et al. (2017), we ~~calculated~~ calculate the onset of under-ice phytoplankton bloom as follows. A bloom onset is defined as the day when bottom-ice PAR exceeds 0.4 W m^{-2} and remains above this value at least for 30 days. This threshold for bottom-ice PAR corresponds to the limit for under-ice algal growth considered in Castellani et al. (2017), assuming an unit conversion (from μmol photon m^{-2} s^{-1} to W m^{-2}) factor of 1/4.56 (Lavoie et al., 2005). Figure 17 shows the spatial variability in the under-ice bloom onset based on the definition above. The bloom ~~took~~ takes place mostly in seasonally ice-covered regions, while it ~~was~~ is absent in most of the pack ice (as indicated by white regions). Unlike Castellani et al. (2017), the under-ice bloom north of 80°N ~~was~~ is absent even without the shading effect. The absence of the bloom in our simulation is due to the presence of snow in this region; despite the extremely low quantity (< 0.01 m; data ~~now~~ not shown), it ~~kept~~ keeps the light level below the threshold for the bloom to occur. The median value of the onset is on the 155th day (June 6) when the shading is accounted (Figure 17a), while it is 10 days earlier without the shading effect (Figure 17b).

Figure 17c shows the spatial variability in the delay in the under-ice bloom onset caused by the ice algal shading. The values range from 5 to 275 days; in some places, the bloom is prevented completely. The present study does confirm the finding of Castellani et al. (2017) that the shading effect is spatially variable and can have a strong impact on the phytoplankton bloom timing under the ice ~~of~~ with high ice algal biomass. However, given the patchiness of ice algal distribution (mostly confined to shelf regions) and the control of the light through the open-water fraction, the impact of the shading on the ~~estimate for the~~ pan-Arctic under-ice annual NPP is negligible. Besides the shading effect, ice algae can contribute to substantial ice melting through light absorption (Kauko et al., 2017), which is not addressed in the present study.

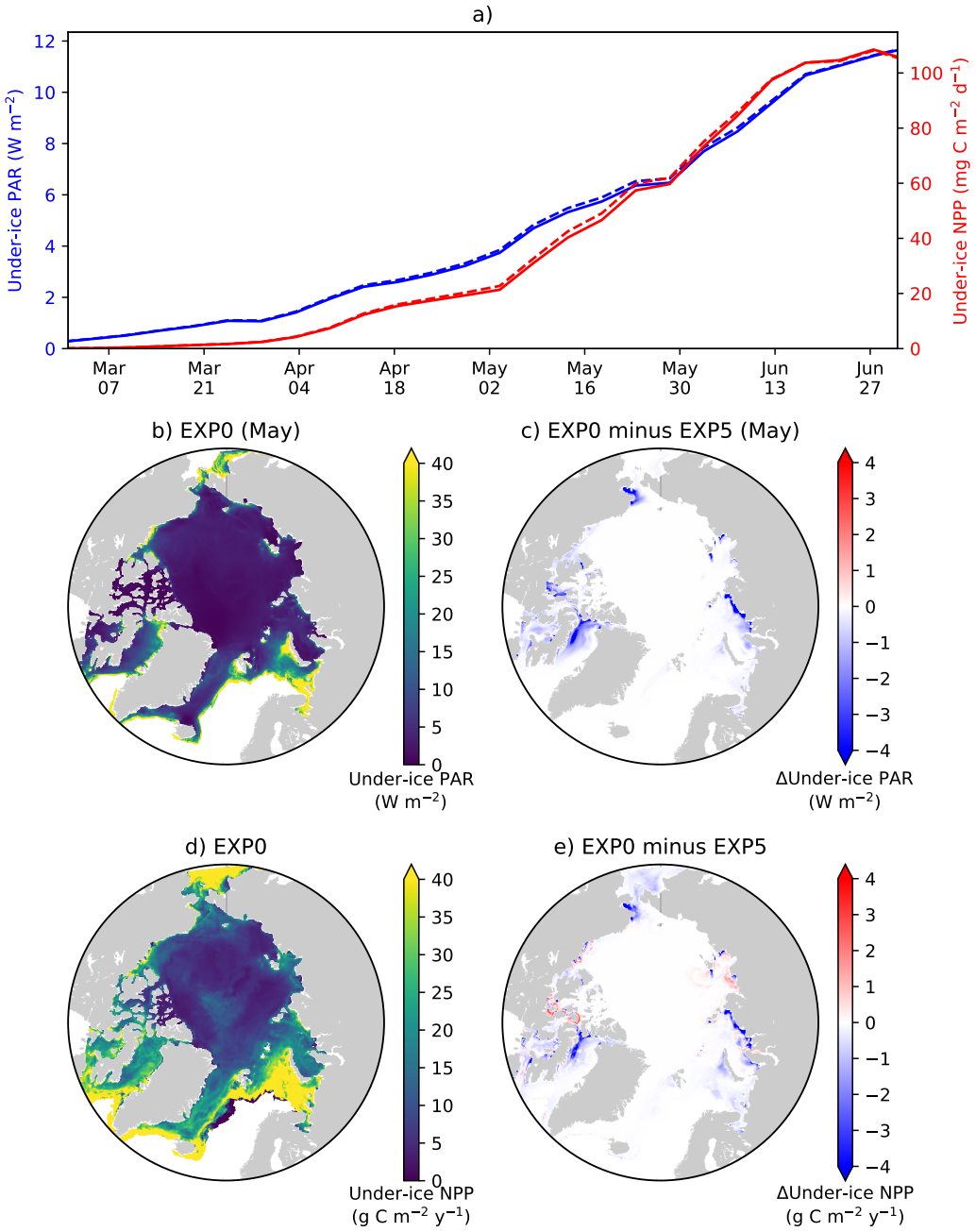

Figure 15. Model sensitivity to shading ~~of~~ by ice algae. a) Time series comparison of modelled pan-Arctic- and 5-day-mean under-ice PAR (blue) and NPP (red) between EXP0 (solid) and EXP5 (dashed) during ~~the year~~ 1979. Spatial maps of b) ~~the~~ monthly-mean under-ice PAR in May in EXP0 and c) its difference from EXP5, d) the under-ice annual NPP in EXP0, and e) its difference from EXP5.

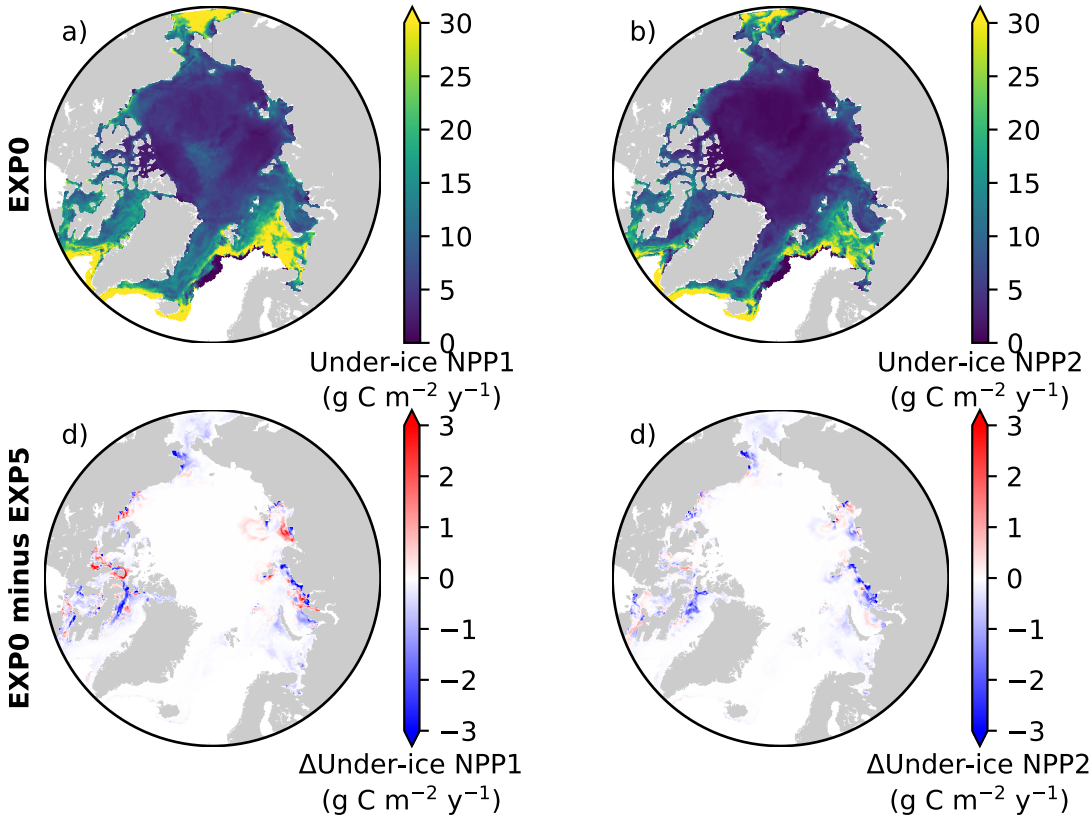

Figure 16. Spatial maps of under-ice annual NPP by a) small and b) large phytoplankton during 1979 in EXP0, and c,d) their respective differences from EXP5.

5 Conclusions

In the present study, we have developed a sea-ice ~~biogeochemical~~ biogeochemistry model which is coupled to NEMO. A number of modifications to the sea-ice physical model used in the standard distribution of NEMO (LIM2), to the ocean biogeochemical model (CanOE), and to the existing pan-Arctic configuration (NAA) were necessary to properly simulate the physical and biogeochemical processes in ice-covered regions. Results of the reference simulation (EXP0) ~~agreed well with observations and previous studies in terms of simulated ice volume and extent and the pan-Arctic annual primary production of ice algae and phytoplankton~~were discussed and compared with previous studies, with a focus on the year 1979; more thorough evaluation of the model performance over the recent decades is planned for future studies. Adopting a high vertical resolution in the upper water column was found to be necessary to properly represent the effects of a meltwater lens on surface nutrients

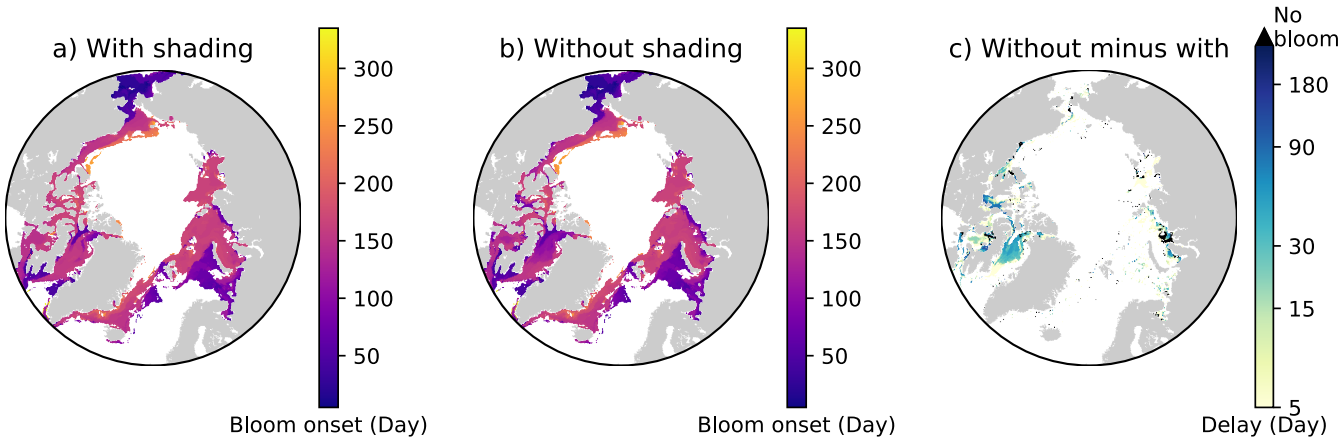

Figure 17. Effects of ice algal shading on the onset of under-ice phytoplankton bloom. Spatial maps showing the bloom onset (as the day from January 1) when the ice algal shading is a) considered and b) neglected and c) the difference between the two cases representing the delay due to the shading in 1979 in EXP0. In c), "No bloom" refers to regions in which the bloom was present in b) but not in a). See ~~the main text~~ Section 4.4 for the definition of bloom onset.

and the formation of a subsurface chlorophyll maximum. Furthermore, the vertical resolution was shown to have an effect on the magnitude of the modelled surface seawater DMS concentration (∼10 % annually and up to ∼20 % seasonally), which in turn influences DMS emissions. Results of the sensitivity experiments demonstrated that: LIM2 requires high-frequency (daily) snowfall forcing data to simulate realistic snow depth (EXP1 and 2); the assumption of no light penetration through snow in LIM2 is unrealistic for simulating an adequate ice algal bloom (EXP3); ~~the advection and eddy diffusion of sea-ice biogeochemical state variables~~ horizontal transport of sea ice contributes to an enhancement of the pan-Arctic ice algal annual ~~GPP~~ NPP by 16 % (EXP4); and attenuation of light by ice algae has local influence on under-ice NPP but is negligible when estimating larger-scale quantities (e.g., pan-Arctic under-ice annual NPP) (EXP5). While we believe that these findings would be qualitatively similar in other years, it would be worthwhile to quantify their interannual variability. The modifications to LIM2, CanOE, and NAA adopted in the present study are also applicable to other submodels and configurations of NEMO (e.g., LIM3, PISCES, ~~and ORCA, respectively~~ORCA) as the code structures are similar, and therefore, can be incorporated into future pan-Arctic biogeochemical studies. The sea-ice biogeochemical model developed in the present study has been embedded into NEMO in a generic way (see Appendix A), and can therefore be easily coupled to the aforementioned sub-models. To our knowledge, such a development has not been done previously within NEMO. Further sensitivity experiments and observational constraints are needed to refine the important parameters (e.g., i_0) for sea-ice biogeochemistry.

Code availability. The model code and the configuration used for conducting model simulations are archived (Hayashida, 2018a).

Table A1. A list of NEMO modules modified to add ocean sulfur cycle and sea-ice biogeochemistry.

Module	Description of the modification
ice_2.F90	Assign arrays for advective and diffusive tendencies of the sea-ice biogeochemical state variables.
limistate_2.F90	Initialize the arrays for the advective and diffusive tendencies.
limrst_2.F90	Restart the arrays for the advective and diffusive tendencies.
limtrp_2.F90	Compute the advective and diffusive tendencies as described in Section 2.3.1.
limthd_zdf_2.F90	Compute the light penetration parameterization through snow and sea ice as described in Section 2.1.
p4zopt.F90	Compute ice-algal shading and under-ice PAR as described in Section 2.2.2.
par_my_trc.F90	Define the number of state and diagnostic variables.
trcini_my_trc.F90	Initialize the state variables.
trcrst_my_trc.F90	Restart the state variables.
trcnam_my_trc.F90	Assign the arrays of the state and diagnostic variables.
trcsms_my_trc.F90	Compute the biological and chemical sources and sinks and ice-ocean fluxes.

Appendix A: Implementation of ocean sulfur cycle and sea-ice biogeochemistry into the NEMO source code

Figure A1 shows the structure of the NEMO v3.4 source code directory (NEMO), which includes the following subdirectories (submodels): OPA_SRC (OPA), LIM_SRC_2 (LIM2), and TOP_SRC (ocean biogeochemistry). The directory TOP_SRC contains two subdirectories: PISCES and MY_TRC. In this study, the directory PISCES contains the source code of CanOE, as CanOE has been developed using the code structure of the PISCES ocean biogeochemical model. The other directory, MY_TRC, consists of a list of generic modules that can be modified by end users to add their own biogeochemical models; we introduced an ocean sulfur cycle and sea-ice biogeochemistry into this interface. Furthermore, we modified a few modules in the directories LIM_SRC_2 and PISCES for the implementation of sea-ice biogeochemistry into the NEMO modelling system (Table A1).

Numerically, the tendencies for the sea-ice biogeochemical state variables are computed at each time step as follows: first, the concentrations of all state variables from the previous time step are transferred from the module trcsms_my_trc.F90 to the module limtrp_2.F90 to compute the advective and diffusive tendencies. The updated concentrations are transferred back to the module trcsms_my_trc.F90 within which the biological and chemical sources and sinks as well as the ice-ocean fluxes of these state variables are computed.

In NEMO, user-specific modules built within MY_TRC are designed to be activated by defining the C preprocessor (CPP) key key_my_trc. As such, we assigned CPP keys for each component of the newly-developed models, which can be activated as needed (Table A2).

Appendix B: Interannual variability during spin up

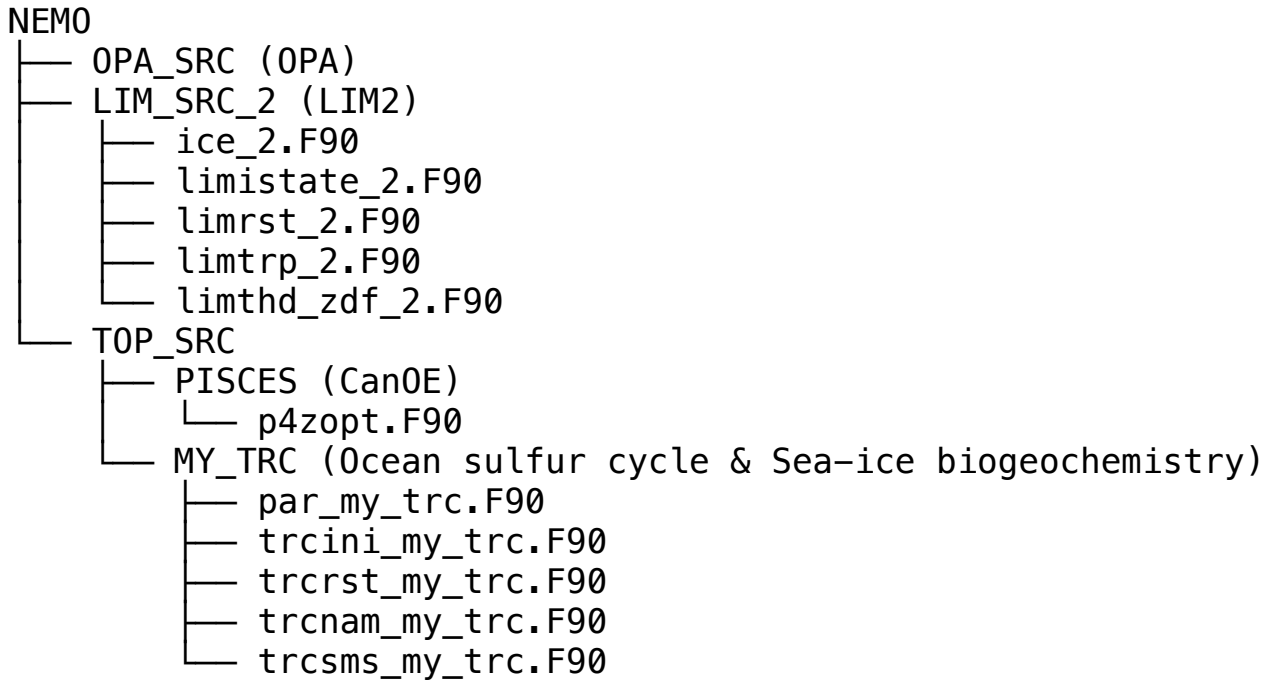

Figure A1. File tree diagram of the OPA-LIM2-CanOE configuration of NEMO v3.4. The modules listed in the diagram (*.F90) have been modified in order to implement ocean sulfur cycle and sea-ice biogeochemistry into the present configuration.

Table A2. A list of CPP keys created in the present study.

CPP key	Description
key_my_trc_ocedms	Activate ocean sulfur cycle.
key_my_trc_iceeco	Activate sea-ice ecosystem.
key_my_trc_icedms	Activate sea-ice sulfur cycle.

The annual-mean time series of modelled snow and ice volumes, ice extent, seawater nitrate, and ice algal and phytoplankton biomass over the 11 years of EXP0 are shown in Figure B1. This time period can be considered as sufficiently long to spin up some of these quantities, while others may require additional time to spin up. However, none of these quantities reach a steady state in the current setup as the model was driven by interannual surface and lateral boundary conditions. The aim of the present analysis is to examine the temporal variability starting from the initial year and compare with findings of previous model studies. Presenting the results from the initial year is often neglected in the literature, but can be useful for future studies.

The annual-mean modelled snow volume stabilizes around 0.8×10^3 km^3 after an initial drop of about 0.1×10^3 km^3 from year 1969 to 1970 (Figure B1a), indicating a spin-up period of a year or so. In contrast, the annual-mean modelled ice volume

variations show an initial reduction during 1969-1971 followed by an overall increase during 1973-1979. The relatively short duration of this simulation does not allow us to distinguish between trends and slow interannual variability, so we cannot determine if the ice volume has spun up based solely on this analysis; this will be addressed in a follow up study. A previous pan-Arctic regional model study of Watanabe (2013) shows a spin-up period of 10 years for modelled ice volume based on a simulation using a fixed annual cycle of atmospheric forcing and restoring of temperature and salinity.

Modelled ice extent shows a decrease in the first 6 years followed by a stabilization in the last 5 years, suggesting that this quantity spun up at year 1975 (Figure B1b). This spin-up time is similar to that found in the pan-Arctic model study of Jin et al. (2012), in which their modelled ice area and extent became comparable to the observations after the first 6 years of simulation.

Annual-mean modelled seawater nitrate concentration integrated over the upper 90 m of the water column shows both increases and decreases during the 11 years (Figure B1b), although the size of the fluctuation ($\sim$20 mmol N m^{-2}) is small relative to its mean state ($\sim$490 mmol N m^{-2}). Similarly to ice volume, a longer simulation would be needed to distinguish between trends and interannual variability in the modelled nitrate concentration. A previous pan-Arctic model study of Dupont (2012) indicated a spin-up period of at least a decade for nitrate in the upper 100 m water column for the model domain he considered. The modelled primary producers (ice algae and phytoplankton) appear to have spun up within a year of the model simulation, as their annual primary production fluctuates around a steady mean following the first year (Figure B1c).

Author contributions. HH wrote the model code, designed and performed the numerical experiments, conducted the analysis, and wrote the manuscript with input from all authors. AHM and NSS supervised the project.

Competing interests. The authors declare that they have no conflict of interest.

Acknowledgements. We thank Achim Randelhoff and two anonymous referees for their thorough review, which greatly improved the presentation of this manuscript. We thank Martin Vancoppenolle for helpful discussion on the LIM model. This study contributes to the SCOR Working group on Biogeochemical Exchange Processes at Sea Ice Interfaces (BEPSII), the Network on Climate and Aerosols: Addressing Key Uncertainties in Remote Canadian Environments (NETCARE), and ArcticNet. We acknowledge funding from NETCARE, ArcticNet, Fisheries and Oceans Canada, and Environment and Climate Change Canada. This research was enabled in part by support provided by WestGrid (www.westgrid.ca) and Compute Canada (www.computecanada.ca). We thank Belaid Moa (University of Victoria) for computational support, Arlan Dirkson (Université du Québec à Montréal) for providing a netCDF version of the PIOMAS monthly-mean ice thickness and concentration gridded data products, and Clark Pennelly (University of Alberta) for providing a modified version of the DFS dataset, and Ken Denman for providing a helpful discussion on growth rates and primary productivity. The original NAA configuration was developed under an NSERC Discovery Grant award to PGM.

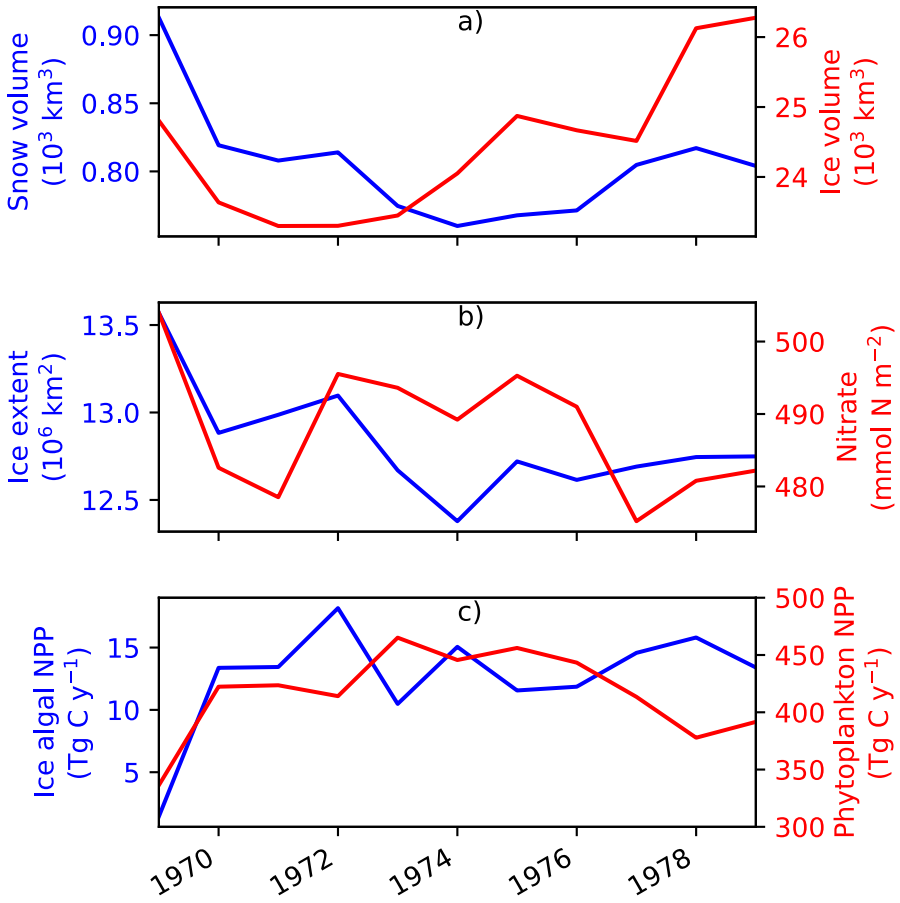

Figure B1. Time series of annual-mean modelled a) snow and ice volumes, b) ice extent and depth-integrated (90 m) seawater nitrate concentration, and c) depth-integrated (3 cm) ice algal NPP and depth-integrated (90 m) phytoplankton NPP in EXP0. The depth-integrated quantities represent averages over the entire model domain.

References

Abraham, C., Steiner, N., Monahan, A., and Michel, C.: Effects of subgrid-scale snow thickness variability on radiative transfer in sea ice, Journal of Geophysical Research: Oceans, 120, 5597–5614, https://doi.org/10.1002/2015JC010741, http://doi.wiley.com/10.1002/2015JC010741, 2015.

Amante, C. and Eakins, B. W.: ETOPO1 1 arc-minute global relief model: procedures, data sources and analysis, US Department of Commerce, National Oceanic and Atmospheric Administration, National Environmental Satellite, Data, and Information Service, National Geophysical Data Center, Marine Geology and Geophysics Division Colorado, 2009.

Arora, V. K., Scinocca, J. F., Boer, G. J., Christian, J. R., Denman, K. L., Flato, G. M., Kharin, V. V., Lee, W. G., and Merryfield, W. J.: Carbon emission limits required to satisfy future representative concentration pathways of greenhouse gases, Geophysical Research Letters, 38, L05 805, https://doi.org/10.1029/2010GL046270, 2011.

Arrigo, K. R.: Sea Ice Ecosystems, Annual Review of Marine Science, 6, 439–467, https://doi.org/10.1146/annurev-marine-010213-135103, http://dx.doi.org/10.1146/annurev-marine-010213-135103, 2014.

Arrigo, K. R., Sullivan, C. W., and Kremer, J. N.: A bio-optical model of Antarctic sea ice, Journal of Geophysical Research: Oceans, 96, 10 581–10 592, https://doi.org/10.1029/91JC00455, http://onlinelibrary.wiley.com.ezproxy.library.uvic.ca/doi/10.1029/91JC00455/abstract, 1991.

Assmy, P., Ehn, J. K., FernÃ¡ndez-MÃ©ndez, M., Hop, H., Katlein, C., Sundfjord, A., Bluhm, K., Daase, M., Engel, A., Fransson, A., Granskog, M. A., Hudson, S. R., Kristiansen, S., Nicolaus, M., Peeken, I., Renner, A. H. H., Spreen, G., Tatarek, A., and Wiktor, J.: Floating Ice-Algal Aggregates below Melting Arctic Sea Ice, PLoS ONE, 8, e76 599, https://doi.org/10.1371/journal.pone.0076599, http://dx.plos.org/10.1371/journal.pone.0076599, 2013.

Aumont, O., Ethé, C., Tagliabue, A., Bopp, L., and Gehlen, M.: PISCES-v2: an ocean biogeochemical model for carbon and ecosystem studies, Geoscientific Model Development, 8, 2465–2513, https://doi.org/10.5194/gmd-8-2465-2015, 2015.

Balmaseda, M. A., Mogensen, K., and Weaver, A. T.: Evaluation of the ECMWF ocean reanalysis system ORAS4, Quarterly Journal of the Royal Meteorological Society, 139, 1132–1161, https://doi.org/10.1002/qj.2063, http://onlinelibrary.wiley.com/doi/10.1002/qj.2063/abstract, 2013.

Bouillon, S., Maqueda, M. A. M., Legat, V., and Fichefet, T.: An elastic–viscous–plastic sea ice model formulated on Arakawa B and C grids, Ocean Modelling, 27, 174–184, http://www.sciencedirect.com/science/article/pii/S1463500309000043, 2009.

Brown, Z. W., Lowry, K. E., Palmer, M. A., van Dijken, G. L., Mills, M. M., Pickart, R. S., and Arrigo, K. R.: Characterizing the subsurface chlorophyll a maximum in the Chukchi Sea and Canada Basin, Deep Sea Research Part II: Topical Studies in Oceanography, 118, 88–104, https://doi.org/10.1016/j.dsr2.2015.02.010, http://linkinghub.elsevier.com/retrieve/pii/S0967064515000399, 2015.

Castellani, G., Losch, M., Lange, B. A., and Flores, H.: Modeling Arctic sea-ice algae: Physical drivers of spatial distribution and algae phenology, Journal of Geophysical Research: Oceans, 122, 7466–7487, https://doi.org/10.1002/2017JC012828, http://onlinelibrary.wiley.com/doi/10.1002/2017JC012828/abstract, 2017.

Crank, J. and Nicolson, P.: A practical method for numerical evaluation of solutions of partial differential equations of the heat-conduction type, Advances in Computational Mathematics, 6, 207–226, https://doi.org/10.1007/BF02127704, https://doi.org/10.1007/BF02127704, 1996.

Dai, A. and Trenberth, K. E.: Estimates of Freshwater Discharge from Continents: Latitudinal and Seasonal Variations, Journal of Hydrometeorology, 3, 660–687, https://doi.org/10.1175/1525-7541(2002)003<0660:EOFDFC>2.0.CO;2, http://journals.ametsoc.org/doi/abs/10.1175/1525-7541(2002)003%3C0660:EOFDFC%3E2.0.CO;2, 2002.

Deal, C., Jin, M., Elliott, S., Hunke, E., Maltrud, M., and Jeffery, N.: Large-scale modeling of primary production and ice algal biomass within arctic sea ice in 1992, Journal of Geophysical Research, 116, C07 004, https://doi.org/10.1029/2010JC006409, http://doi.wiley.com/10.1029/2010JC006409, 2011.

Dee, D. P., Uppala, S. M., Simmons, A. J., Berrisford, P., Poli, P., Kobayashi, S., Andrae, U., Balmaseda, M. A., Balsamo, G., Bauer, P., Bechtold, P., Beljaars, A. C. M., van de Berg, L., Bidlot, J., Bormann, N., Delsol, C., Dragani, R., Fuentes, M., Geer, A. J., Haimberger, L., Healy, S. B., Hersbach, H., Hólm, E. V., Isaksen, L., Kållberg, P., Köhler, M., Matricardi, M., McNally, A. P., Monge-Sanz, B. M., Morcrette, J.-J., Park, B.-K., Peubey, C., de Rosnay, P., Tavolato, C., Thépaut, J.-N., and Vitart, F.: The ERA-Interim reanalysis: configuration and performance of the data assimilation system, Quarterly Journal of the Royal Meteorological Society, 137, 553–597, https://doi.org/10.1002/qj.828, http://onlinelibrary.wiley.com/doi/10.1002/qj.828/abstract, 2011.

Dirkson, A., Merryfield, W. J., and Monahan, A.: Impacts of Sea Ice Thickness Initialization on Seasonal Arctic Sea Ice Predictions, Journal of Climate, 30, 1001–1017, https://doi.org/10.1175/JCLI-D-16-0437.1, http://journals.ametsoc.org.ezproxy.library.uvic.ca/doi/abs/10.1175/JCLI-D-16-0437.1, 2016.

Dupont, F.: Impact of sea-ice biology on overall primary production in a biophysical model of the pan-Arctic Ocean, Journal of Geophysical Research: Oceans, 117, C00D17, https://doi.org/10.1029/2011JC006983, http://onlinelibrary.wiley.com.ezproxy.library.uvic.ca/doi/10.1029/2011JC006983/abstract, 2012.

Dupont, F., Higginson, S., Bourdallé-Badie, R., Lu, Y., Roy, F., Smith, G. C., Lemieux, J.-F., Garric, G., and Davidson, F.: A high-resolution ocean and sea-ice modelling system for the Arctic and North Atlantic oceans, Geosci. Model Dev., 8, 1577–1594, https://doi.org/10.5194/gmd-8-1577-2015, http://www.geosci-model-dev.net/8/1577/2015/, 2015.

Dussin, R., Barnier, B., Brodeau, L., and Molines, J. M.: The making of the Drakkar Forcing Set DFS5, DRAKKAR/MyOcean Rep. 01–04, 16, 2016.

Eppley, R. W.: Temperature and phytoplankton growth in the sea, Fish. Bull, 70, 1063–1085, 1972.

Fichefet, T. and Maqueda, M. A. M.: Sensitivity of a global sea ice model to the treatment of ice thermodynamics and dynamics, Journal of Geophysical Research: Oceans, 102, 12 609–12 646, https://doi.org/10.1029/97JC00480, http://onlinelibrary.wiley.com.ezproxy.library.uvic.ca/doi/10.1029/97JC00480/abstract, 1997.

Flato, G. M. and Brown, R. D.: Variability and climate sensitivity of landfast Arctic sea ice, Journal of Geophysical Research: Oceans, 101, 25 767–25 777, https://doi.org/10.1029/96JC02431, http://onlinelibrary.wiley.com.ezproxy.library.uvic.ca/doi/10.1029/96JC02431/abstract, 1996.

Garcia, H. E., Locarnini, R. A., Boyer, T. P., Antonov, J. I., Baranova, O. K., Zweng, M. M., Reagan, J. R., and Johnson, D. R.: World Ocean Atlas 2013, Volume 3: Dissolved Oxygen, Apparent Oxygen Utilization, and Oxygen Saturation, s. Levitus, Ed., A. Mishonov Technical Ed.; NOAA Atlas NESDIS 75, 27 pp., 2014.

Garrison, D. L., Ackley, S. F., and Buck, K. R.: A physical mechanism for establishing algal populations in frazil ice, Nature, 306, 363–365, https://doi.org/10.1038/306363a0, http://www.nature.com/nature/journal/v306/n5941/abs/306363a0.html, 1983.

Gosselin, M., Levasseur, M., Wheeler, P. A., Horner, R. A., and Booth, B. C.: New measurements of phytoplankton and ice algal production in the Arctic Ocean, Deep Sea Research Part II: Topical Studies in Oceanography, 44, 1623–1644, http://www.sciencedirect.com/science/article/pii/S0967064597000544, 1997.

Grenfell, T. C. and Maykut, G. A.: The optical properties of ice and snow in the Arctic Basin, Journal of Glaciology, 18, 445–463, http://adsabs.harvard.edu/abs/1977JGlac..18..445G, 1977.

Hashimoto, S., Horimoto, N., Yamaguchi, Y., Ishimaru, T., and Saino, T.: Relationship between net and gross primary production in the Sagami Bay, Japan, Limnology and oceanography, 50, 1830–1835, 2005.

Hayashida, H.: CSIB v1 source code, https://doi.org/10.5281/zenodo.1435254, https://zenodo.org/record/1435254, 2018a.

Hayashida, H.: Modelling sea-ice and oceanic dimethylsulfide production and emissions in the Arctic, PhD Thesis, University of Victoria, Victoria, BC, Canada, https://dspace.library.uvic.ca//handle/1828/10486, 2018b.

Hayashida, H., Steiner, N., Monahan, A., Galindo, V., Lizotte, M., and Levasseur, M.: Implications of sea-ice biogeochemistry for oceanic production and emissions of dimethyl sulfide in the Arctic, Biogeosciences, 14, 3129–3155, https://doi.org/10.5194/bg-14-3129-2017, https://www.biogeosciences.net/14/3129/2017/, 2017.

Hu, X. and Myers, P. G.: A Lagrangian view of Pacific water inflow pathways in the Arctic Ocean during model spin-up, Ocean Modelling, 71, 66–80, https://doi.org/10.1016/j.ocemod.2013.06.007, http://linkinghub.elsevier.com/retrieve/pii/S1463500313001157, 2013.

Hu, X. and Myers, P. G.: Changes to the Canadian Arctic Archipelago Sea Ice and Freshwater Fluxes in the Twenty-First Century under the Intergovernmental Panel on Climate Change A1B Climate Scenario, Atmosphere-Ocean, 52, 331–350, https://doi.org/10.1080/07055900.2014.942592, http://www.tandfonline.com/doi/abs/10.1080/07055900.2014.942592, 2014.

Jin, M., Deal, C. J., Wang, J., Shin, K.-H., Tanaka, N., Whitledge, T. E., Lee, S. H., and Gradinger, R. R.: Controls of the landfast ice–ocean ecosystem offshore Barrow, Alaska, Annals of Glaciology, 44, 63–72, http://www.ingentaconnect.com/content/igsoc/agl/2006/00000044/00000001/art00012, 2006.

Jin, M., Deal, C., Lee, S. H., Elliott, S., Hunke, E., Maltrud, M., and Jeffery, N.: Investigation of Arctic sea ice and ocean primary production for the period 1992–2007 using a 3-D global ice–ocean ecosystem model, Deep Sea Research Part II: Topical Studies in Oceanography, 81–84, 28–35, https://doi.org/10.1016/j.dsr2.2011.06.003, 2012.

Jin, M., Popova, E. E., Zhang, J., Ji, R., Pendleton, D., Varpe, Ø., Yool, A., and Lee, Y. J.: Ecosystem model intercomparison of under-ice and total primary production in the Arctic Ocean, Journal of Geophysical Research: Oceans, 121, 934–948, https://doi.org/10.1002/2015JC011183, http://doi.wiley.com/10.1002/2015JC011183, 2015.

Jin, M., Deal, C., Maslowski, W., Matrai, P., Roberts, A., Osinski, R., Lee, Y. J., Frants, M., Elliott, S., Jeffery, N., Hunke, E., and Wang, S.: Effects of Model Resolution and Ocean Mixing on Forced Ice-Ocean Physical and Biogeochemical Simulations Using Global and Regional System Models, Journal of Geophysical Research: Oceans, 123, 358–377, https://doi.org/10.1002/2017JC013365, http://onlinelibrary.wiley.com/doi/10.1002/2017JC013365/full, 2018.

Kauko, H. M., Taskjelle, T., Assmy, P., Pavlov, A. K., Mundy, C. J., Duarte, P., Fernández-Méndez, M., Olsen, L. M., Hudson, S. R., Johnsen, G., Elliott, A., Wang, F., and Granskog, M. A.: Windows in Arctic sea ice: Light transmission and ice algae in a refrozen lead, Journal of Geophysical Research: Biogeosciences, 122, 2016JG003 626, https://doi.org/10.1002/2016JG003626, http://onlinelibrary.wiley.com/doi/10.1002/2016JG003626/abstract, 2017.

Lauvset, S. K., Key, R. M., Olsen, A., van Heuven, S., Velo, A., Lin, X., Schirnick, C., Kozyr, A., Tanhua, T., Hoppema, M., Jutterström, S., Steinfeldt, R., Jeansson, E., Ishii, M., Perez, F. F., Suzuki, T., and Watelet, S.: A new global interior ocean mapped climatology: the $1^\circ \times 1^\circ$ GLODAP version 2, Earth System Science Data, 8, 325–340, https://doi.org/10.5194/essd-8-325-2016, http://oceanrep.geomar.de/31183/, 2016.

Lavoie, D., Denman, K., and Michel, C.: Modeling ice algal growth and decline in a seasonally ice-covered region of the Arctic (Resolute Passage, Canadian Archipelago), Journal of Geophysical Research, 110, C11 009, https://doi.org/10.1029/2005JC002922, http://doi.wiley.com/10.1029/2005JC002922, 2005.

Legendre, L., Ackley, S. F., Dieckmann, G. S., Gulliksen, B., Horner, R., Hoshiai, T., Melnikov, I. A., Reeburgh, W. S., Spindler, M., and Sullivan, C. W.: Ecology of sea ice biota, Polar Biology, 12, 429–444, https://doi.org/10.1007/BF00243114, http://link.springer.com.ezproxy.library.uvic.ca/article/10.1007/BF00243114, 1992.

Leu, E., Mundy, C. J., Assmy, P., Campbell, K., Gabrielsen, T. M., Gosselin, M., Juul-Pedersen, T., and Gradinger, R.: Arctic spring awakening – Steering principles behind the phenology of vernal ice algal blooms, Progress in Oceanography, 139, 151–170, https://doi.org/10.1016/j.pocean.2015.07.012, http://www.sciencedirect.com/science/article/pii/S0079661115001640, 2015.

Loose, B., McGillis, W. R., Schlosser, P., Perovich, D., and Takahashi, T.: Effects of freezing, growth, and ice cover on gas transport processes in laboratory seawater experiments, Geophysical Research Letters, 36, L05 603, https://doi.org/10.1029/2008GL036318, http://onlinelibrary.wiley.com.ezproxy.library.uvic.ca/doi/10.1029/2008GL036318/abstract, 2009.

Madec, G.: NEMO ocean engine, Tech. Rep. 27, Institut Pierre Simon Laplace (ISPL), 2008.

Maykut, G. A. and Untersteiner, N.: Some results from a time-dependent thermodynamic model of sea ice, Journal of Geophysical Research, 76, 1550–1575, https://doi.org/10.1029/JC076i006p01550, http://onlinelibrary.wiley.com.ezproxy.library.uvic.ca/doi/10.1029/JC076i006p01550/abstract, 1971.

Melnikov, I. A., Kolosova, E. G., Welch, H. E., and Zhitina, L. S.: Sea ice biological communities and nutrient dynamics in the Canada Basin of the Arctic Ocean, Deep Sea Research Part I: Oceanographic Research Papers, 49, 1623–1649, https://doi.org/10.1016/S0967-0637(02)00042-0, http://linkinghub.elsevier.com/retrieve/pii/S0967063702000420, 2002.

Miller, L. A., Fripiat, F., Else, B. G., Bowman, J. S., Brown, K. A., Collins, R. E., Ewert, M., Fransson, A., Gosselin, M., Lannuzel, D., Meiners, K. M., Michel, C., Nishioka, J., Nomura, D., Papadimitriou, S., Russell, L. M., Sørensen, L. L., Thomas, D. N., Tison, J.-L., van Leeuwe, M. A., Vancoppenolle, M., Wolff, E. W., and Zhou, J.: Methods for biogeochemical studies of sea ice: The state of the art, caveats, and recommendations, Elementa: Science of the Anthropocene, 3, https://doi.org/10.12952/journal.elementa.000038, http://elementascience.org:80/article/info:doi/10.12952/journal.elementa.000038, 2015.

Morel, A.: Optical modeling of the upper ocean in relation to its biogenous matter content (case I waters), Journal of Geophysical Research: Oceans, 93, 10 749–10 768, https://doi.org/10.1029/JC093iC09p10749, http://onlinelibrary.wiley.com.ezproxy.library.uvic.ca/doi/10.1029/JC093iC09p10749/abstract, 1988.

Mortenson, E., Hayashida, H., Steiner, N., Monahan, A., Blais, M., Gale, M. A., Galindo, V., Gosselin, M., Hu, X., Lavoie, D., and Mundy, C. J.: A model-based analysis of physical and biological controls on ice algal and pelagic primary production in Resolute Passage, Elem Sci Anth, 5, https://doi.org/10.1525/elementa.229, http://www.elementascience.org/articles/10.1525/elementa.229/, 2017.

Olsen, L. M., Laney, S. R., Duarte, P., Kauko, H. M., Fernández-Méndez, M., Mundy, C. J., Rösel, A., Meyer, A., Itkin, P., Cohen, L., Peeken, I., Tatarek, A., Różańska-Pluta, M., Wiktor, J., Taskjelle, T., Pavlov, A. K., Hudson, S. R., Granskog, M. A., Hop, H., and Assmy, P.: The seeding of ice algal blooms in Arctic pack ice: The multiyear ice seed repository hypothesis, Journal of Geophysical Research: Biogeosciences, p. 2016JG003668, https://doi.org/10.1002/2016JG003668, http://onlinelibrary.wiley.com/doi/10.1002/2016JG003668/abstract, 2017.

Pabi, S., van Dijken, G. L., and Arrigo, K. R.: Primary production in the Arctic Ocean, 1998–2006, Journal of Geophysical Research: Oceans, 113, C08 005, https://doi.org/10.1029/2007JC004578, http://onlinelibrary.wiley.com/doi/10.1029/2007JC004578/abstract, 2008.

Popova, E. E., Yool, A., Coward, A. C., Dupont, F., Deal, C., Elliott, S., Hunke, E., Jin, M., Steele, M., and Zhang, J.: What controls primary production in the Arctic Ocean? Results from an intercomparison of five general circulation models with biogeochemistry, Journal of Geophysical Research: Oceans, 117, C00D12, https://doi.org/10.1029/2011JC007112, http://onlinelibrary.wiley.com/doi/10.1029/2011JC007112/abstract, 2012.

Prather, M. J.: Numerical advection by conservation of second-order moments, Journal of Geophysical Research: Atmospheres, 91, 6671–6681, https://doi.org/10.1029/JD091iD06p06671, http://onlinelibrary.wiley.com.ezproxy.library.uvic.ca/doi/10.1029/JD091iD06p06671/abstract, 1986.

Rampal, P., Weiss, J., Marsan, D., and Bourgoin, M.: Arctic sea ice velocity field: General circulation and turbulent-like fluctuations, Journal of Geophysical Research: Oceans, 114, https://doi.org/10.1029/2008JC005227, https://agupubs-onlinelibrary-wiley-com.ezproxy.library.uvic.ca/doi/full/10.1029/2008JC005227, 2009.

Rampal, P., Bouillon, S., Bergh, J., and Ólason, E.: Arctic sea-ice diffusion from observed and simulated Lagrangian trajectories, The Cryosphere, 10, 1513–1527, https://doi.org/10.5194/tc-10-1513-2016, http://www.the-cryosphere.net/10/1513/2016/, 2016.

Rebreanu, L., Vanderborght, J.-P., and Chou, L.: The diffusion coefficient of dissolved silica revisited, Marine Chemistry, 112, 230–233, https://doi.org/10.1016/j.marchem.2008.08.004, http://www.sciencedirect.com/science/article/pii/S0304420308001400, 2008.

Sakshaug, E.: Primary and Secondary Production in the Arctic Seas, in: The Organic Carbon Cycle in the Arctic Ocean, edited by Stein, R. and MacDonald, R. W., pp. 57–81, Springer Berlin Heidelberg, https://doi.org/10.1007/978-3-642-18912-8_3, http://link.springer.com.ezproxy.library.uvic.ca/chapter/10.1007/978-3-642-18912-8_3, 2004.

Sakshaug, E., Bricaud, A., Dandonneau, Y., Falkowski, P. G., Kiefer, D. A., Legendre, L., Morel, A., Parslow, J., and Takahashi, M.: Parameters of photosynthesis: definitions, theory and interpretation of results, Journal of Plankton Research, 19, 1637–1670, https://doi.org/10.1093/plankt/19.11.1637, https://academic.oup.com/plankt/article/19/11/1637/1420276, 1997.

Schweiger, A., Lindsay, R., Zhang, J., Steele, M., Stern, H., and Kwok, R.: Uncertainty in modeled Arctic sea ice volume, Journal of Geophysical Research: Oceans, 116, C00D06, https://doi.org/10.1029/2011JC007084, http://onlinelibrary.wiley.com.ezproxy.library.uvic.ca/doi/10.1029/2011JC007084/abstract, 2011.

Stefels, J., Steinke, M., Turner, S., Malin, G., and Belviso, S.: Environmental constraints on the production and removal of the climatically active gas dimethylsulphide (DMS) and implications for ecosystem modelling, Biogeochemistry, 83, 245–275, https://doi.org/10.1007/s10533-007-9091-5, http://link.springer.com.ezproxy.library.uvic.ca/article/10.1007/s10533-007-9091-5, 2007.

Steiner, N. S., Sou, T., Deal, C., Jackson, J. M., Jin, M., Popova, E., Williams, W., and Yool, A.: The Future of the Subsurface Chlorophyll-a Maximum in the Canada Basin - A Model Intercomparison, Journal of Geophysical Research: Oceans, 120, 387–409, https://doi.org/10.1002/2015JC011232, http://doi.wiley.com/10.1002/2015JC011232, 2015.

Tedesco, L., Miettunen, E., An, B. W., Happala, J., and Kaartokallio, H.: Long-term mesoscale variability of modelled sea-ice primary production in the northern Baltic Sea, Elem Sci Anth, 5, https://doi.org/10.1525/elementa.223, http://www.elementascience.org/articles/10.1525/elementa.223/, 2017.

Thorndike, A. S.: Diffusion of sea ice, Journal of Geophysical Research: Oceans, 91, 7691–7696, https://doi.org/10.1029/JC091iC06p07691, http://onlinelibrary.wiley.com.ezproxy.library.uvic.ca/doi/10.1029/JC091iC06p07691/abstract, 1986.

Uppala, S. M., KÅllberg, P. W., Simmons, A. J., Andrae, U., Bechtold, V. D. C., Fiorino, M., Gibson, J. K., Haseler, J., Hernandez, A., Kelly, G. A., Li, X., Onogi, K., Saarinen, S., Sokka, N., Allan, R. P., Andersson, E., Arpe, K., Balmaseda, M. A., Beljaars, A. C. M., Berg, L. V. D., Bidlot, J., Bormann, N., Caires, S., Chevallier, F., Dethof, A., Dragosavac, M., Fisher, M., Fuentes, M., Hagemann, S., Hólm, E., Hoskins, B. J., Isaksen, L., Janssen, P. a. E. M., Jenne, R., Mcnally, A. P., Mahfouf, J.-F., Morcrette, J.-J., Rayner, N. A., Saunders, R. W., Simon, P.,

Sterl, A., Trenberth, K. E., Untch, A., Vasiljevic, D., Viterbo, P., and Woollen, J.: The ERA-40 re-analysis, Quarterly Journal of the Royal Meteorological Society, 131, 2961–3012, https://doi.org/10.1256/qj.04.176, http://onlinelibrary.wiley.com/doi/10.1256/qj.04.176/abstract, 2005.

Vancoppenolle, M. and Tedesco, L.: Numerical models of sea ice biogeochemistry, in: Sea Ice, pp. 492–515, Wiley-Blackwell, 3 edn., https://doi.org/10.1002/9781118778371.ch20, https://onlinelibrary-wiley-com.ezproxy.library.uvic.ca/doi/abs/10.1002/9781118778371.ch20, 2016.

Vancoppenolle, M., Goosse, H., de Montety, A., Fichefet, T., Tremblay, B., and Tison, J.-L.: Modeling brine and nutrient dynamics in Antarctic sea ice: The case of dissolved silica, Journal of Geophysical Research, 115, C02 005, https://doi.org/10.1029/2009JC005369, http://doi.wiley.com/10.1029/2009JC005369, 2010.

Vancoppenolle, M., Bouillon, S., Fichefet, T., Goosse, H., Lecomte, O., Maqueda, M. A. M., and Madec, G.: The Louvain-la-Neuve sea ice model, Tech. rep., Université catholique de Louvain, ftp://ftp.elic.ucl.ac.be/lecomte/LIM3_users_guide_2012.pdf, 2012.

Vancoppenolle, M., Meiners, K. M., Michel, C., Bopp, L., Brabant, F., Carnat, G., Delille, B., Lannuzel, D., Madec, G., Moreau, S., Tison, J.-L., and van der Merwe, P.: Role of sea ice in global biogeochemical cycles: emerging views and challenges, Quaternary Science Reviews, 79, 207–230, https://doi.org/10.1016/j.quascirev.2013.04.011, http://www.sciencedirect.com/science/article/pii/S0277379113001431, 2013.

Warren, S. G., Rigor, I. G., Untersteiner, N., Radionov, V. F., Bryazgin, N. N., Aleksandrov, Y. I., and Colony, R.: Snow Depth on Arctic Sea Ice, Journal of Climate, 12, 1814–1829, https://doi.org/10.1175/1520-0442, http://journals.ametsoc.org.ezproxy.library.uvic.ca/doi/abs/10.1175/1520-0442(1999)012%3C1814:SDOASI%3E2.0.CO;2, 1999.

Watanabe, E.: Linkages among halocline variability, shelf-basin interaction, and wind regimes in the Beaufort Sea demonstrated in pan-Arctic Ocean modeling framework, Ocean Modelling, 71, 43–53, https://doi.org/10.1016/j.ocemod.2012.12.010, http://www.sciencedirect.com/science/article/pii/S1463500312001874, 2013.

Watanabe, E., Onodera, J., Harada, N., Aita, M. N., Ishida, A., and Kishi, M. J.: Wind-driven interannual variability of sea ice algal production in the western Arctic Chukchi Borderland, Biogeosciences, 12, 6147–6168, https://doi.org/10.5194/bg-12-6147-2015, http://www.biogeosciences.net/12/6147/2015/, 2015.

Windnagel, A., Brandt, M., Fetterer, F., and Meier, W.: Sea Ice Index Version 3 Analysis, NSIDC Special Report 19, https://nsidc.org/sites/nsidc.org/files/files/NSIDC-special-report-19.pdf, 2017.

Wolf-Gladrow, D. A., Zeebe, R. E., Klaas, C., Körtzinger, A., and Dickson, A. G.: Total alkalinity: The explicit conservative expression and its application to biogeochemical processes, Marine Chemistry, 106, 287–300, https://doi.org/10.1016/j.marchem.2007.01.006, http://www.sciencedirect.com/science/article/pii/S0304420307000047, 2007.

Zeebe, R. E., Eicken, H., Robinson, D. H., Wolf-Gladrow, D., and Dieckmann, G. S.: Modeling the heating and melting of sea ice through light absorption by microalgae, Journal of Geophysical Research: Oceans, 101, 1163–1181, https://doi.org/10.1029/95JC02687, http://onlinelibrary.wiley.com.ezproxy.library.uvic.ca/doi/10.1029/95JC02687/abstract, 1996.

Zhang, J. and Rothrock, D. A.: Modeling Global Sea Ice with a Thickness and Enthalpy Distribution Model in Generalized Curvilinear Coordinates, Monthly Weather Review, 131, 845–861, https://doi.org/10.1175/1520-0493(2003)131<0845:MGSIWA>2.0.CO;2, http://journals.ametsoc.org/doi/abs/10.1175/1520-0493%282003%29131%3C0845%3AMGSIWA%3E2.0.CO%3B2, 2003.

Zhang, J., Spitz, Y. H., Steele, M., Ashjian, C., Campbell, R., Berline, L., and Matrai, P.: Modeling the impact of declining sea ice on the Arctic marine planktonic ecosystem, Journal of Geophysical Research: Oceans, 115, C10 015, https://doi.org/10.1029/2009JC005387, http://onlinelibrary.wiley.com.ezproxy.library.uvic.ca/doi/10.1029/2009JC005387/abstract, 2010.